

Corosion, Passivity and Metallurgy

by

Bernard Baroux

Professeur à l'Institut National polytechnique de Grenoble

- **Introduction to the aqueous corrosion of metals and alloys**
- **Passivity and Passive films**
- **Passivity breakdown**
- **Metallurgical effects**

Part I: Introduction to the aqueous corrosion of metals and alloys

by

Bernard Baroux

Institut National Polytechnique de Grenoble

Corrosion is an irreversible phenomenon which results from the basic thermodynamic characteristics of the materials and the nature of their environment. In this lecture we will look at the water corrosion phenomena applicable to metals and alloys, but excluding both high temperature oxidation phenomena and corrosion of non-metallic materials

Experimental Evidences

- Formation of rust and other corrosion products



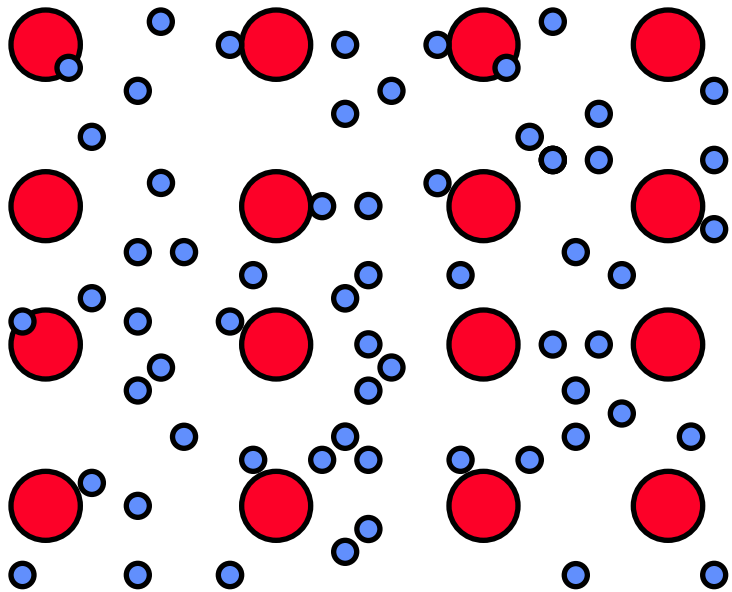
Metallurgical effects

- Electrochemical (anodic) dissolution



⇒ loss of weight and pollution...

What is a metal ?



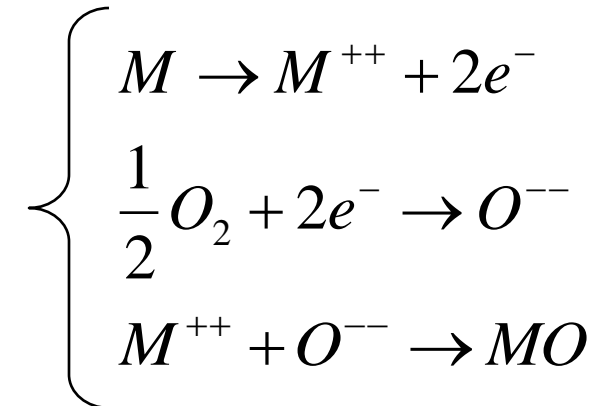
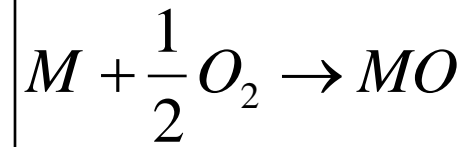
A metal is an assembly of cations (positive) arranged in a lattice structure immersed in a gas of delocalized electrons (negative) which ensure the cohesion of the structure.

A metal is a reservoir of electrons.
Consequences:

- 1) A metal is a good conductor of electricity and heat.
- 2) The electron gas reflects light waves ⇒ optical properties
- 3) A metal is ductile (dislocations easy to displace)
- 4) A metal is oxidizable (easy separation of cations and electrons).

The oxidation of metals (example of a *divalent metal*)

Dry oxidation



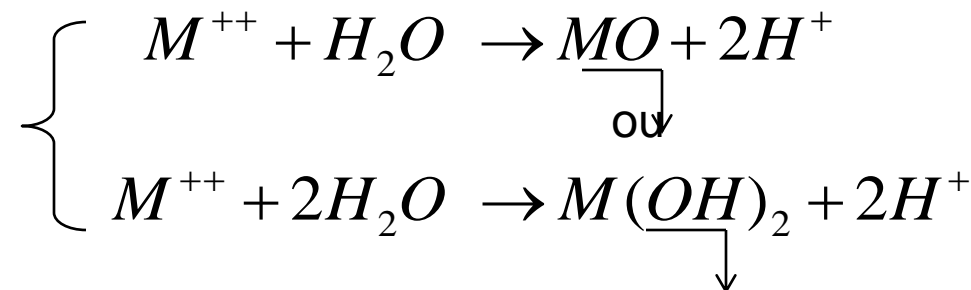
Water passivation



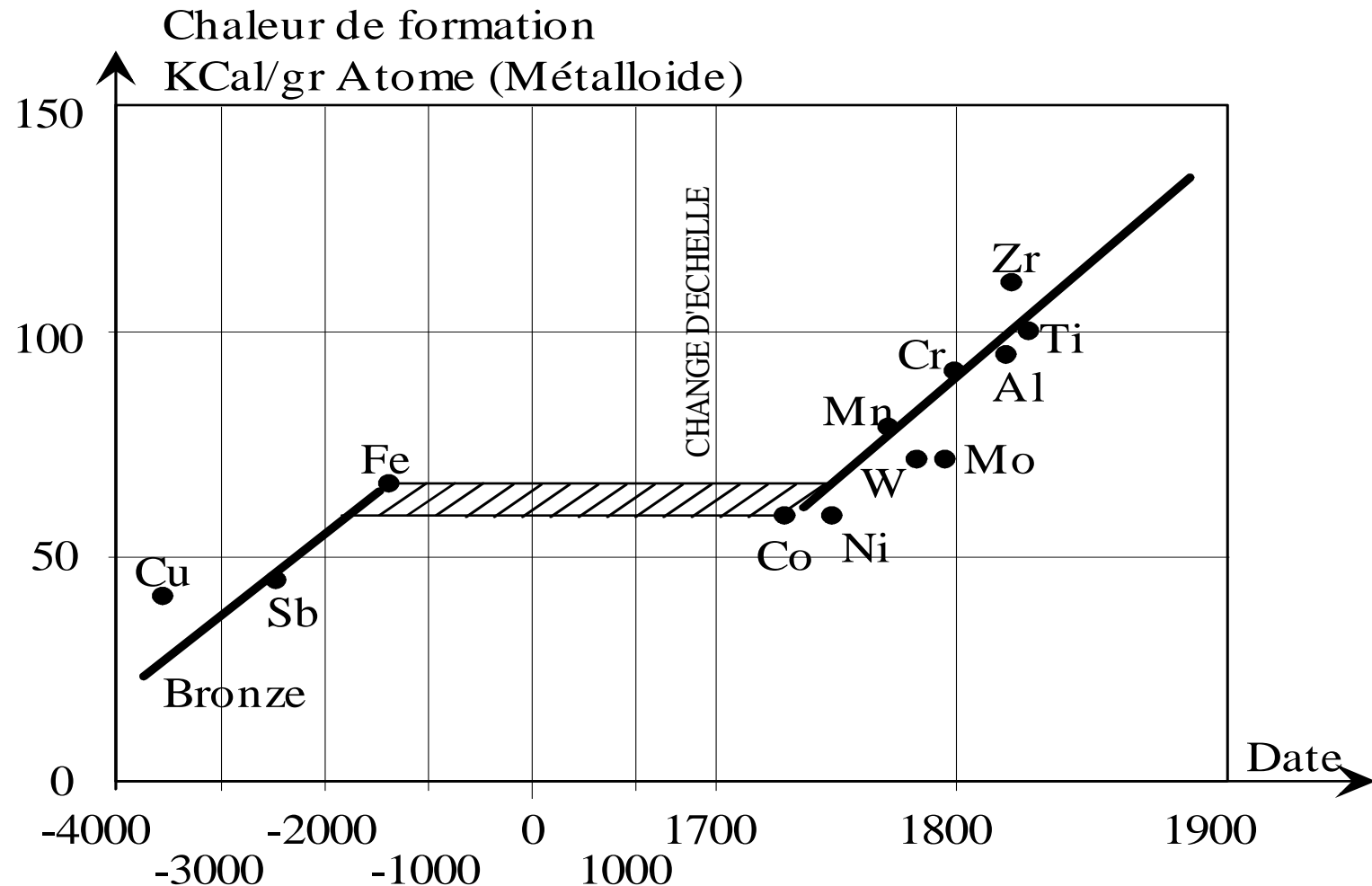
Water dissolution



Precipitation of an oxide
or a hydroxide (rust)



Consequences on the history of metallurgy



Consequences on the Corrosion resistance : The Paradox of passivity

The more oxidisable materials can protect themselves by the formation of their own layer of corrosion in the form of a very thin protective film (called a passive film).

For these materials, the question of corrosion resistance no longer arises in terms of rate of dissolution, but in terms of the stability of the protective oxide.

These materials are described as "stainless", quite simply (but this paradox is only apparent) because their oxidation is fast enough and intense enough to inhibit any subsequent corrosion.

Example: the Corrosion resistance of S.S. results from their Chromium content (more than 12%)

The predominant role of water in Corrosion processes

The oxygen in the iron oxides is drawn essentially from the molecules of water and not at all or only very slightly from the oxygen in the air, as is most often thought (the oxygen only encourages the cathodic reaction as will be explained later).

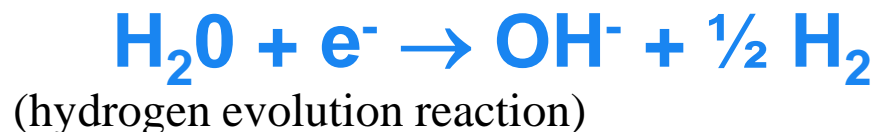
In temperate climates, atmospheric corrosion may be considered a water corrosion phenomenon due to the presence of a film of water on the surface of the metal which generally constitutes a cold surface encouraging the formation of condensation.

Oxydoreduction of water

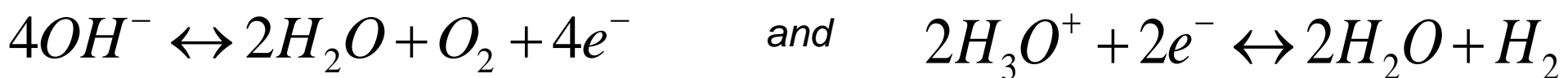
Oxidation:



Reduction:



Other instances of oxido-reductive processes



Etc...

The Bronsted Acidobasicity of Water

Water is a Bronsted amphotер

Bronsted acids*



Bronsted bases*



Acid-base balance



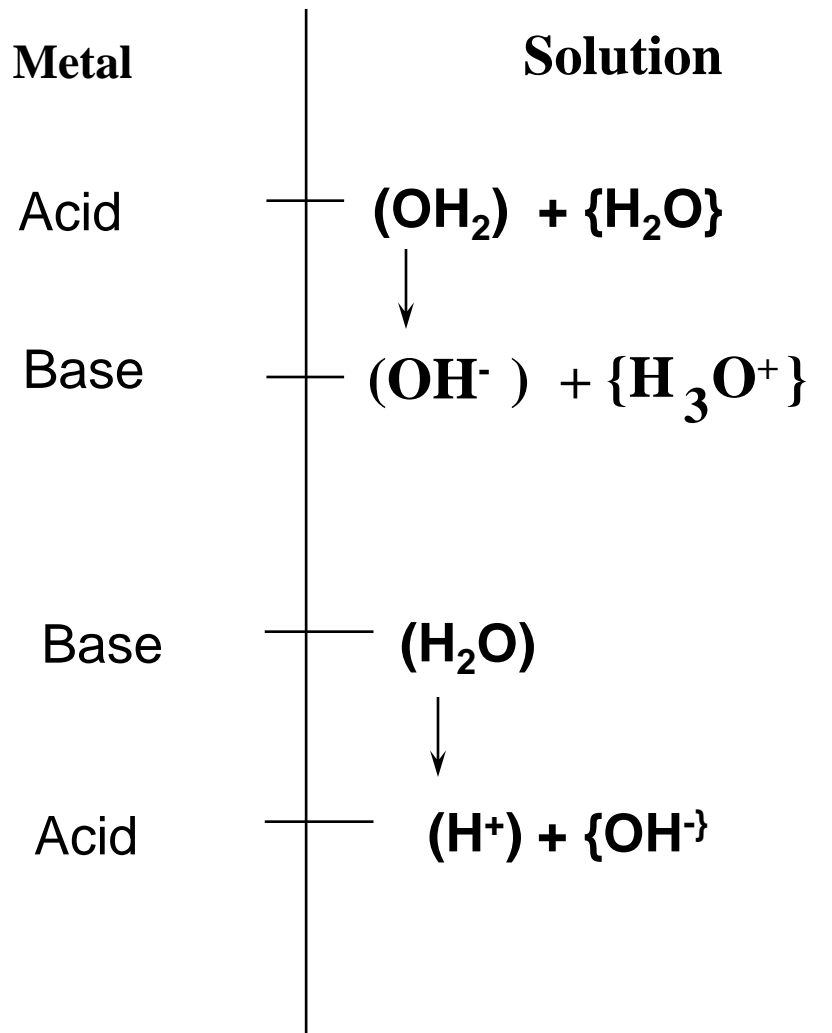
H_3O^+ = hydronium ion
= protonated water
(or hydrated proton)

OH^- = hydroxyl ion
= deprotonated water

(*Conjugated acids and bases are indicated in italics)

Dissociation of water on metal surfaces

(Bronsted acidobasicity)



The consequences of water dissociation:

(1) Adsorbed surface charge

$$\sigma_{\text{ad}} = q[H^+_{\text{ad}} - \text{OH}^-_{\text{ad}}]$$

(2) Potential drop

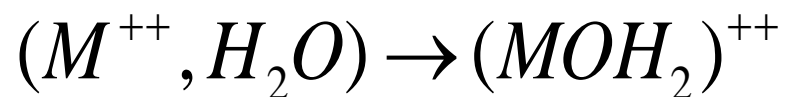
at the metal/electrolyte interface

$$V_H = \sigma_{\text{ad}} / C_H$$

Formation de complexes hydratés

(Acidobasicité de Lewis)

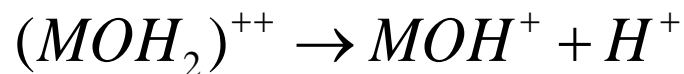
cation solvaté → cation hydraté



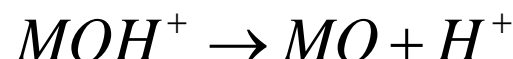
Hydrolyse des complexes hydratés

(Acidobasicité de Bronsted)

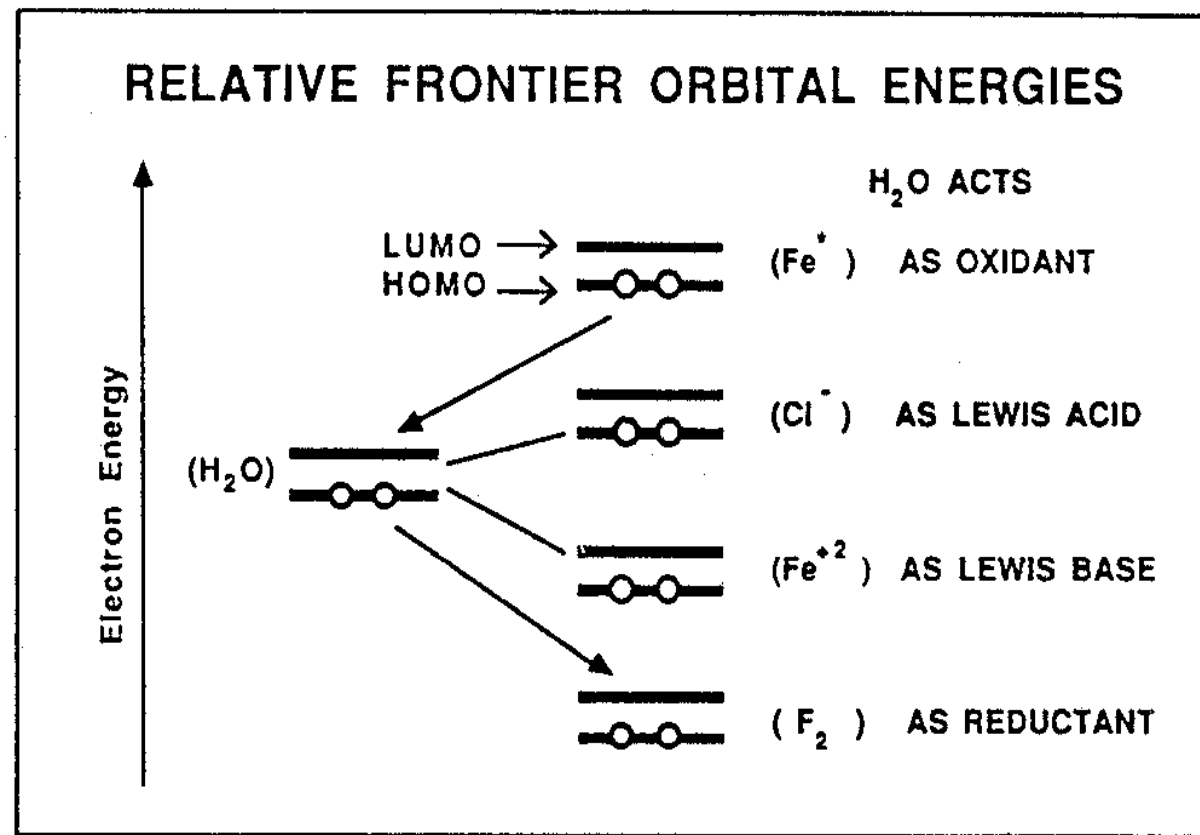
Hydrolyse



Précipitation de l 'oxyde

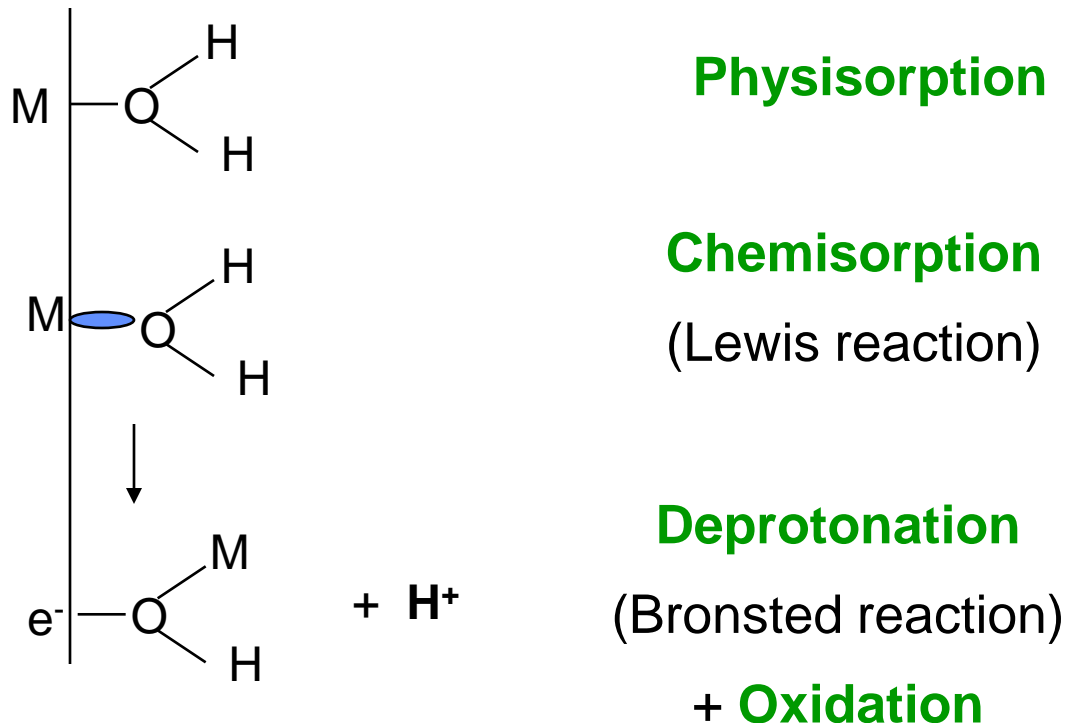


Oxydoreduction and Lewis acidobasicity of water

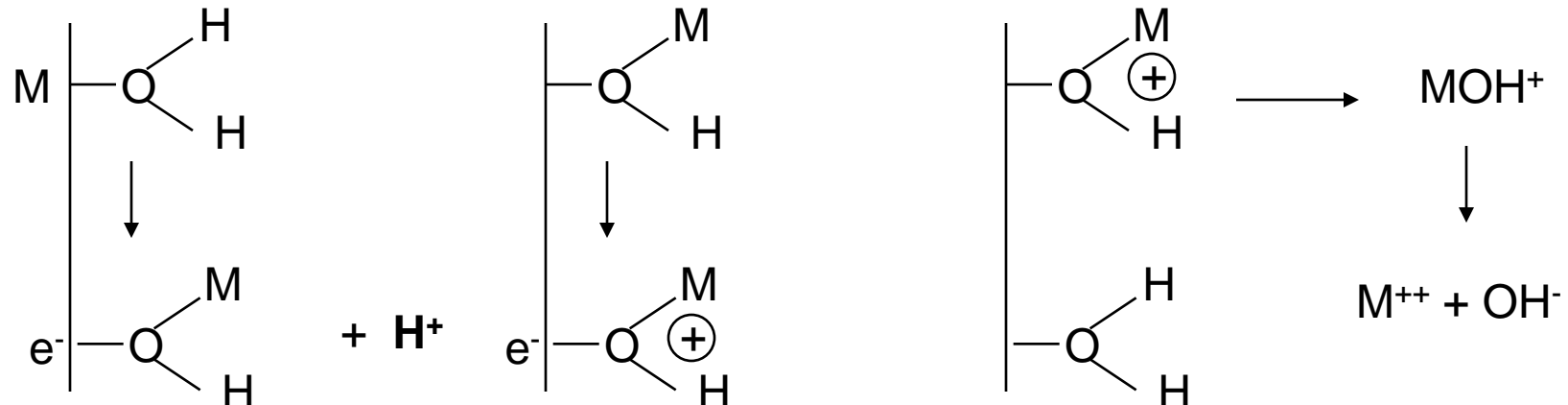


Metal water interactions

The first steps



Water corrosion



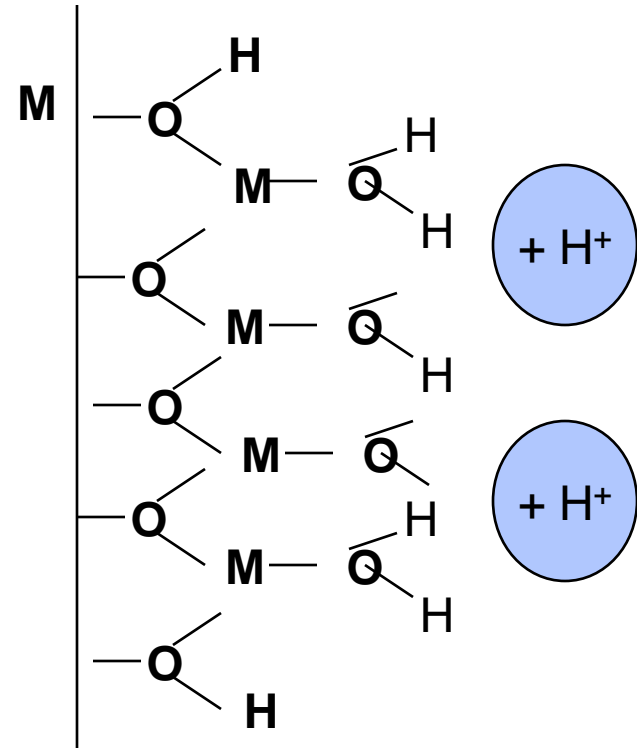
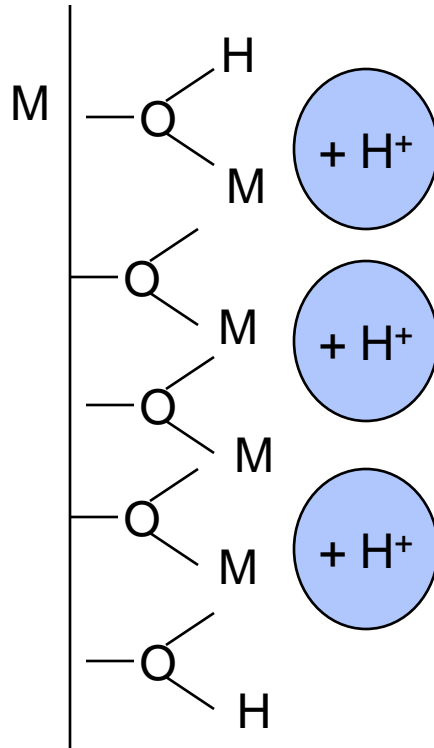
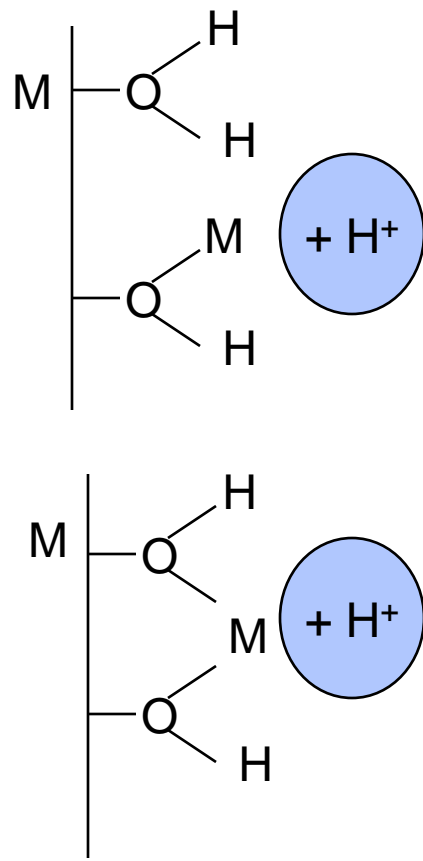
Bockris mechanism for iron dissolution

Oxidation

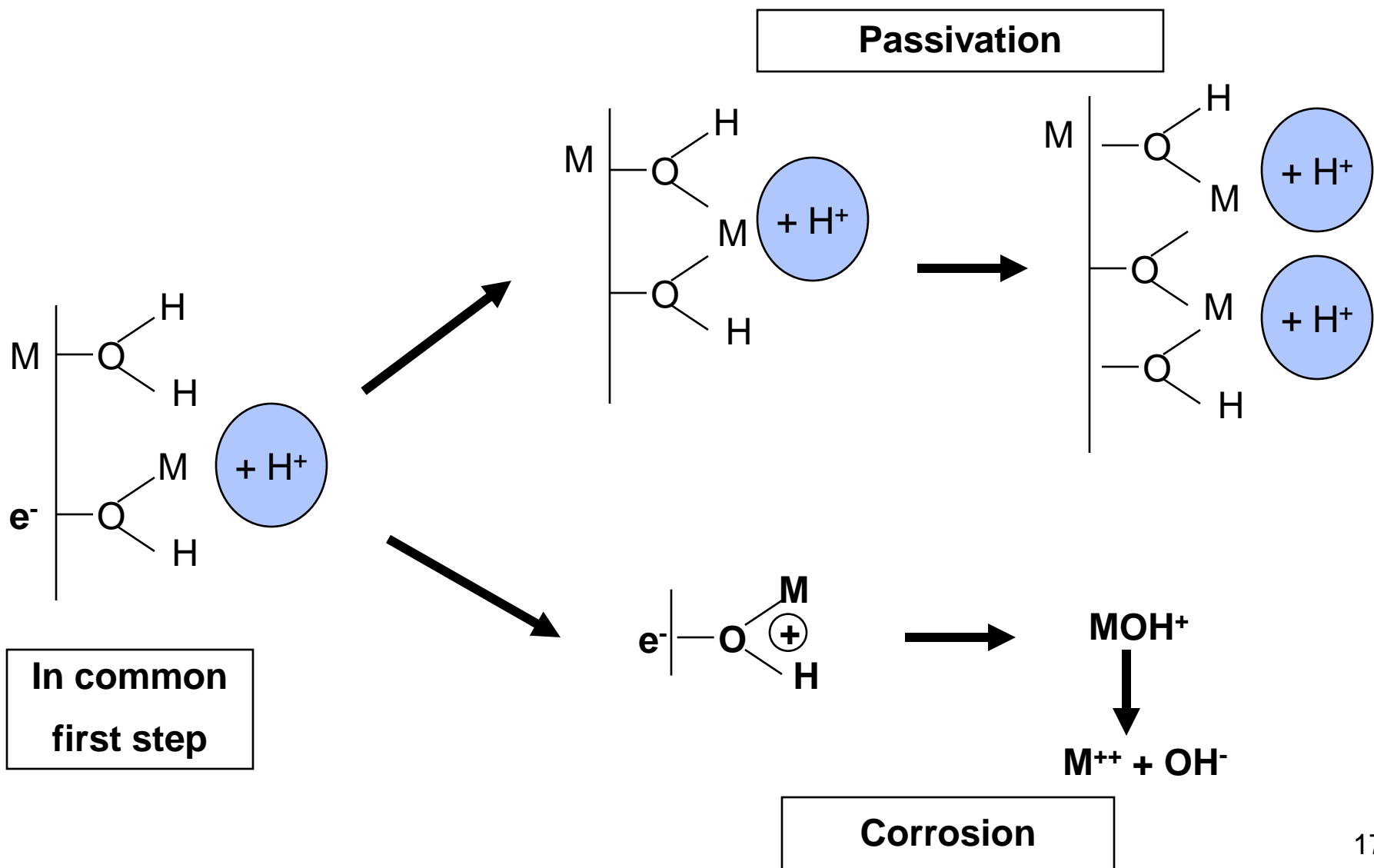
Dissolution

- (1) $\text{Fe(OH}_2\text{)} \rightarrow (\text{FeOH}) + \text{H}^+ + \text{e}^-$
- (2) $(\text{FeOH}) \rightarrow (\text{FeOH}^+) + \text{e}^-$
- (3) $(\text{FeOH}^+) \rightarrow \text{Fe}^{++} + \text{OH}^-$

Water passivation



Competition between water corrosion and passivation processes (summary)



Chloride assisted corrosion process

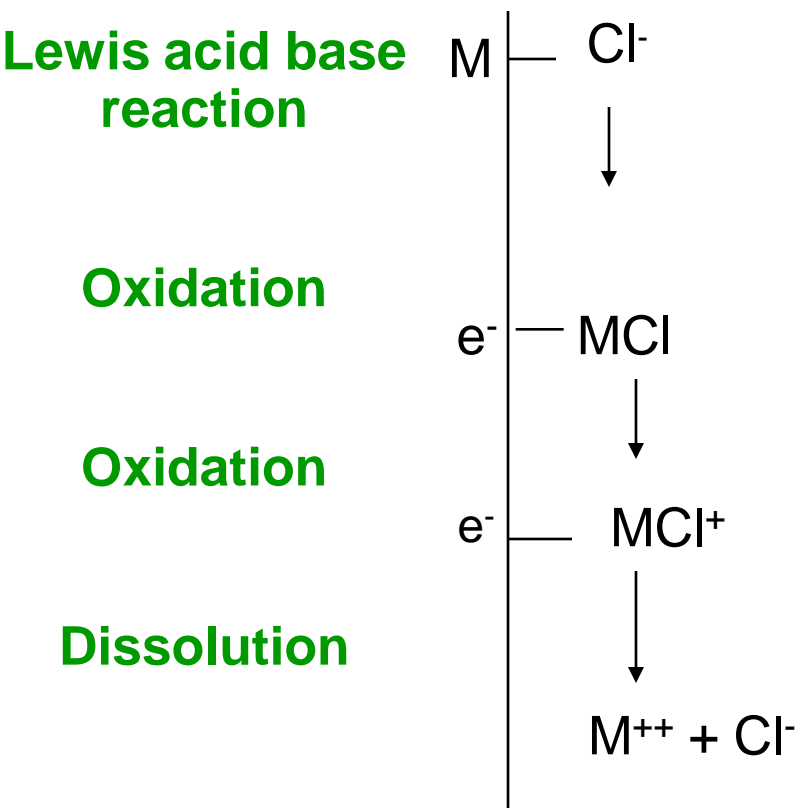
Adsorption of a chloride ion

Lewis acid base reaction

Oxidation

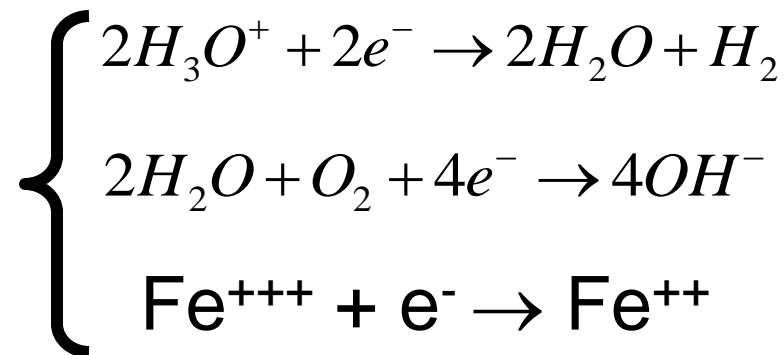
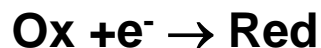
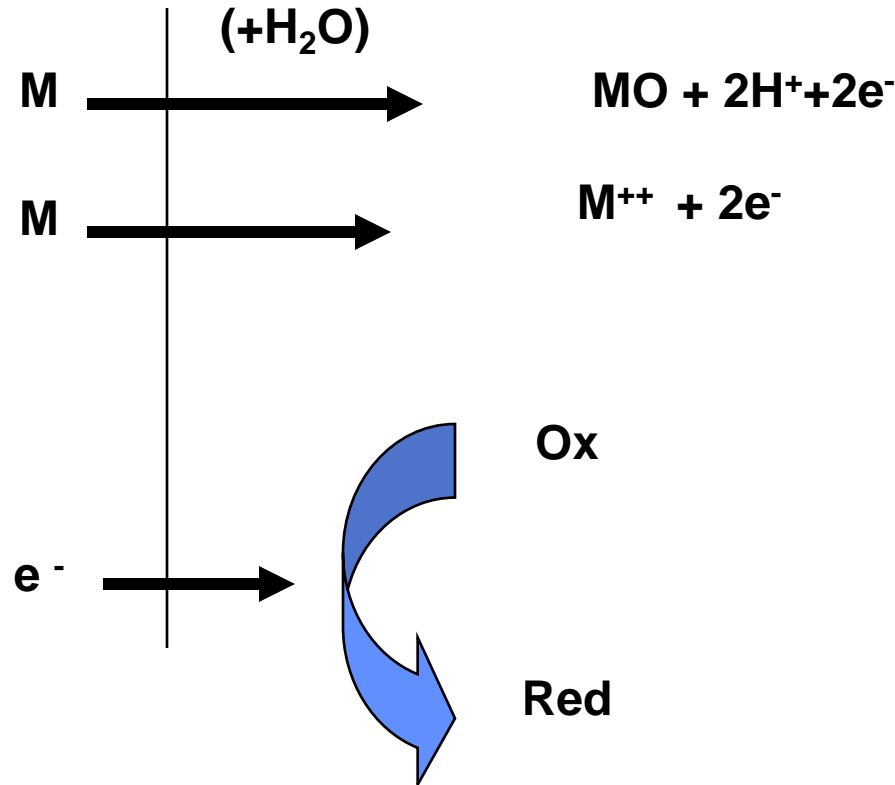
Oxidation

Dissolution

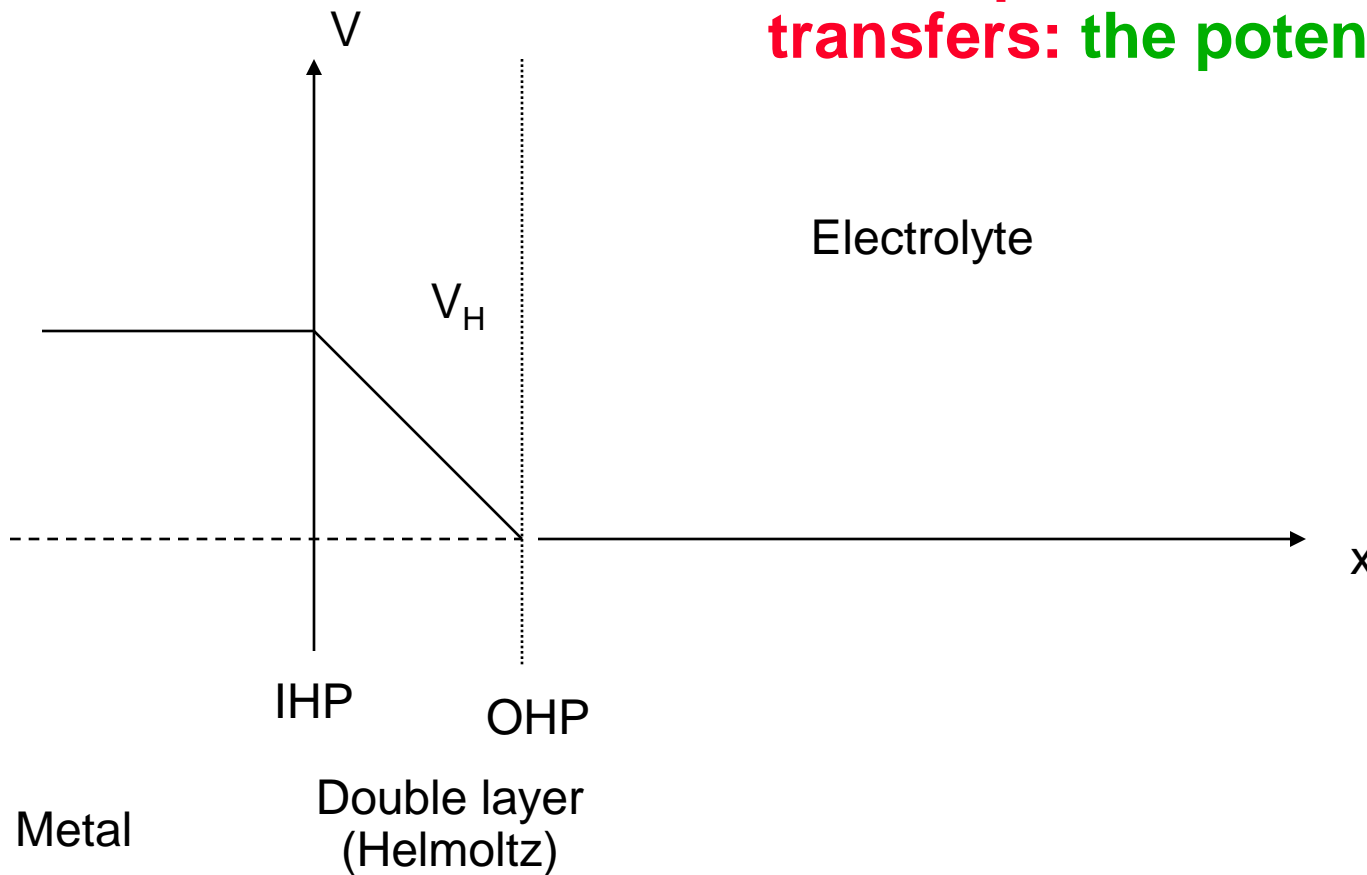


Corrosion outlook:

Anodic
(electron producing)
and cathodic
(electron consuming)
reactions



Consequence of the charge transfers: the potential drop

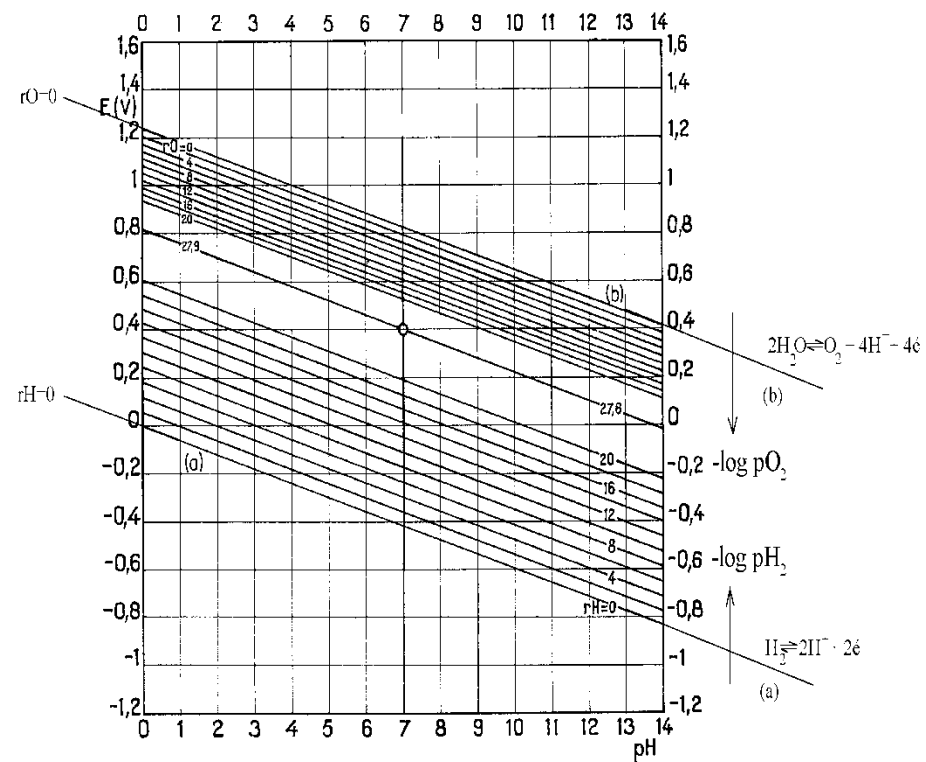


The Charge transfers (electrons and ions) between the metal and the aqueous solution produces a potential difference

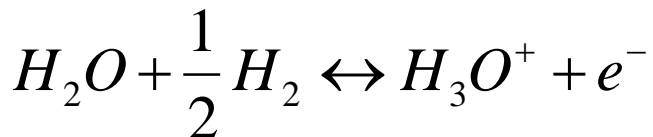
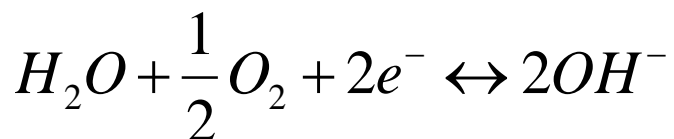
Effect of the potential drop on the electrochemical equilibria of water

V is the potential difference between water and the electron reservoir,

The Standard hydrogen electrode ($V=0$) is defined by $pH=0$ and $p(H_2)=1\text{ Atm}$



Electrochemical equilibria



Law of mass action

$$\begin{aligned} V &= 1.23^{\text{Volts}} + \frac{kT}{q} (\ln(H^+) + \frac{1}{4} \ln(pO_2)) \\ &= 1.23^{\text{Volts}} - 60^{\text{mV}} (pH - \frac{1}{4} \log(pO_2)) \end{aligned}$$

$$V = \frac{kT}{q} (\ln(H^+) - \ln \sqrt{pH_2}) = -60^{\text{mV}} (pH + \log \sqrt{pH_2})$$

Corrosion equilibria

At a metal electrode, several potential and pH dependent reactions occur

(1) Anodic dissolution:



(2) Dissolution or Precipitation of the oxide



(3) Passivation



Assuming local equilibria, the mass action law writes

$$V = cst. + 2.3 \frac{kT}{2q} \log(c)$$

$$pH + \frac{1}{2} \log(c) = cst.$$

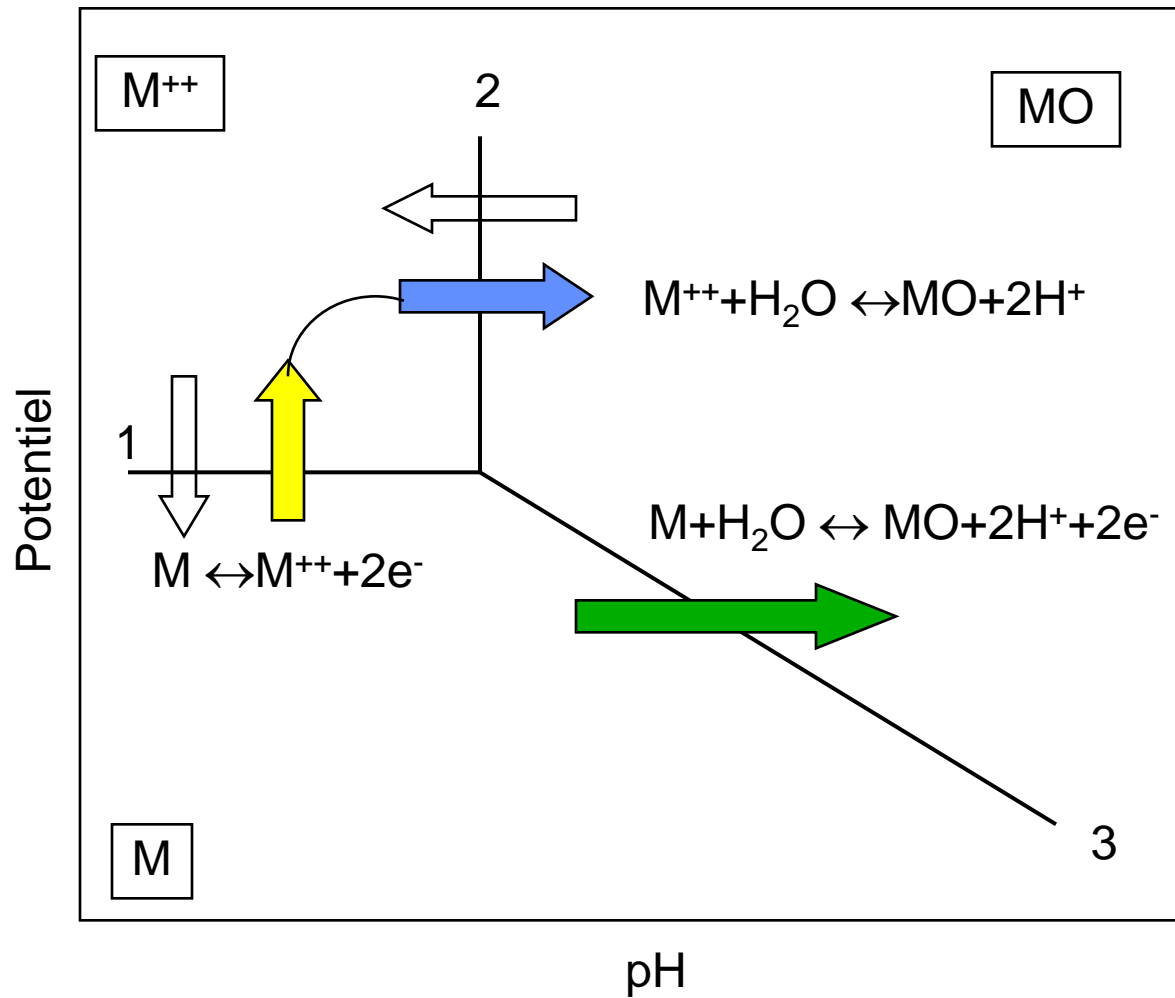
$$V + 2.3 \frac{kT}{q} pH = cst.$$

Where **c** is the concentration in dissolved cations near the metal interface.

C results from the balance between the dissolution rate and the diffusion flow **J** □ **c** from the metal surface to the solution bulk (where **c=0**)

The dissolution rate is then proportionnal to **c**

The Pourbaix diagrams of metals



$$c = [M^{++}]$$

$$(1) V = cst. + 2.3 \frac{kT}{2q} \log(c)$$

$$(2) pH + \frac{1}{2} \log(c) = cst.$$

$$(3) V + 2.3 \frac{kT}{q} pH = cst.$$

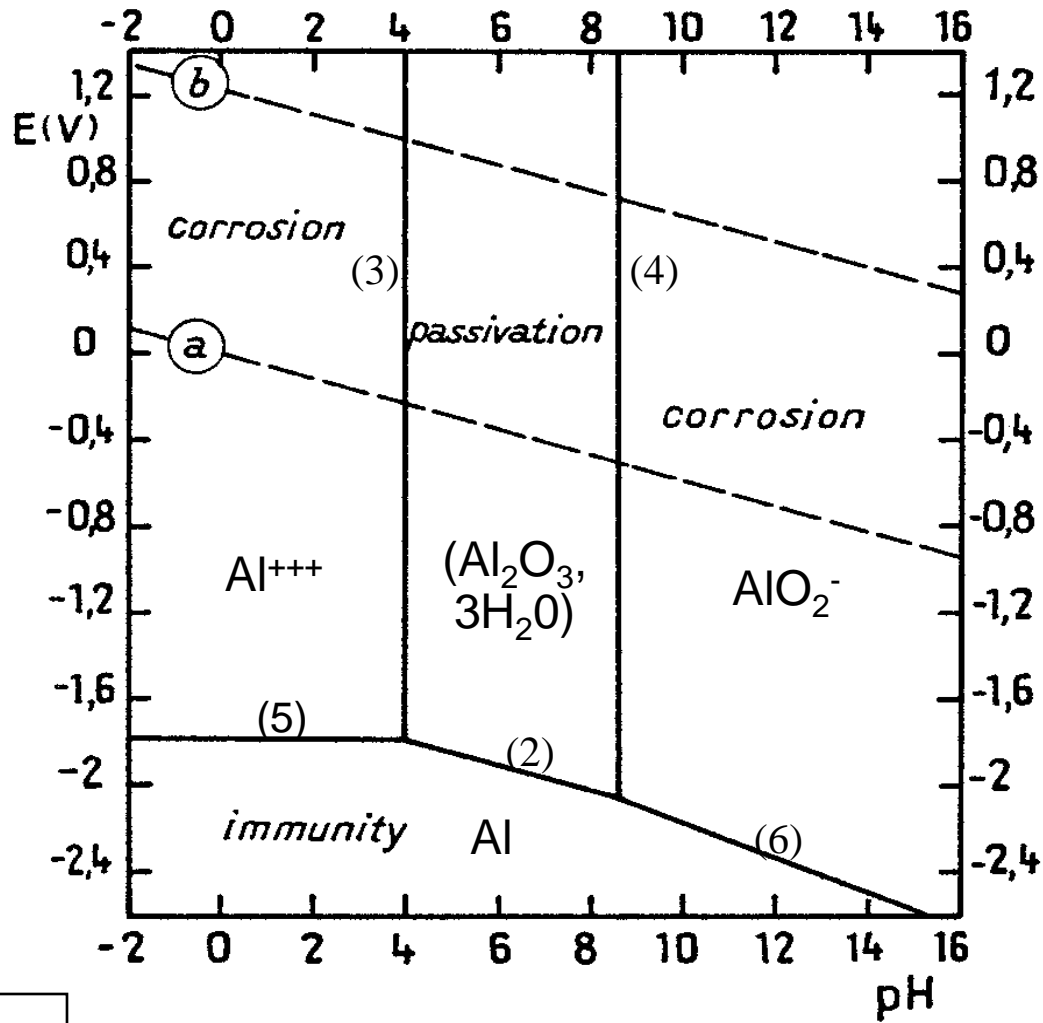
$M \rightarrow M^{++}$: anodic dissolution

$M \rightarrow MO$: passivation

$M^{++} \rightarrow MO$: rust precipitation

In diffusion controlled kinetics, the corrosion current j is proportionnal to the concentration c in solute cations near the surface. An arbitrary concentration $c = 10^{-6} M$ is chosen, below which corrosion is disregarded

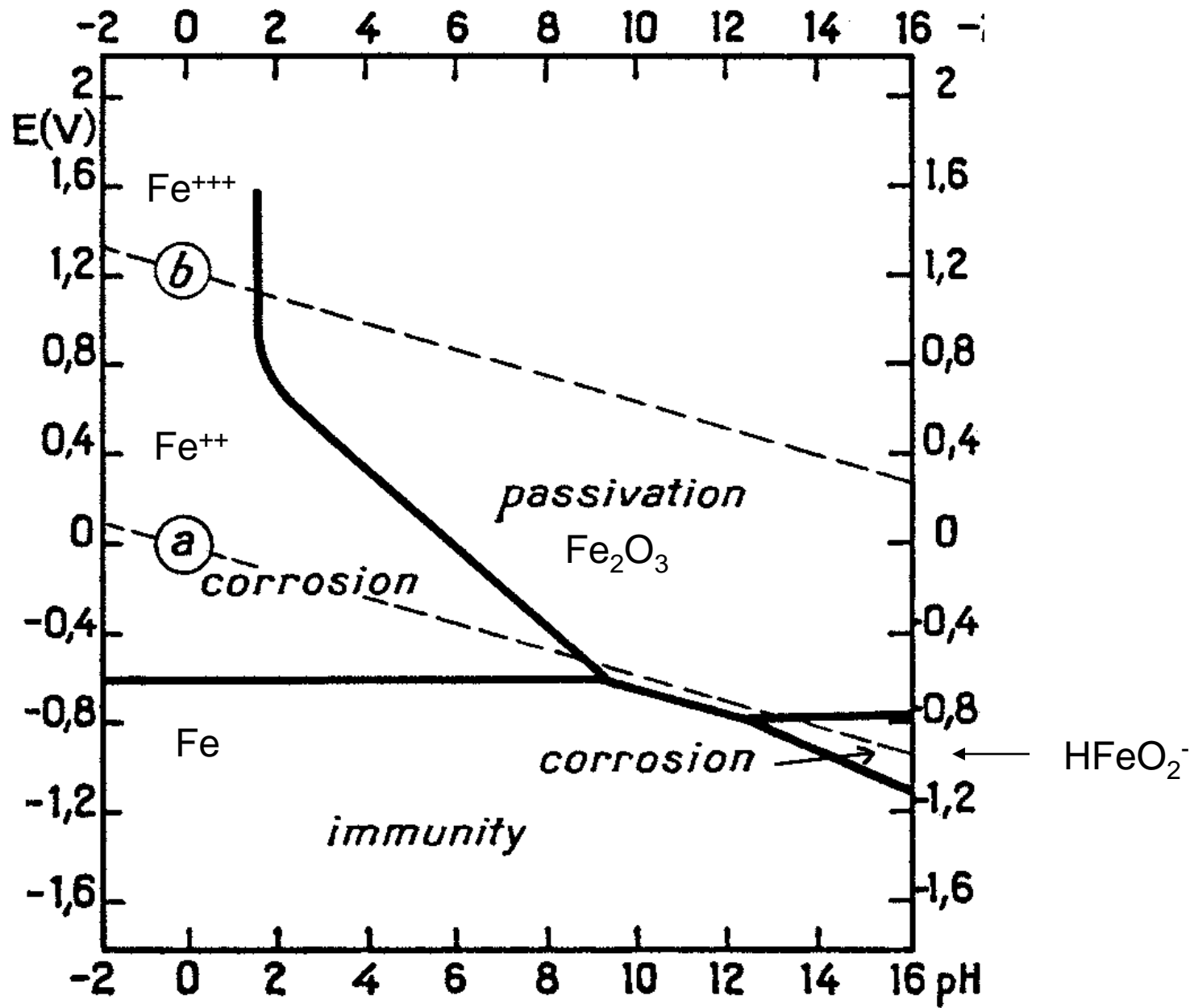
Pourbaix diagram of Aluminium



- (1) $\text{Al}^{+++} + 2 \text{H}_2\text{O} \leftrightarrow \text{AlO}_2^- + 4 \text{H}^+$
- (2) $\text{Al} + 3 \text{H}_2\text{O} \leftrightarrow \text{Al}_2\text{O}_3 + 6 \text{H}^+ + 6 \text{e}^-$
- (3) $2\text{Al}^{+++} + 3 \text{H}_2\text{O} \leftrightarrow \text{Al}_2\text{O}_3 + 6 \text{H}^+$
- (4) $\text{Al}_2\text{O}_3 + \text{H}_2\text{O} \leftrightarrow 2\text{AlO}_2^- + 2 \text{H}^+$
- (5) $\text{Al} \leftrightarrow \text{Al}^{+++} + 3 \text{e}^-$
- (6) $\text{Al} + 2 \text{H}_2\text{O} \leftrightarrow \text{AlO}_2^- + 4 \text{H}^+ + 3 \text{e}^-$

NB: this diagram is drawn for 1 $\mu\text{M/l}$
concentrations in solute species

Pourbaix diagram of Iron



Effect of the potential drop on the Corrosion kinetics.

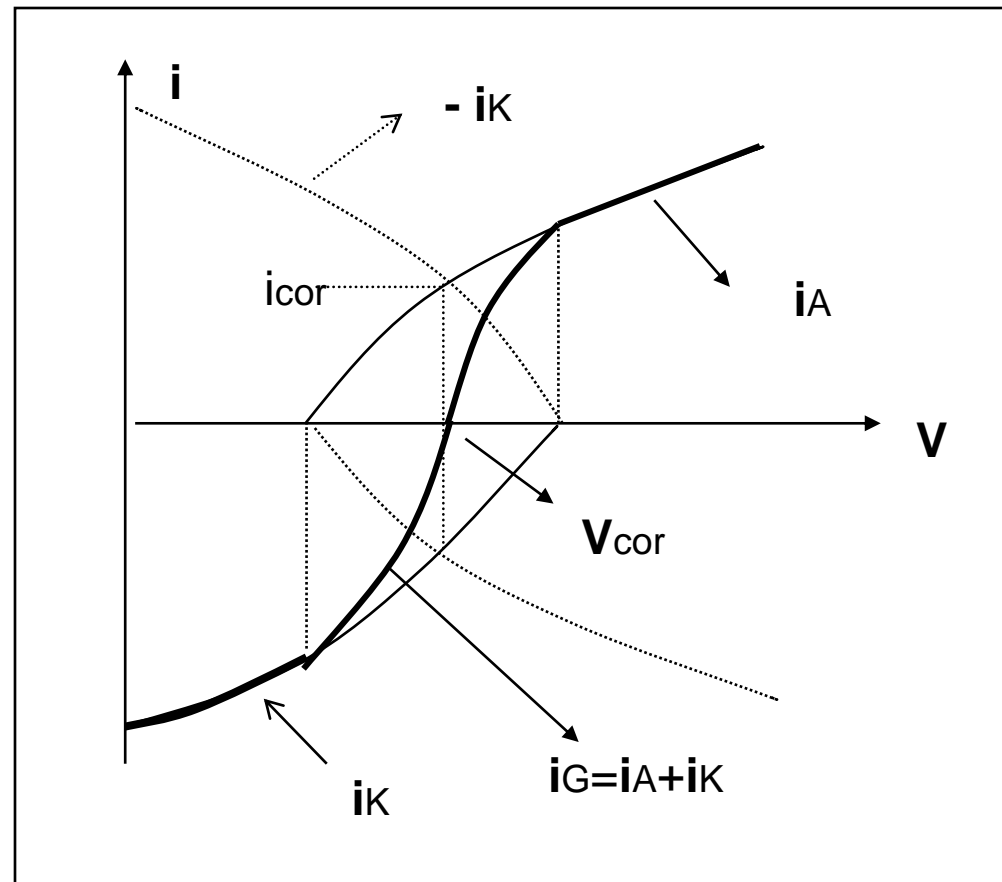
Polarisation curves:

Both anodic and cathodic currents depend on the potential difference

V = Electrode potential

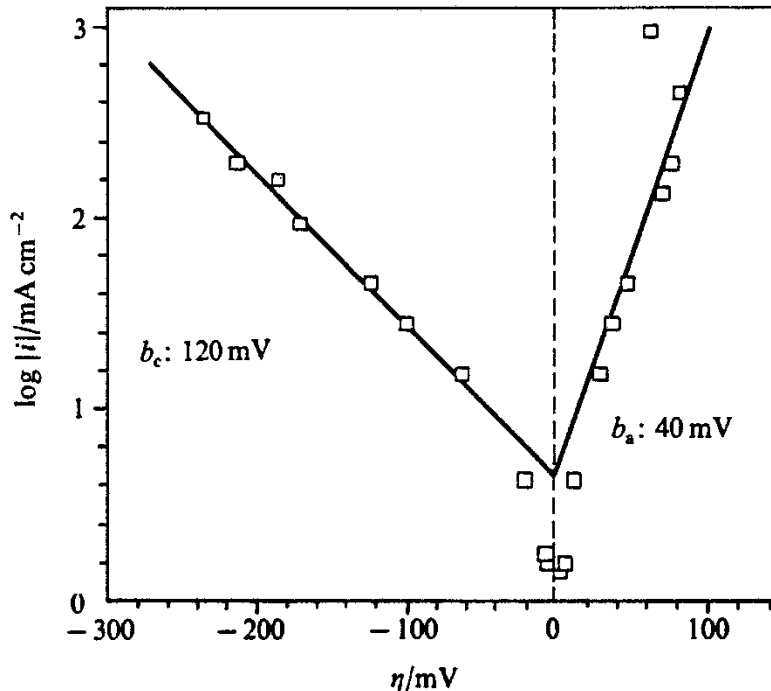
V_{cor} = Corrosion potential

I = Current density



The Tafel law

CU in $\text{H}_2\text{SO}_4(0.5\text{M}) + \text{CuSO}_4(0.075\text{M})$



The Tafel law:

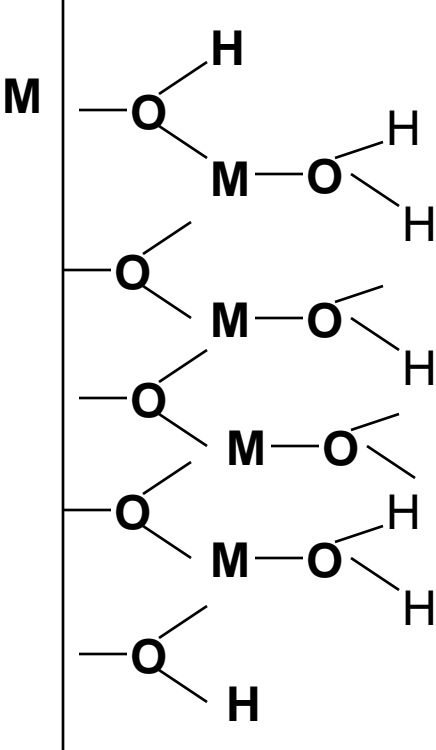
$$V = \text{cst} + b \log i$$

$$I = B \cdot \exp(2.3 V / b)$$

In the cathodic domain: Proton reduction
In the anodic domain: Anodic dissolution

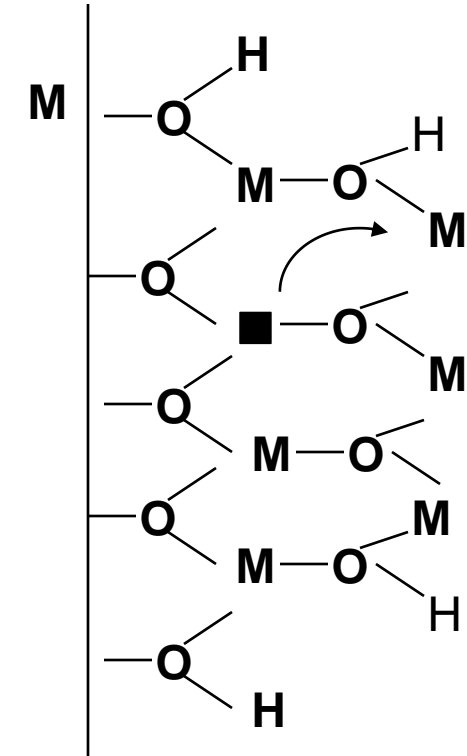
Part II) Passive films

From passive layer to passive film:
ion hopping and water deprotonation



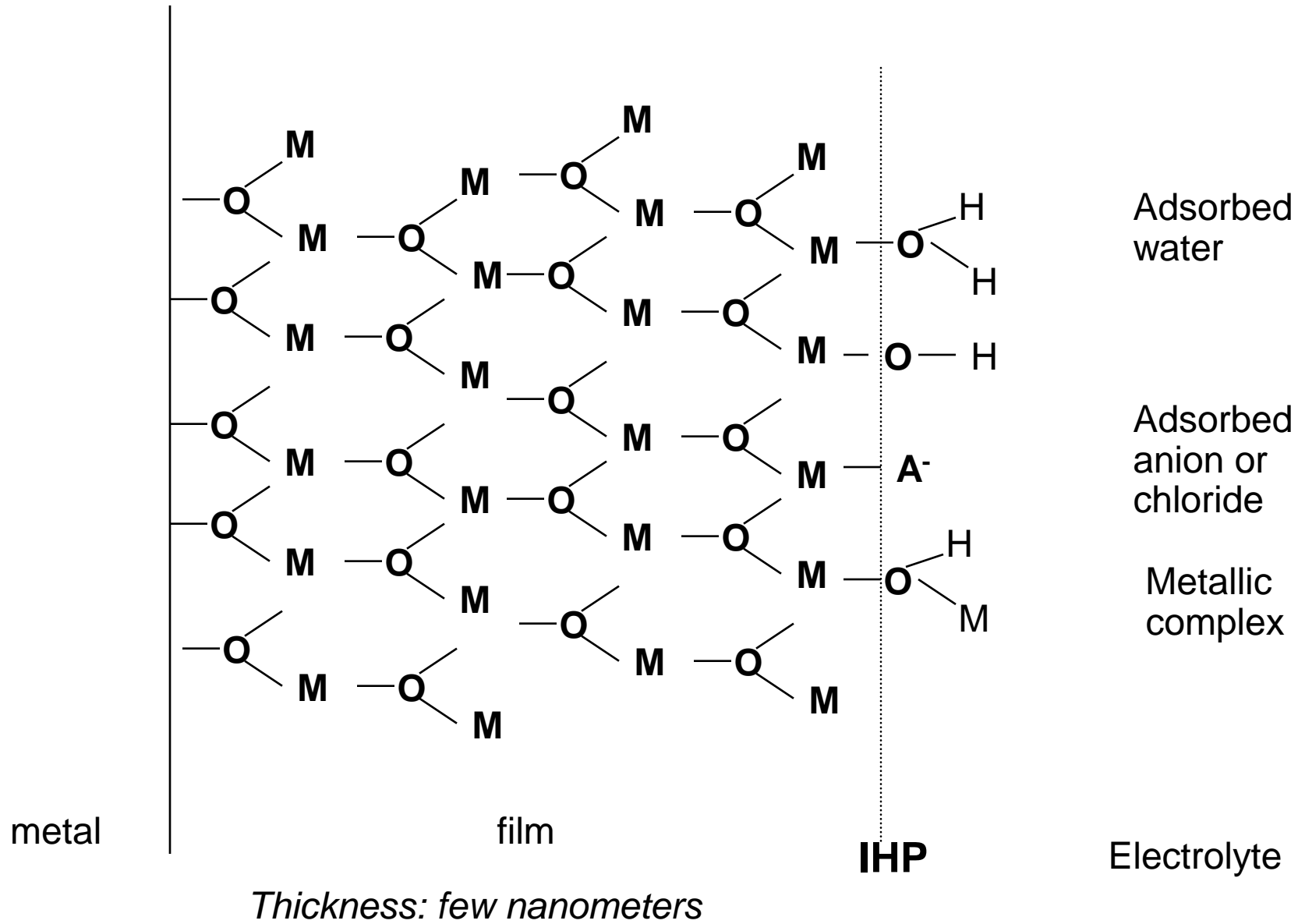
(a) First (hydrated)
oxide layer

- (a) Formation of the first oxide monolayer
- (b) Cation hopping and formation of a second layer.
- (c) Vacancy ■ migrates toward the metal
- (d) The process is repeated (Passive Film growth)

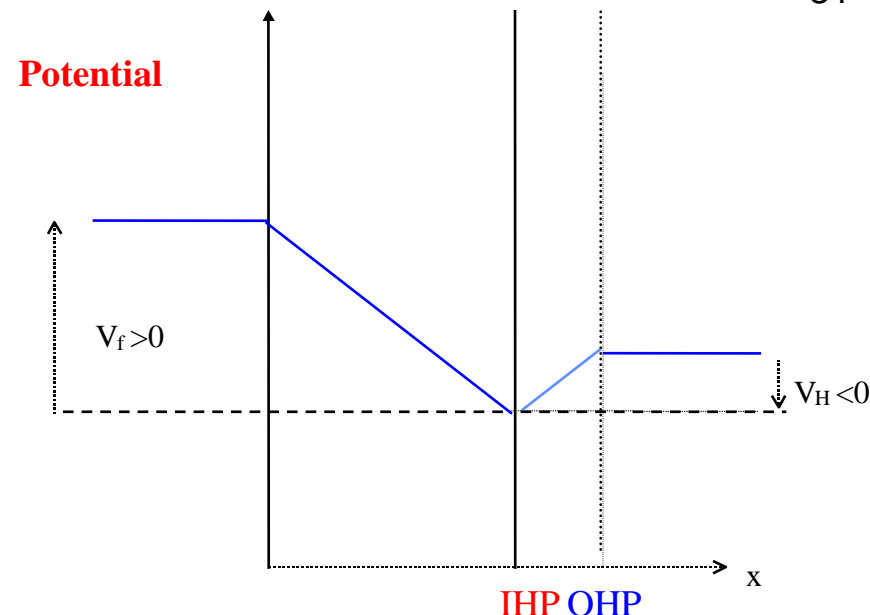
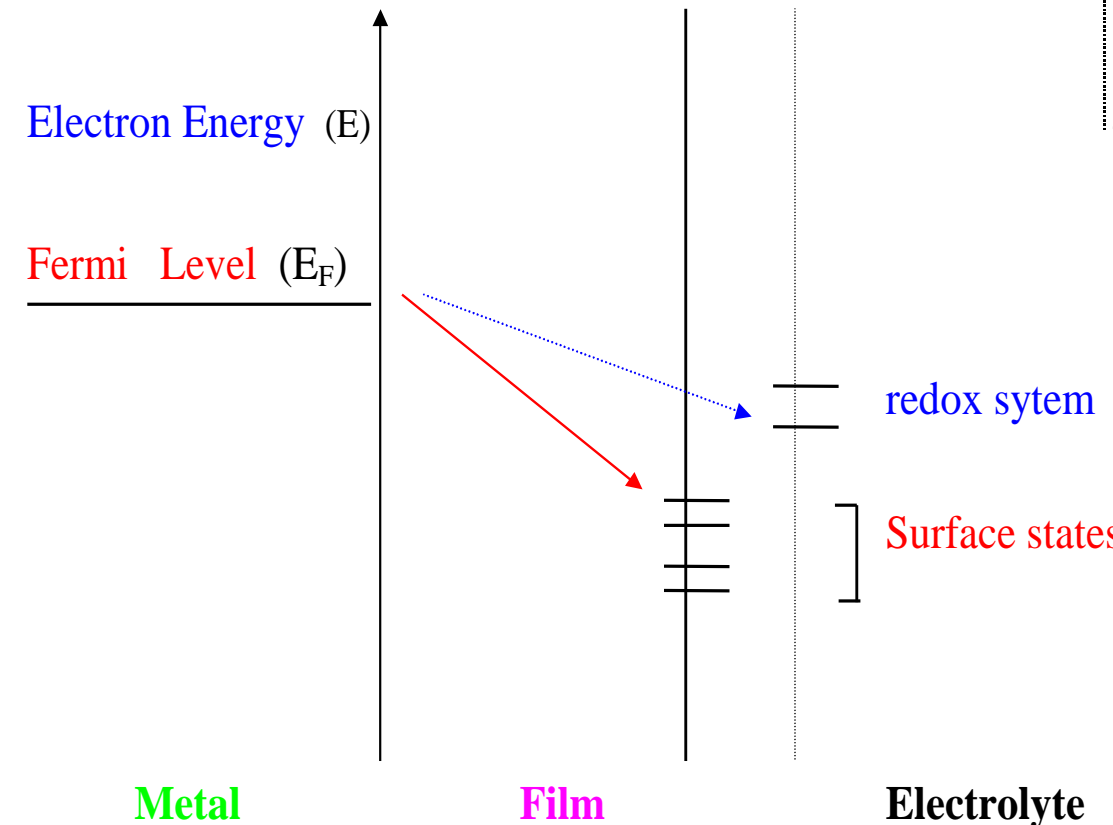


(b) ion hopping and
film growth

(over)simplified model of passive film



The Electric field



$L \sim 30 \text{ \AA}^\circ \text{ (example)}$
 $F \sim 10^6 \text{ V/cm} = 10 \text{ mV/\AA}$

Electron transfer from metal to electrolyte redox system (e.g. $\text{Fe}^{+++}/\text{Fe}^{++}$) or on metallic complexes (MOH^+ type) located at IHP

Density: $F = \sigma_{ss}/\epsilon \sim 10^6 \text{ V/cm} \Leftrightarrow \sigma_{ss}/q \sim 10^{14} \text{ cm}^{-2}$

Effect of the electric field

- **Ionic conduction**
 - The electric field drives the positively charged species (cations, anionic vacancies...) toward the outer interface, and the negatively charged species (anions, cationic vacancies ...) toward the inner interface
- **Electrostriction**
 - Strong electric field produce a so called electrostriction force, perpendicularly to the field, This force is normally equilibrated by the cohesion forces in the oxide. A decrease in these cohesion forces may therefore produce local breakdown of the passive film (Sato)

Défauts ponctuels

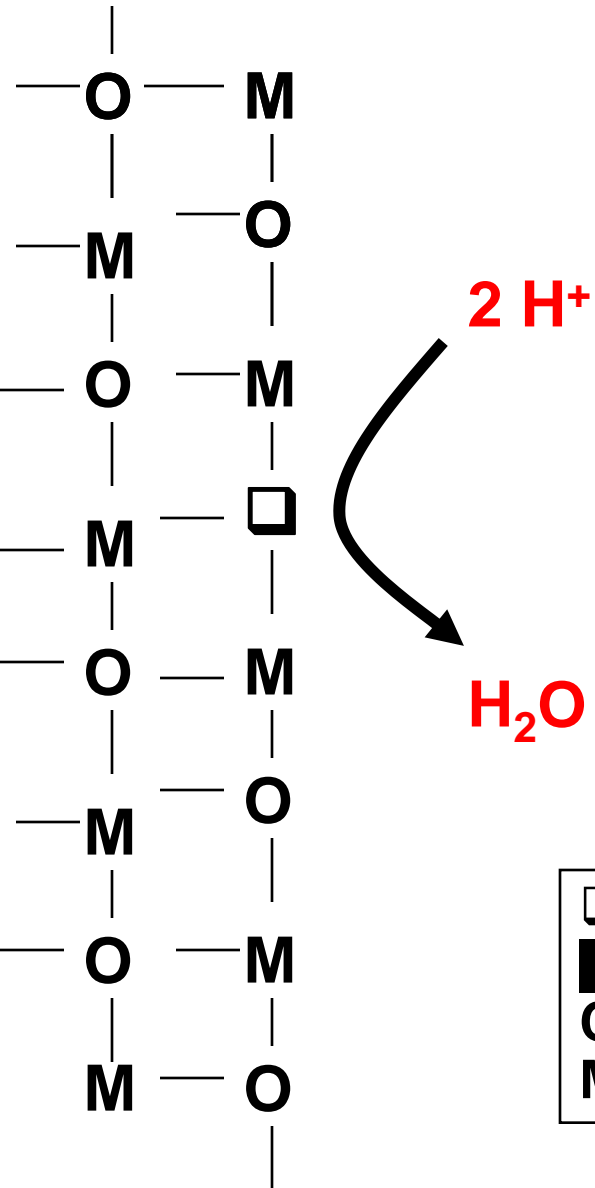
Pour les films passifs minces, on considère généralement que la densité en défauts ponctuels (ions en excès et lacunes) est très faible:

$$\rho \ll 1/L^3 \sim 10^{20} \text{ cm}^{-3} \text{ (pour } L \sim 2\text{nm})$$

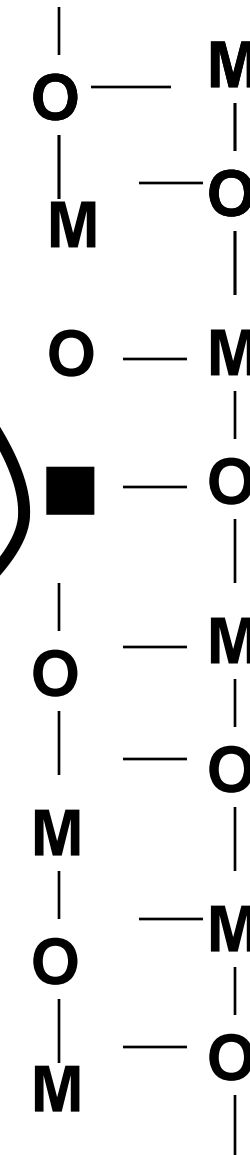
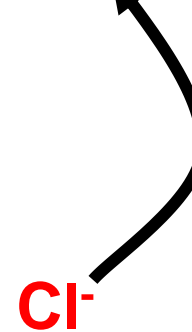
Les défauts ponctuels sont chargés et agissent comme pièges électroniques

Suivant leur charge, ils migrent vers le métal ou l'interface externe qui peuvent constituer des sources ou des puits de défauts.

Acidic attack



Cation Vacancies Injection

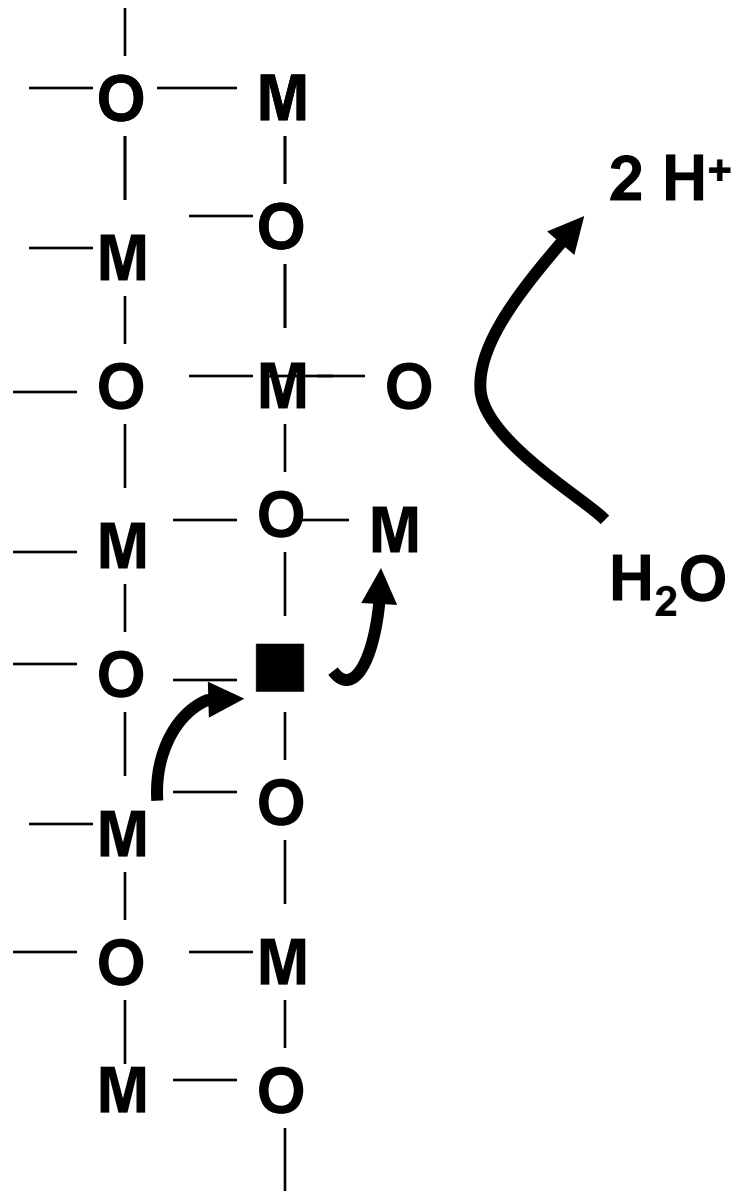


Point defects produced by corrosion

- \square = oxygen vacancy
- \blacksquare = cation vacancy
- Cl^- = anion
- MCl^+ = unstable complex

Cation vacancies migrate toward the metal film interface where they annihilate

Oxygen deposition



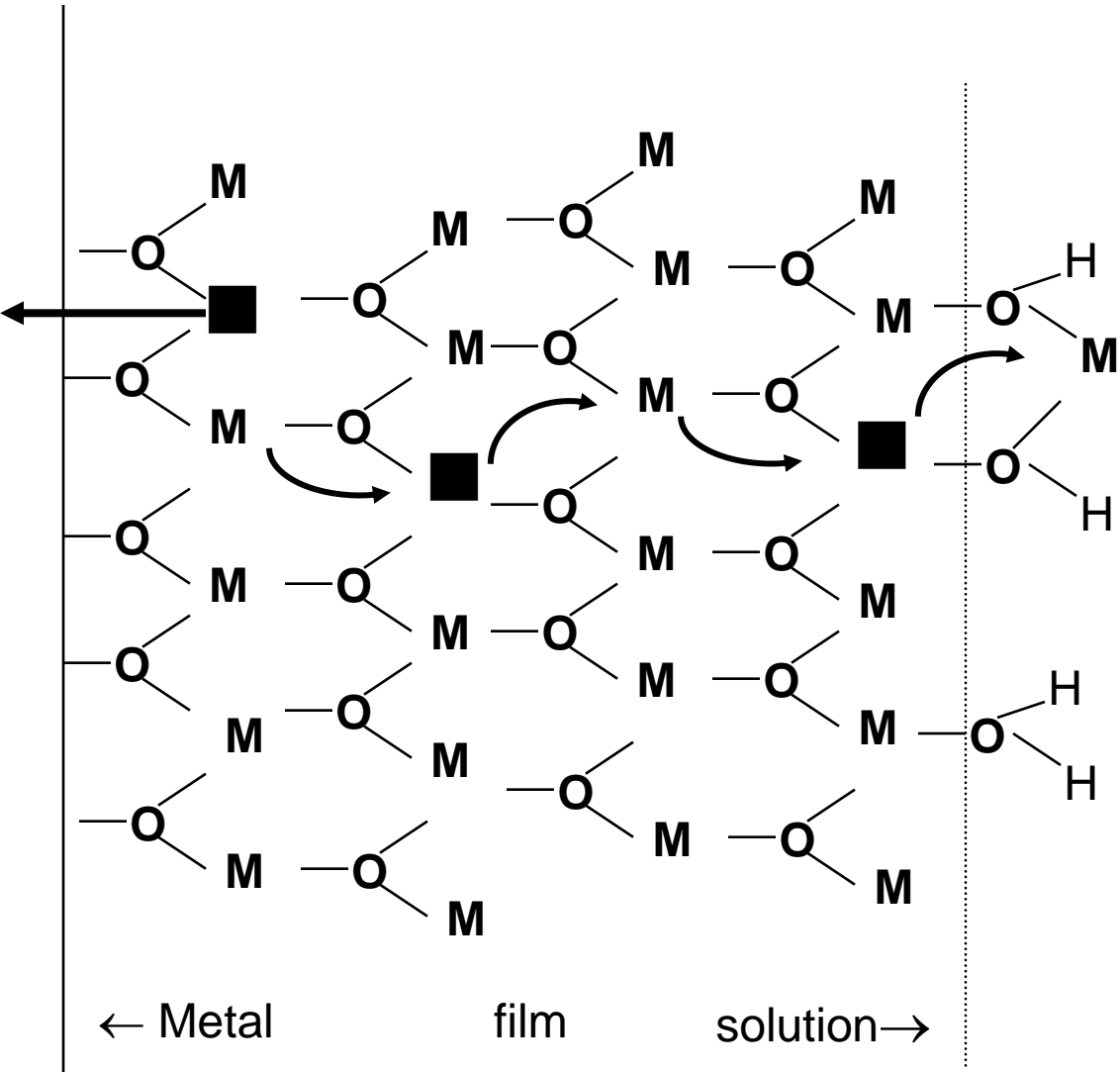
**Water deprotonation produces
Oxygen anions excess**

Cation hopping \Rightarrow film growth

Growth kinetics is controlled by the cation migration rate from the mf interface (\Leftrightarrow vacancies migration to the mf interface)

**Cation vacancies produced
by the film growth**

Croissance des films (details)



- Un cation est transféré du film vers le film hydraté d'extrême surface où il prend la place d'un proton qui est rejeté en solution
- Le processus global se résume à une déprotonation de l'eau et à une injection de lacunes cationiques dans le film
- Sous l'effet du champ électrique les lacunes cationiques créées sont drainées par le champ électrique vers l'interface métal-film où elles s' anihilent

Capacité de croissance

La Croissance du film implique le transfert d'une charge par unité de surface:

$$dQ = \frac{Zq}{\delta^3} dL$$

où δ^3 est le volume cationique moyen et $v = \frac{Zq}{\delta^3} \sim 18 \text{ Cb/mm}^3$ dans le cas de ZrO_2

Et engendre une augmentation dV de chute de potentiel $V=F.L$ à travers le film:

$$dV = F dL + L dF.$$

if $dF \sim 0$ then $F = dV/dL = v / C$

$C=v/F$ est la capacité de croissance

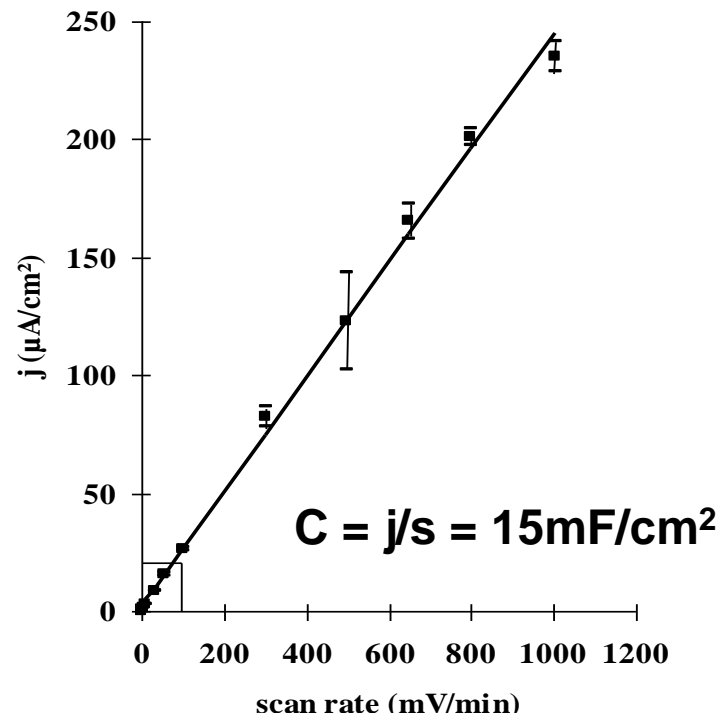
$$C = 15 \text{ mF/cm}^2$$

pour $F = 1.2 \cdot 10^6 \text{ V/cm}$ ($1/F \sim 8 \text{ nm/V}$)

L'augmentation de potentiel d'électrode est entièrement absorbée par la croissance du film

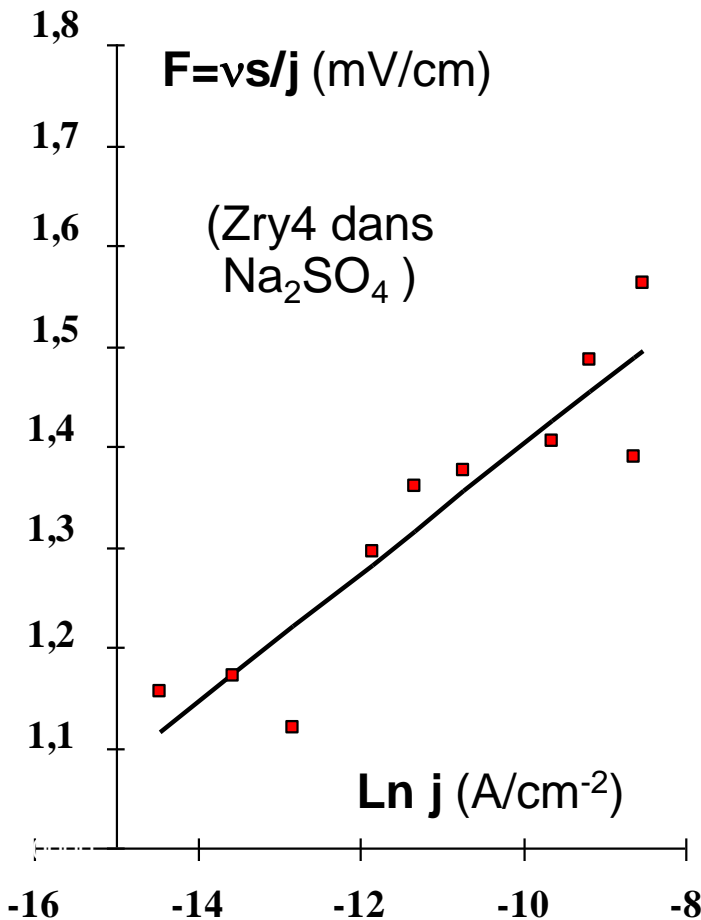
Zry4 poli 4000 dans Na_2SO_4 1M pH 6.6 23°C désaéré. Tracé de courbes de polarisation à plusieurs vitesses de balayage s. Le courant mesuré est sensiblement constant dans le domaine passif. j est sa valeur pour $V = 1 \text{ V/SCE}$.

la Capacité $C = j/s = j dt/dV = dQ/dV$ est sensiblement constante et proche d'une capacité de croissance.



Loi du Champ fort

(mise en évidence expérimentale)



Une analyse plus fine des résultats précédents montre que $C=j/s$ et donc aussi $F = vs/j$ ne sont pas rigoureusement constants et varient linéairement avec $\ln j$:

$$F = vs/j = F^* \cdot \ln(j/j^*)$$

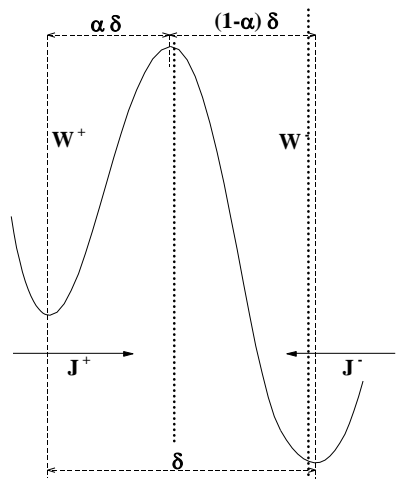
Avec $F^* = 9 \cdot 10^4 \text{ V/cm}$

$$j^* = 0,7 \cdot 10^{-9} \text{ A/cm}^2$$

D'où la loi dite du Champ fort :

$$j = j^* \exp \frac{F}{F^*}$$

Loi du Champ fort: justification théorique



Transport thermiquement activé:

$$J^+ = K_0 \exp -W^+/kT$$

Effet du Champ électrique:

$$W^+ = W_0 - ZqF\alpha\delta$$

$$\Rightarrow J = K(\exp ZqF\alpha\delta/kT - \exp -ZqF(1-\alpha)\delta/kT)$$

$$\alpha=0,5 \Rightarrow$$

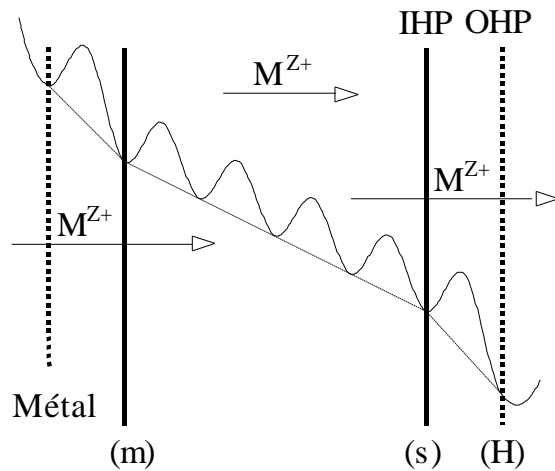
$$J = 2KF^* \sinh \frac{F}{F^*}$$

Où $2K$ est la conductivité et $F^* = \frac{kT}{Z\alpha q\delta}$

pour $Z\alpha=2$ et $\delta \sim 1$ nm) on trouve:

$$F^* \sim 10^5 V/cm$$

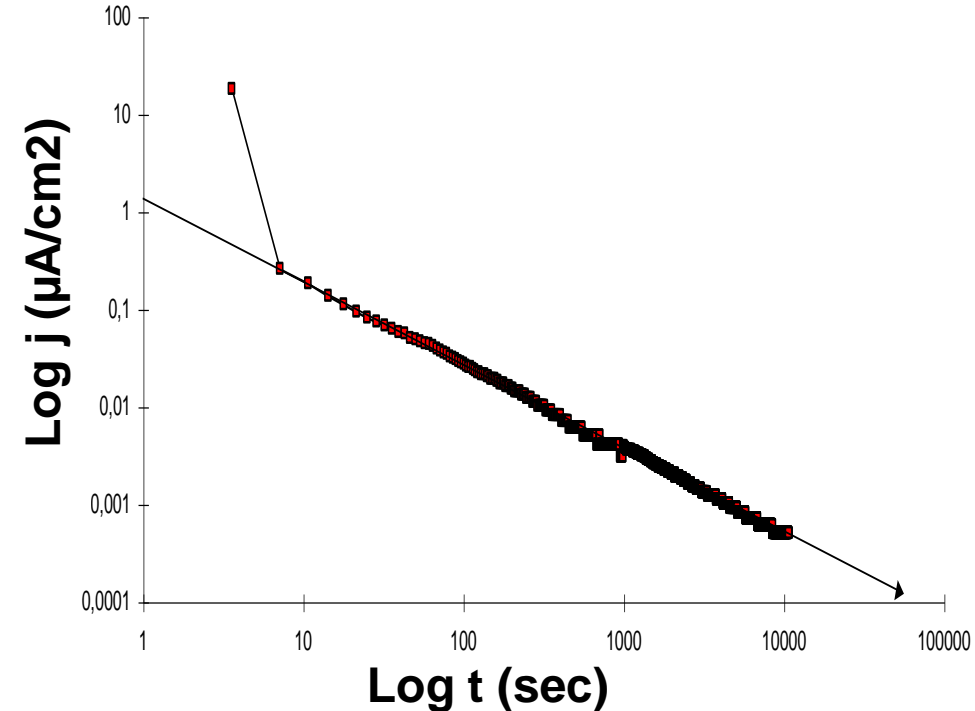
Loi d'Ohm: $F \ll F^* \Rightarrow J = 2K.F$



Loi du Champ Fort :

$$F \gg F^* \Rightarrow J = K \cdot \exp \frac{F}{F^*}$$

Loi de croissance en mode potentiostatique (Loi Logarithmique Directe)



Chronoampèremétrie potentiostatique

Réalisée sur Zry4 poli 4000 polarisé à 1 V/SCE dans Na_2SO_4 1M pH 6.6 23°C désaéré.

$$m = d(\ln j)/d(\ln t) \rightarrow -1 \text{ quand } t \rightarrow \infty$$

Approximation au premier ordre

$$\begin{aligned} LF &= L_0 F_0 = V_f = \text{cst.} \Rightarrow L dF + F dL = 0 \\ \Rightarrow F_0(L - L_0) + L_0(F - F_0) &= 0 \\ \Rightarrow F/F_0 &= 2 - L/L_0 \end{aligned}$$

$dL/dt = \text{cst.} \exp F/F^* \Rightarrow$
 $L - L_0 = a \cdot \ln(1+t/\tau)$

(Où a et τ sont des constantes vis-à-vis du temps, mais dépendent de V_f)

$$j = v \cdot dL/dt = va/(1+t/\tau) \Rightarrow$$

Loi de Mott:

$$\frac{1}{j} \approx \frac{1}{j_0} \left(1 + \frac{t}{\tau}\right)$$

Compléments

Loi logarithmique inverse

(Approximation au second ordre)

L'approximation au premier ordre pour le champ donne

$$F_0 - F = b \cdot \ln(1 + t/\tau)$$

En reportant cette valeur dans l'équation

$$1/L = F / V_f$$

on obtient une approximation au second ordre pour L:

$$1/L = 1/L_0 - b \cdot \ln(1 + t/\tau)$$

Epaisseur limite

En mode potentiostatique stationnaire

$$J = K_{fs} \exp \frac{F}{F^*} = \frac{1}{\delta^3} \cdot \frac{dL}{dt} + J_{dis}(V_H)$$

$$\Rightarrow L = \uparrow(t)$$

$$\text{Une épaisseur limite} \quad \bar{L} = \frac{V_f}{\bar{F}}$$

est atteinte lorsque $F = \bar{F} = F^* \ln \frac{J_{dis}}{K_{fs}}$

$$\frac{d \bar{L}}{dV_f} = \frac{1}{\bar{F}} \quad \sim 10^{-6} \text{ cm/V} = 1 \text{ \AA}/10 \text{ mV}$$

Loi de croissance

loin de l'épaisseur limite:

$$\frac{dL}{dt} \approx \delta^3 \cdot K_{fs} \exp \frac{F}{F^*} = \delta^3 \cdot K_{fs} \exp \frac{V_f}{LF^*}$$

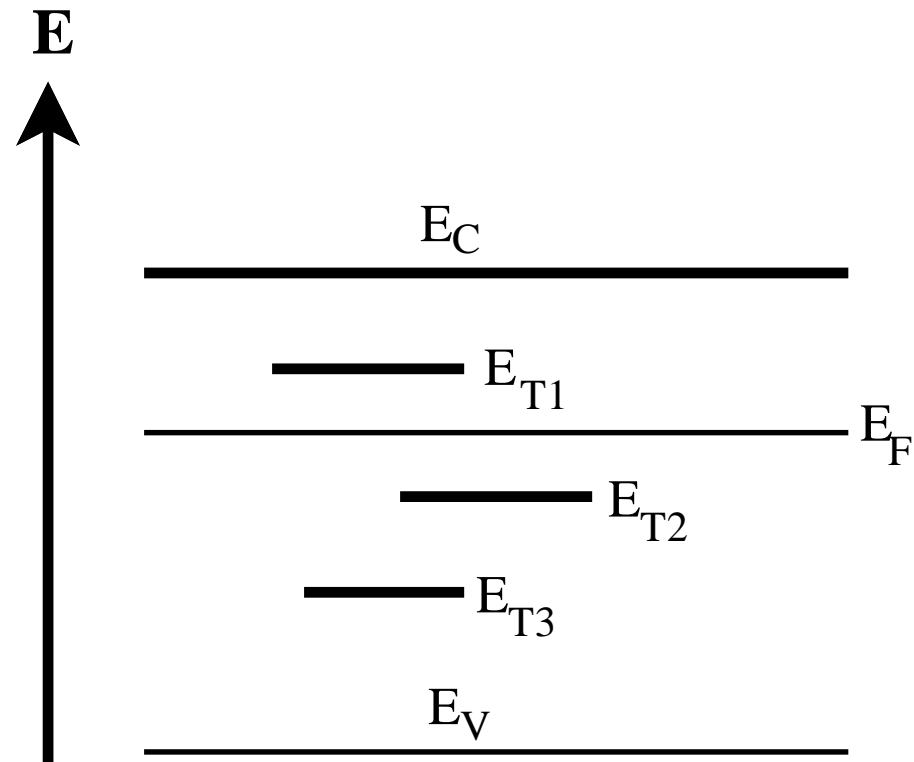
Les électrons dans le film

L'hypothèse $\sigma_f=0$ (film non chargé) est totalement arbitraire

Le film passif est susceptible de contenir des charges ioniques et des charges électroniques ($\Rightarrow \sigma_f \neq 0$)

Les Charges ioniques sont constituées par les défauts fonctionnels (ions et lacunes) dues à la croissance, à la corrosion , aux défauts de structure, etc...

Les charges électroniques résultent du piégeage des électrons sur des niveaux accepteurs, ou à leur dépêgeage à partir de niveaux donneurs, en équilibre avec le niveau de Fermi du métal et les niveaux de valence et de conduction de l'oxyde (comportement semi-conducteur)



- Niveau de conduction (E_c)
- Niveau de valence (E_v)
- Niveaux pièges (E_T)
- Niveau de Fermi (E_F)

Loi d'action de masse et loi de Fermi Dirac

à l'approximation semi classique

Soit $N(E)$ le nombre d ' « états » électroniques à l 'énergie E

Chaque « état » électronique peut être vide (oxydé) ou occupé (réduit)

. **Red \leftrightarrow Ox + e⁻ (metal)**

Un niveau peut être accepteur (neutre si vide, négatif si occupé) ou donneur (neutre si occupé, positif si vide)

On notera n le nombre d'états occupés et $N-n$ = nombre d'états vides.
La loi d'action de masse s'écrit:

$$n \cdot \exp -E/kT = \text{cst.} (N-n) \cdot \exp -E_F/kT$$

La probabilité d 'occupation n/N
d 'un état est donc donnée par:

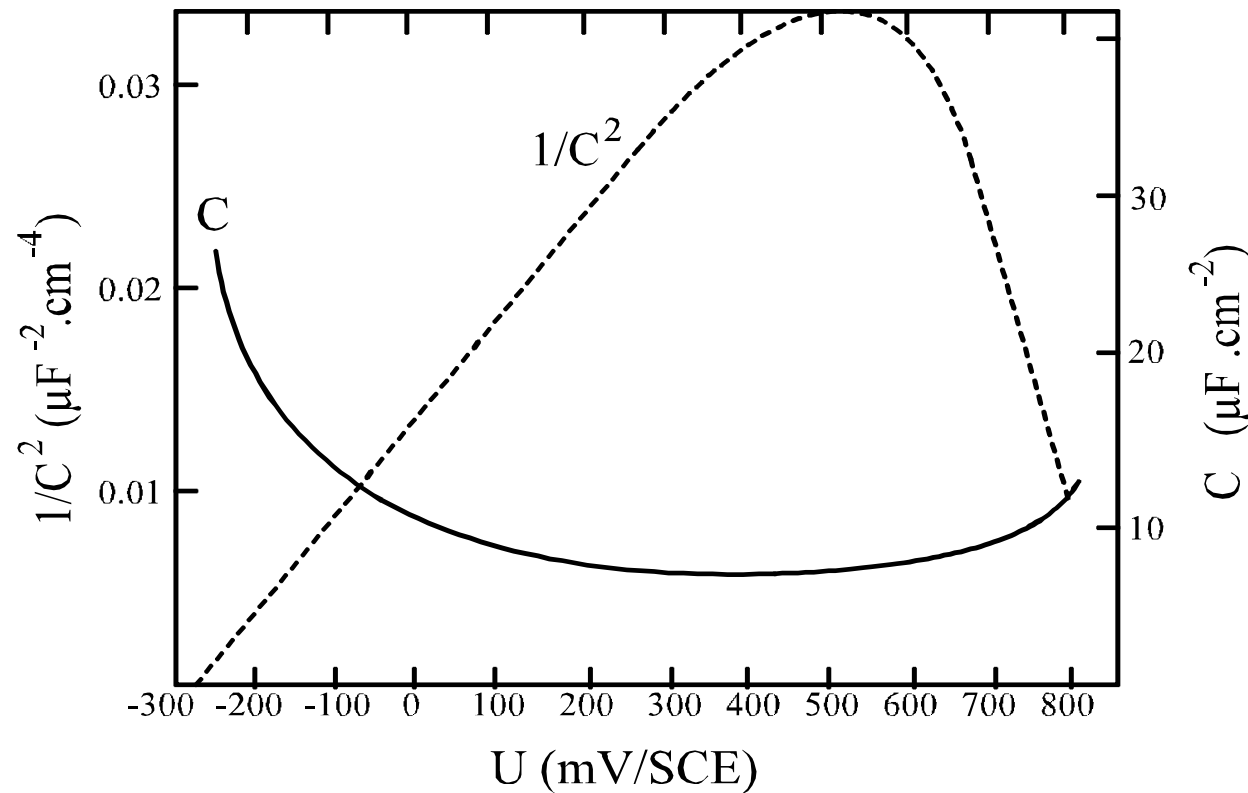
$$\frac{n}{N-n} = \exp \frac{E_F - E}{kT}$$

Qui est formellement analogue
à la loi de Fermi-Dirac:

$$n / N = \frac{1}{1 + \exp \frac{E - E_F}{kT}}$$

A très basse température, on peut considérer les niveaux d 'énergie comme pleins en dessous du niveau de Fermi, vides au dessus

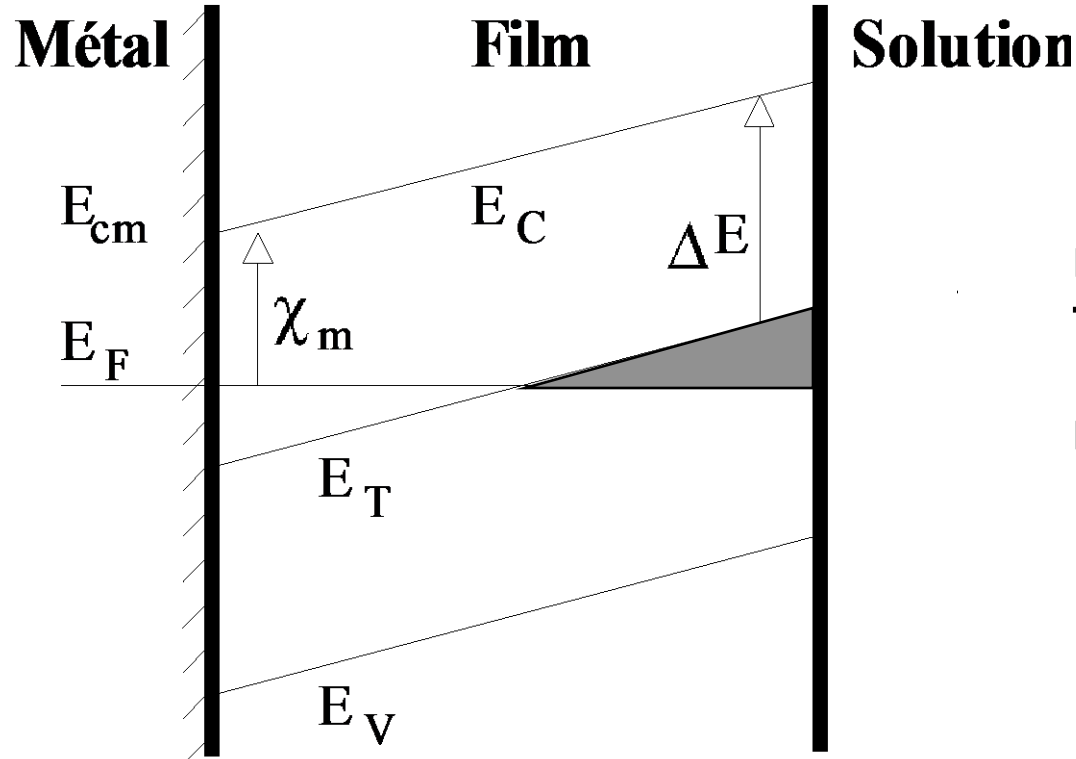
Mise en évidence des propriétés semi-conductrices des films passifs: comportement de Mott Schottky



Typical C^{-2} vs. V Diagram on an Fe electrode passivated in borate buffer (pH 8,4)

La Capacité d 'interface suit une loi de Mott –Schottky
due au piegeage-dépiegage des electrons dans le film

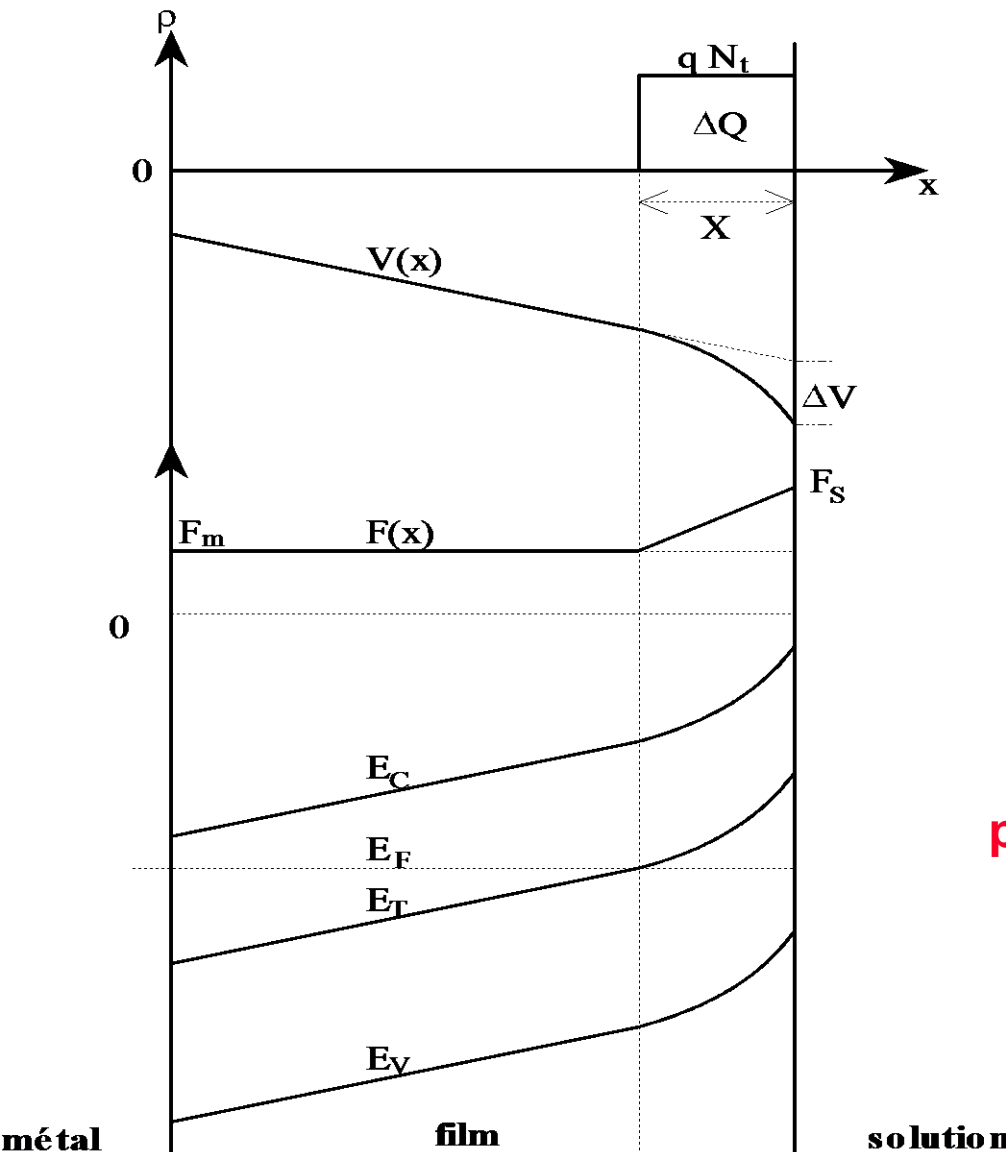
Effet du champ électrique sur le comportement semi-conducteur des films passifs



La répartition des niveaux d'énergie est fortement perturbée par le champ électrique qui règne dans le film

Modèle simplifié : Les niveaux sont remplis en dessous du niveau de Fermi, vides au dessus

Capacité de Charge d'espace.



$$X = \lambda \sqrt{\frac{q \Delta V}{kT}}$$

$$\Rightarrow [\Delta Q]^2 = 2\varepsilon q N \Delta V$$

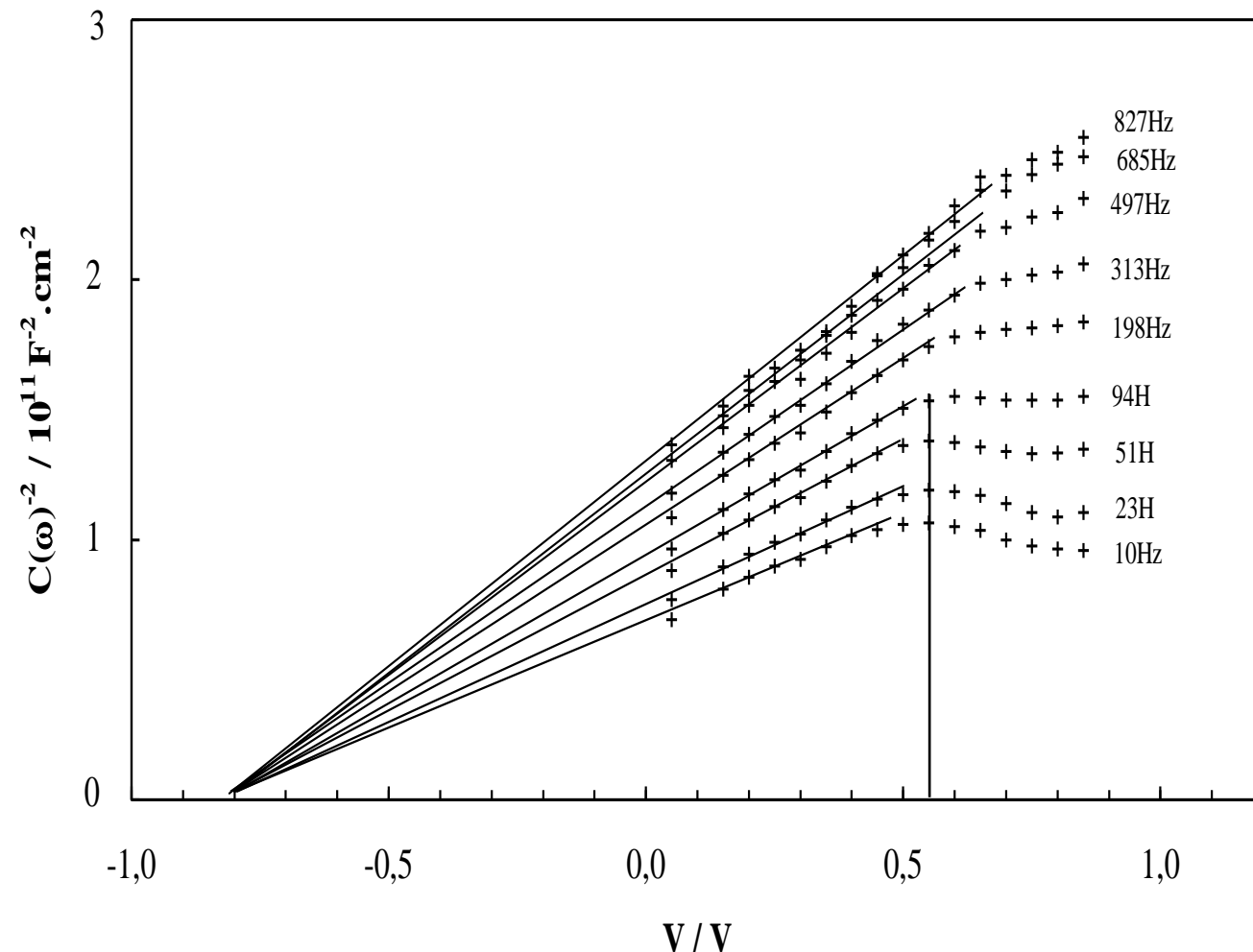
$$\text{Capacité } C = d\Delta Q/d\Delta V$$

$$\boxed{\frac{1}{C^2} = \frac{2(V_0 - V)}{N\varepsilon kT}}$$

Où V_0 est le
potentiel de bandes plates « apparent »

$C = 1 \mu\text{F}/\text{cm}^2$
pour $N = 10^{20} \text{ cm}^{-3}$ et $V - V_0 = 200 \text{ mV}$

solution



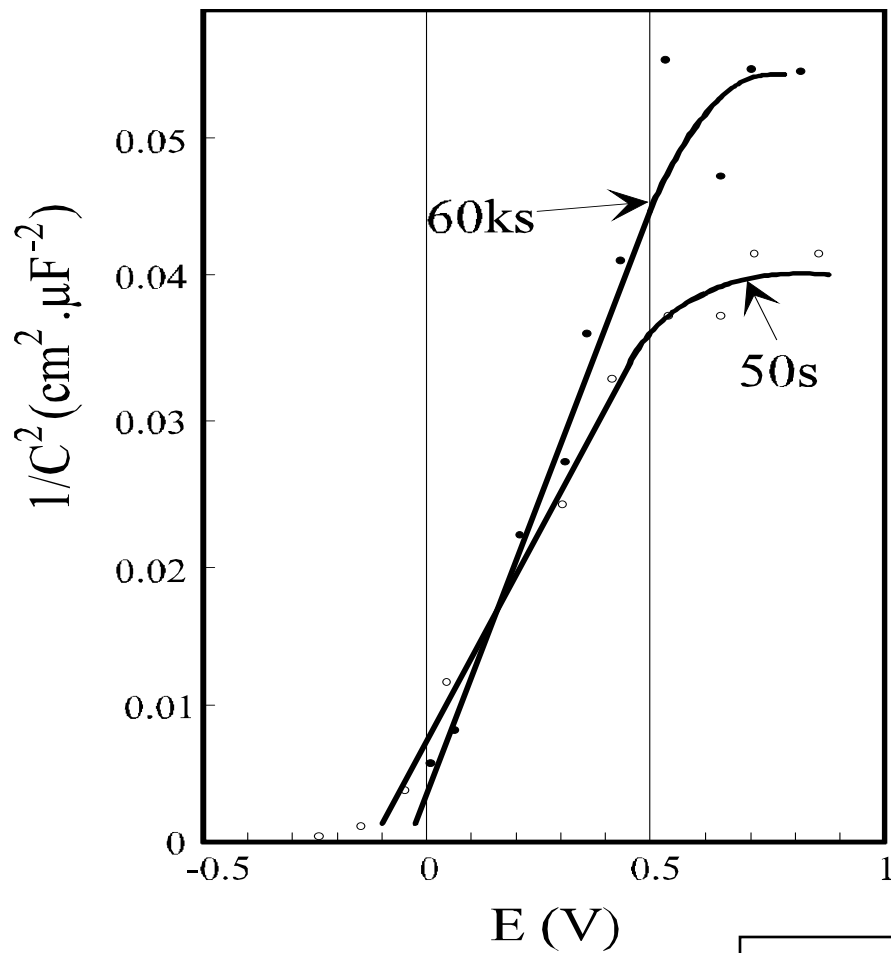
Other Instances of M.S. behaviour (1)

$$\frac{1}{C^2} = (V - V_0) \frac{2}{N \varepsilon k T}$$

M.S. Diagram obtained on a mechanically polished AISI430 type steel, in deaerated NaCl (0.02M) pH6.6 after polarising 16h at +200mV/SCE.

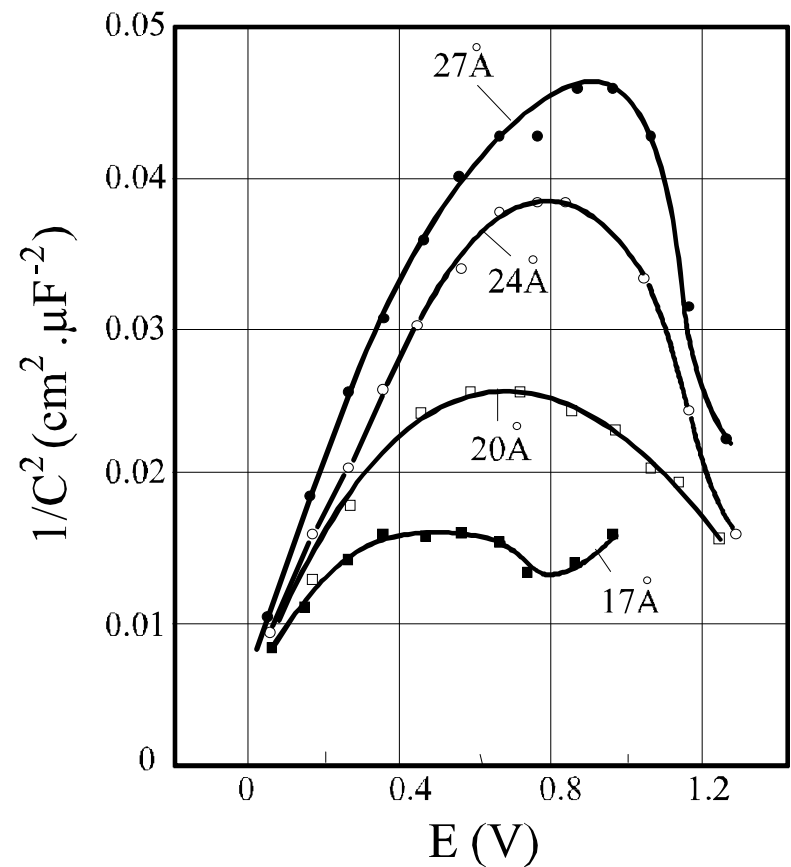
Impedance was measured using several frequencies: The frequency dispersion reflects the time needed for the trapping-detraping process

Other Instances of M.S. behaviour (2,3)



Effect of the polarisation time

$$\frac{1}{C^2} = \frac{2(V_0 - V)}{N\varepsilon kT}$$



Effect of the film thickness

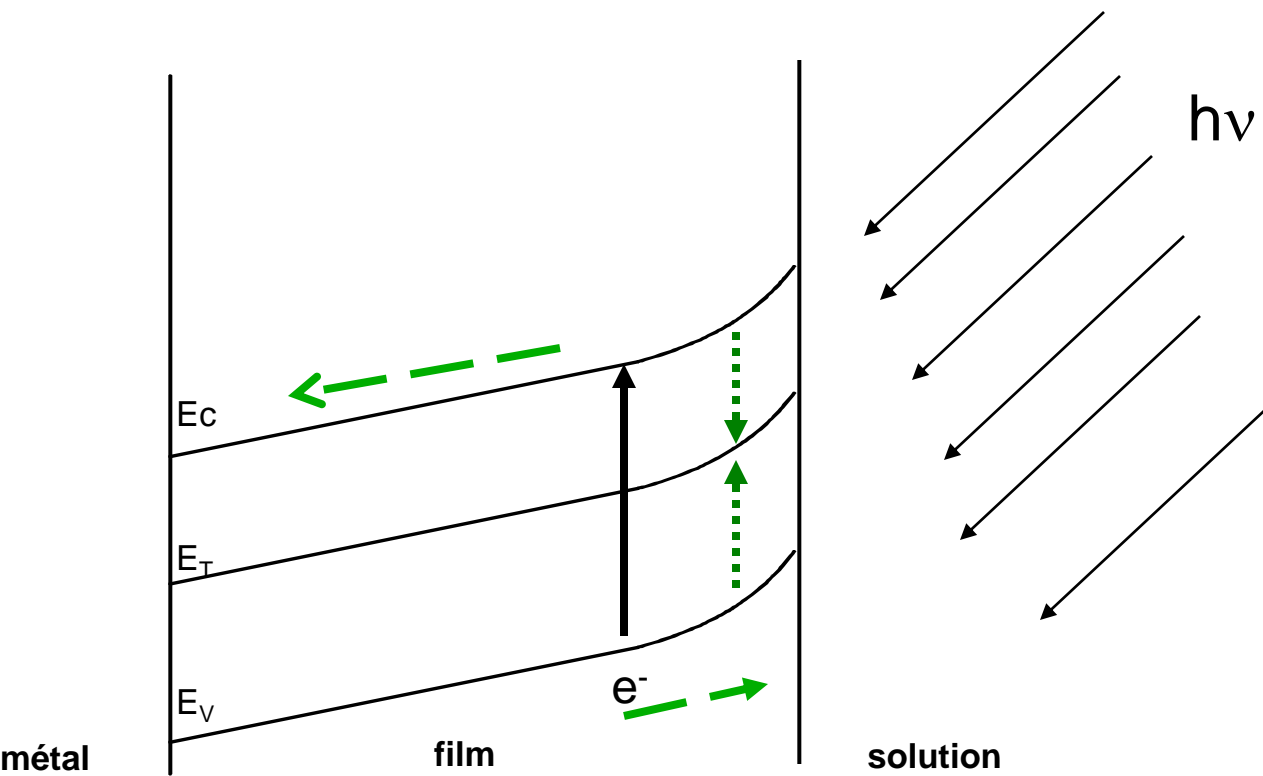


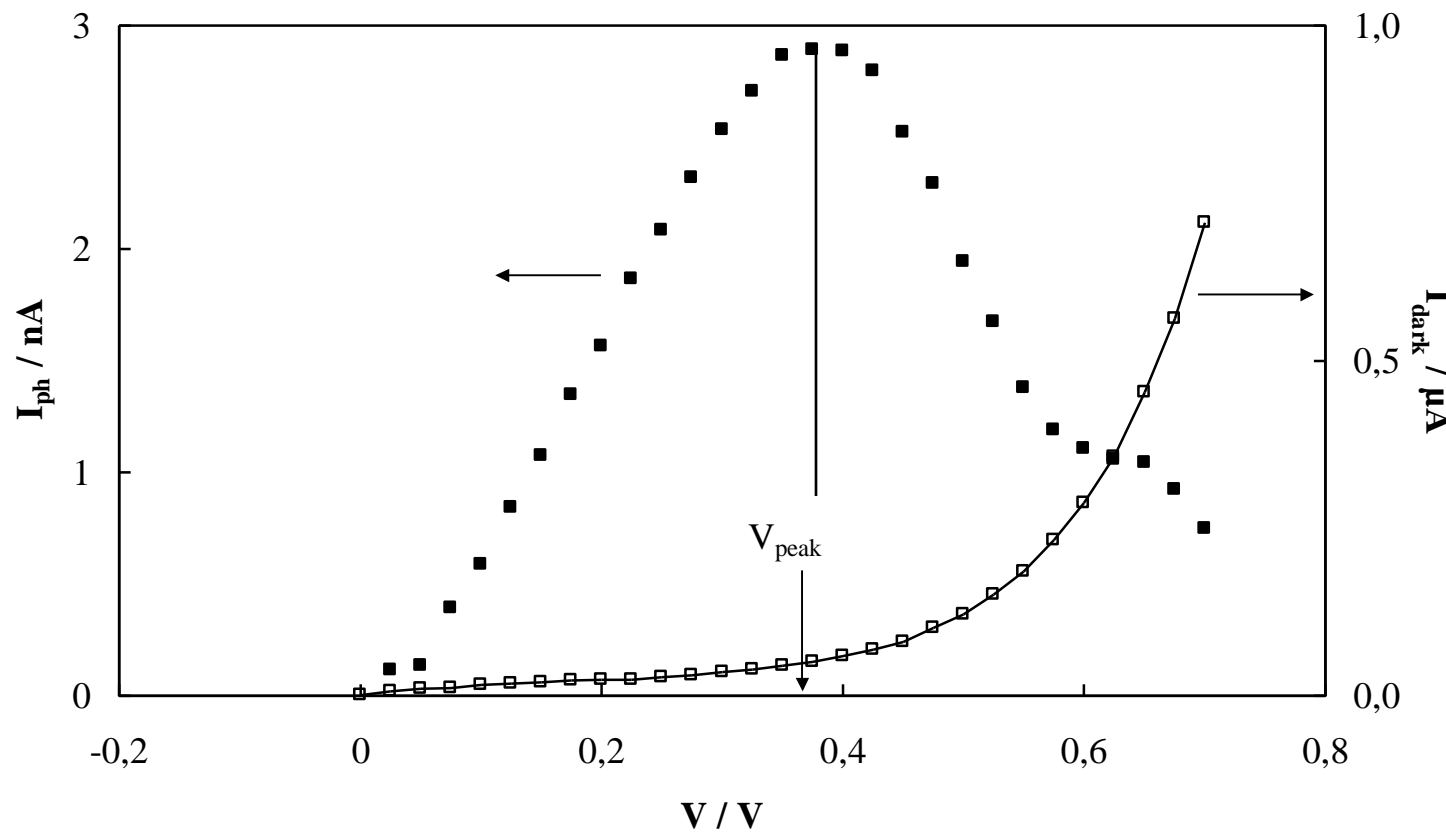
Photo-electrochemical effects

→ Formation of an electron hole pair

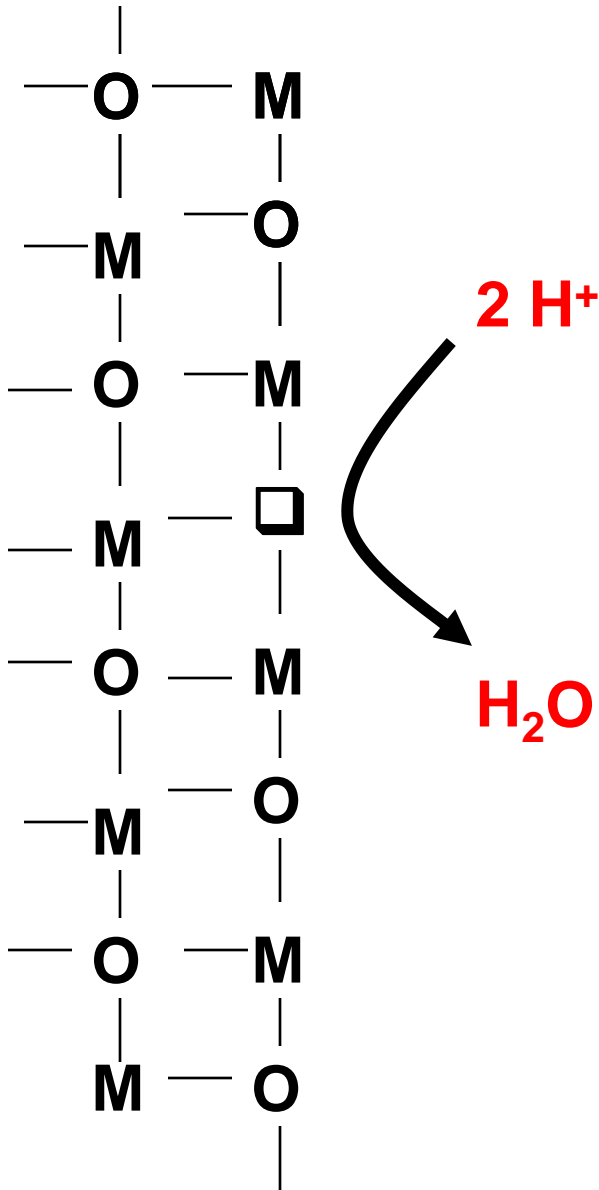
→ Pair annihilation : recombination on an electron trap energy level

→ photocurrent

An instance of PEC response of passive films

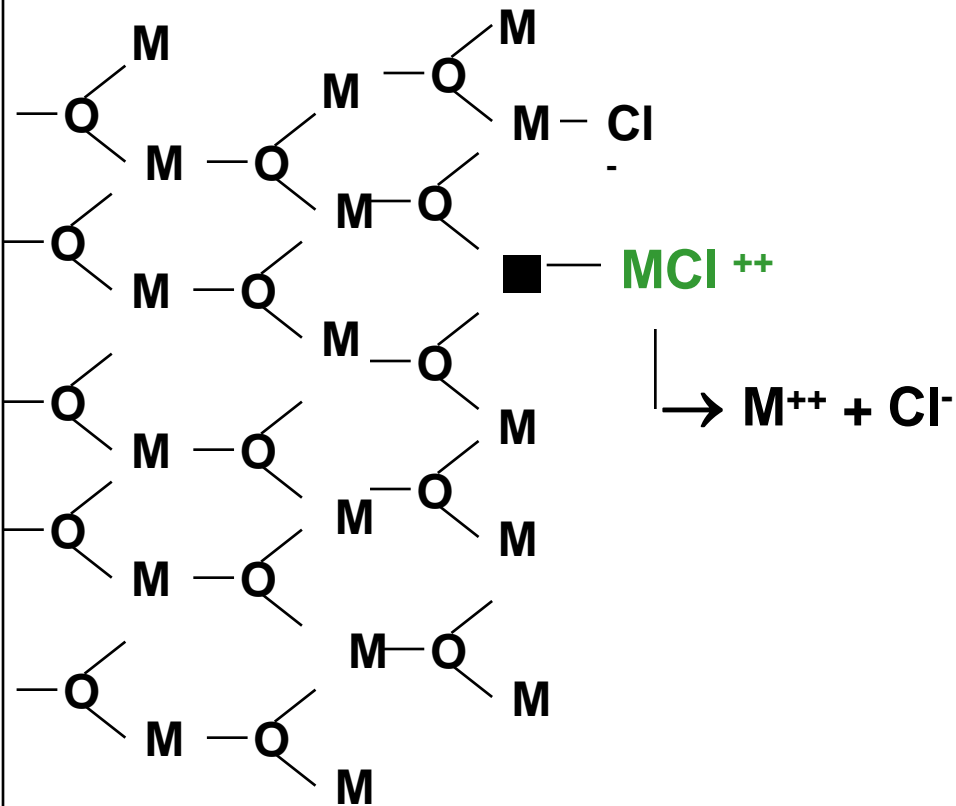


Potential dependence of the photocurrent (■) and dark current (□) for a passive film formed in $\text{NaCl } 0.02\text{mol} \cdot \text{dm}^{-3}$, $\text{Ar}10\% \text{H}_2$ ($t_p=15\text{h}30$), $\text{pH}_f=3.0$. Experimental conditions: $\text{pHm}=5.2$, sweep rate $0.1\text{V}/120\text{s}$. $\lambda=501.7\text{nm}$, $P=60\text{mW} \cdot \text{cm}^{-2}$, light modulation frequency 45Hz .



Corrosion of passive films: The acidic attack

- The first step of acidic attack results in the net transfer of a negative charge (O^-) from the film to the environment.
- **The reaction rate is then expected to decrease when the electrode potential increases**
- When the O^- vacancies are in a sufficient amount, the cationic bond is weakened leading to the film dissolution
- **This corrosion is expected to be uniform on all the surface**



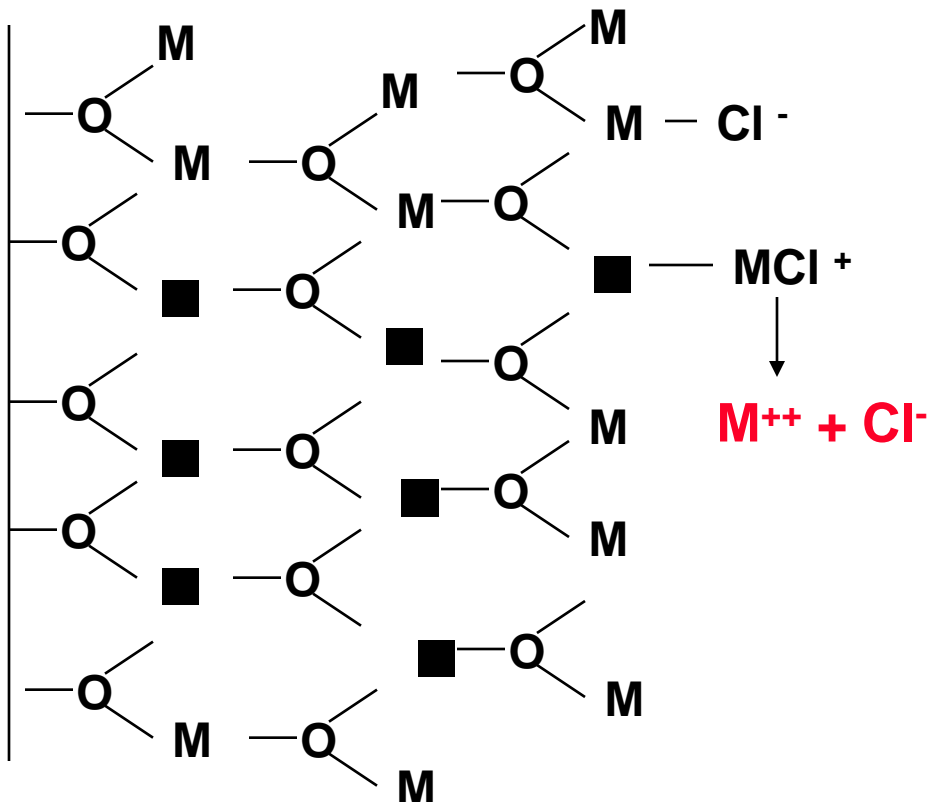
Corrosion in chloride containing electrolytes:

The vacancy Injection process

- 1) Chloride ions favours the action dissolution et the atomic scale, creating cation vacancies inside the film.**
- 2) Under the effect of the electric field**, cation vacancies migrates toward the metal/film interface, where they eliminate proportionally to their concentration $\Rightarrow \frac{dX}{dt} = J \cdot K \cdot X$ leading to the stationnary concentration $X = J/K$

Destabilising effect of cation vacancies

(Role of the Chloride ions)



- 1) Choride ions favours the action dissolution et the atomic scale, creating cation vacancies inside the film.
- 2) Under the effect of the electric field, these vacancies migrate toward the metal/film interface, where they eliminate proportionally to their concentration $\Rightarrow \frac{dX}{dt} = J - K \cdot X$ leading to the stationnary concentration $X = J/K$
- 3) When the vacancy concentration increases , the passive film cohesion decreases. At a critical value X_{crit} the film may locally break down .
- 4) Electrostriction theory: When the cohesion forces do not counterbalance the electrostriction forces, «local» film breakdown may occur (cf. N.Sato) .

NB: The mechanical breakdown should release the mechanical stresses around the breakdown point. This form of corrosion is then expected to be localized

The Pit nucleation potential

1) The vacancies creation rate J increases with the solution chloride content and electrode potential :

$$J = \text{cst.} c^n \cdot \exp V_{fs}/\phi = \text{cst.} c^n \cdot \exp (1-\gamma)V_E/\phi$$

where $\gamma = dV_f/dV_E$ is a share coefficient

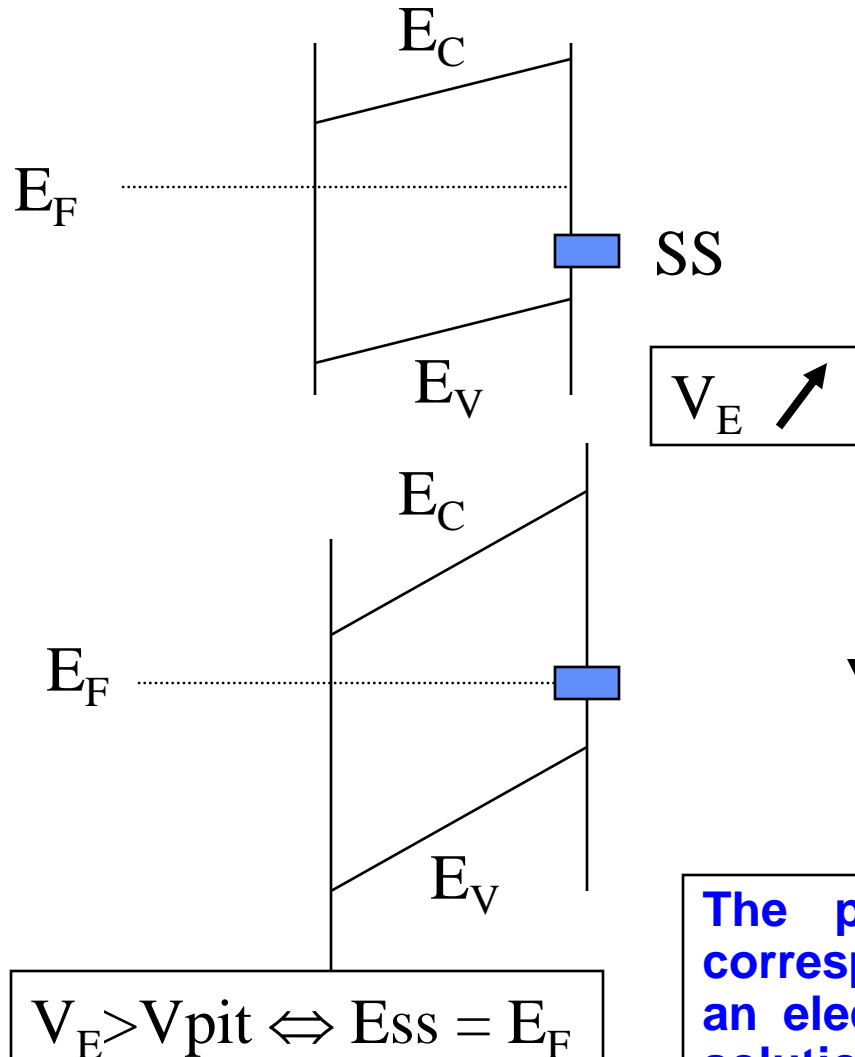
2) A pit nucleation potential may be defined as:

$$J(C, V_{pit}) = KX_{crit}$$

It decreases when the chloride concentration increases

The Pit Nucleation potential (details)

$$V_E < V_{\text{pit}} \Leftrightarrow E_{\text{ss}} < E_F$$



Below the pitting potential:

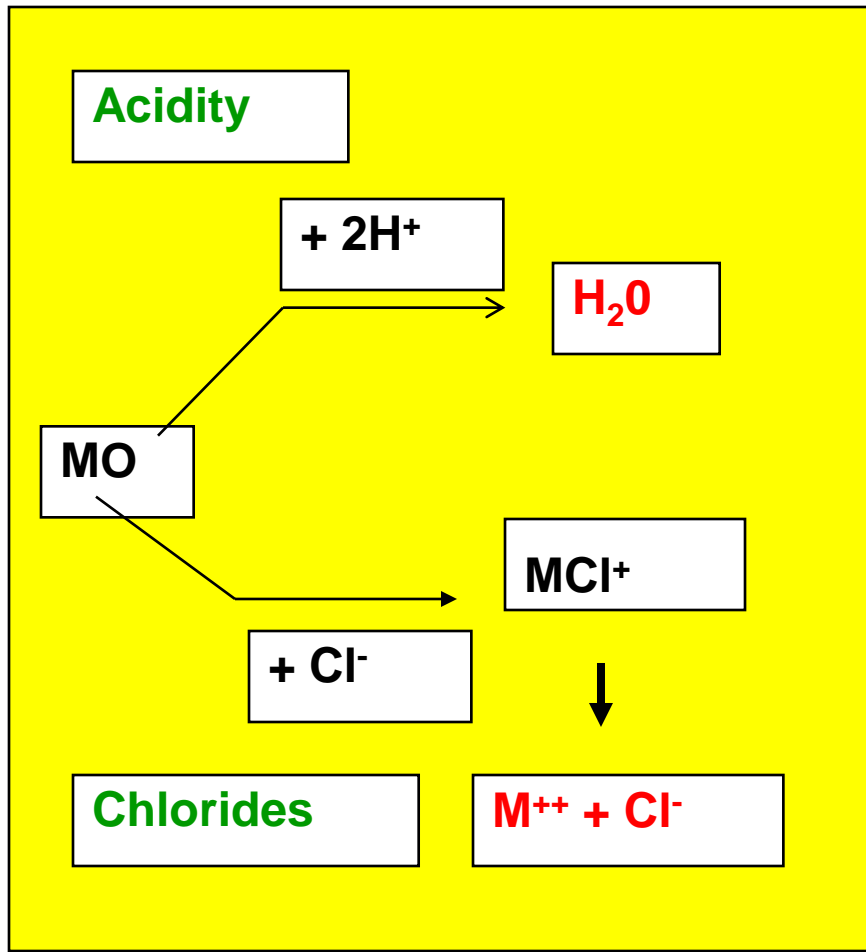
Any increase in electrode potential is concentrated inside the passive film. Then the potential drop at the outer interface keeps constant. The vacancy concentration in the film is negligible and does not depend on electrode potential

Above the pitting potential:

The metal Fermi level is pinned on the electron surface states energy level. Then the potential drop within the film is constant and any increase in electrode potential concentrates at the film electrolyte interface. The vacancy concentration in the film quickly increases with electrode potential

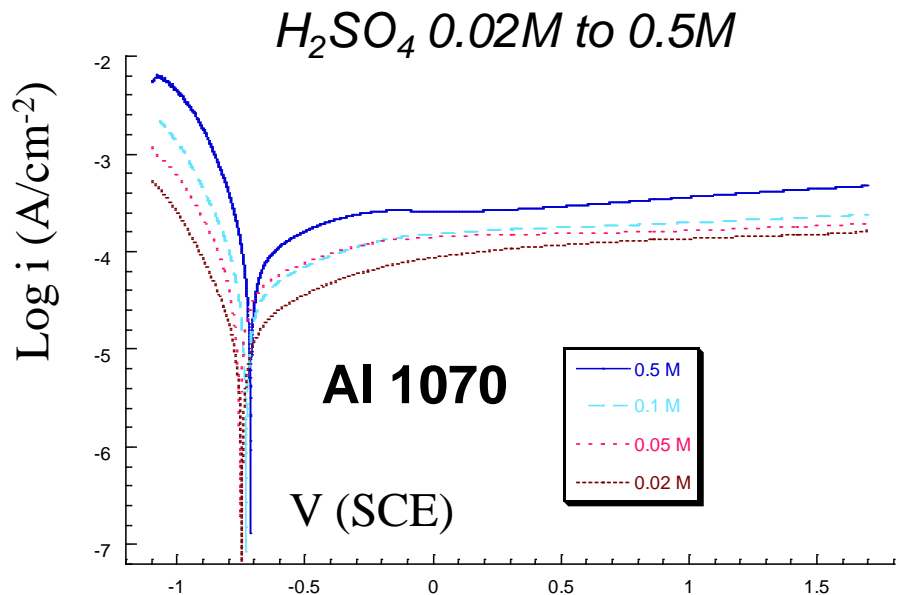
The pit nucleation potential could simply correspond to the pinning of the Fermi level on an electron acceptor level present at the film solution interface.

Part III: Passivity breakdown

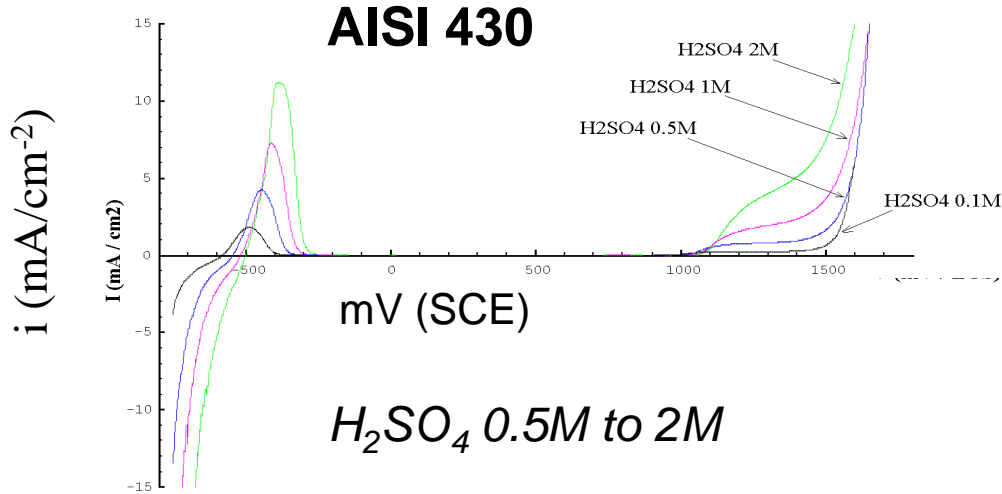


CORROSION RISK	<i>Quasi-neutral</i>	<i>Acidic</i>
<i>Chloride free</i>	NO	UNIFORM CORROSION
<i>Chloride containing</i>	LOCALISED CORROSION	HAZARD!!

Polarisation curves in acidic media

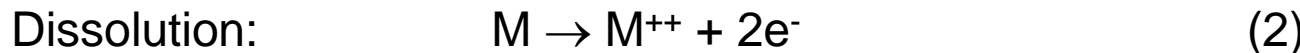
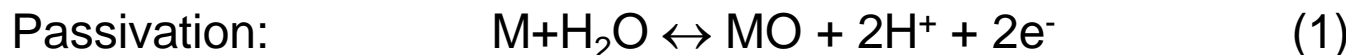


Aluminium alloys



Stainless steels

Modelling the polarisation curve (1)



$$\text{Fraction passivée (recouverte par MO)} = \theta$$

$$\text{Activité du proton en surface} \propto \xi = H^+ \exp - \frac{qV}{kT}$$

Loi d'action de masse (1) : $1 - \theta \propto \theta \xi^2 = \theta / u^2$ avec:

$$u = \xi_{1/2} / \xi = [\xi_{1/2} / H^+] \exp \frac{qV}{kT} \Rightarrow \exp \frac{qV}{kT} \propto u \cdot H^+ / \xi_{1/2}$$

$$\theta = \frac{u^2}{1+u^2}$$

= 0 pour les potentiels cathodiques et/ou les milieux acides
= 1 pour les potentiels anodiques et/ou les milieux basiques

Loi cinétique (2)
(Tafel) :

$$i \propto [1 - \theta] \exp \frac{\beta qV}{kT} \propto [H^+]^\beta \frac{u^\beta}{1+u^2}$$

Modelling the polarisation curve (2)

$$i \propto [1 - \theta] \exp \frac{\beta q V}{kT} \propto [H^+]^\beta \frac{u^\beta}{1 + u^2}$$

avec $u = [\xi_{1/2} / H^+] \exp \frac{qV}{kT}$

Qui varie comme u^β pour les potentiels cathodiques et/ou les milieux acides

Qui varie comme $u^{\beta-2}$ pour les potentiels anodiques et/ou les milieux basiques

Si $\beta < 2$, cette fonction présente un maximum i_{crit} pour $u=u_{\text{crit}}$, $V=V_{\text{crit}}$, avec:

$u_{\text{crit}}^2 = \beta/(2-\beta)$ ($\Rightarrow \theta = \beta/2$) . Il en résulte que:

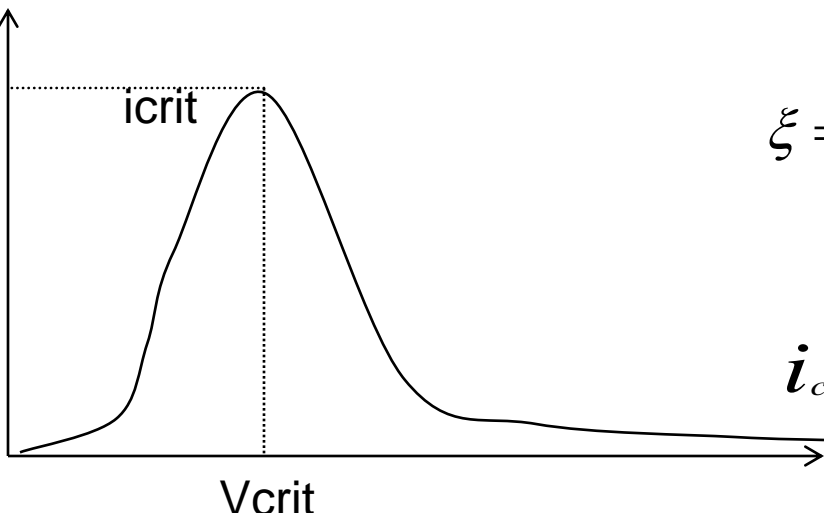
(1) V_{crit} suit une loi Nernstienne :

$$\xi = H^+ \exp - \frac{qV_{\text{crit}}}{kT} = \xi_{\text{crit}} = \xi_{1/2} / [\beta/(2-\beta)]^{1/2}$$

(2) i_{crit} décroît linéairement avec le pH :

$$i_{\text{crit}} \propto [H^+]^\beta$$

$$\Rightarrow \log i_{\text{crit}} = \text{cst.} - \beta \cdot \text{pH}$$

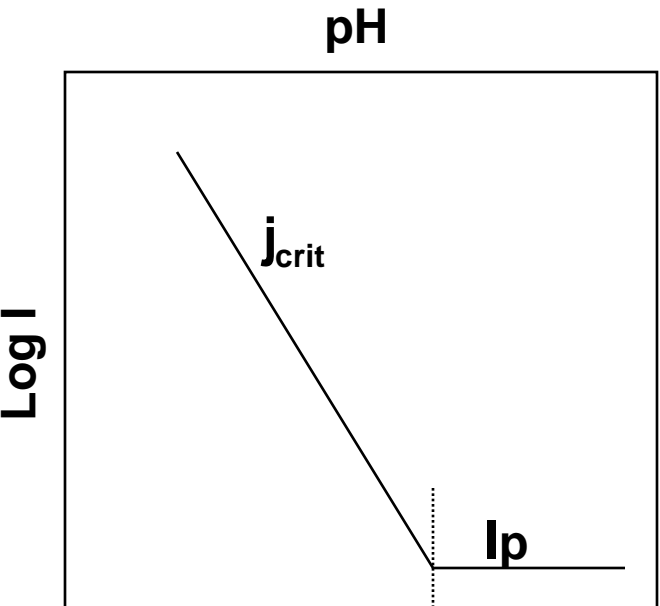
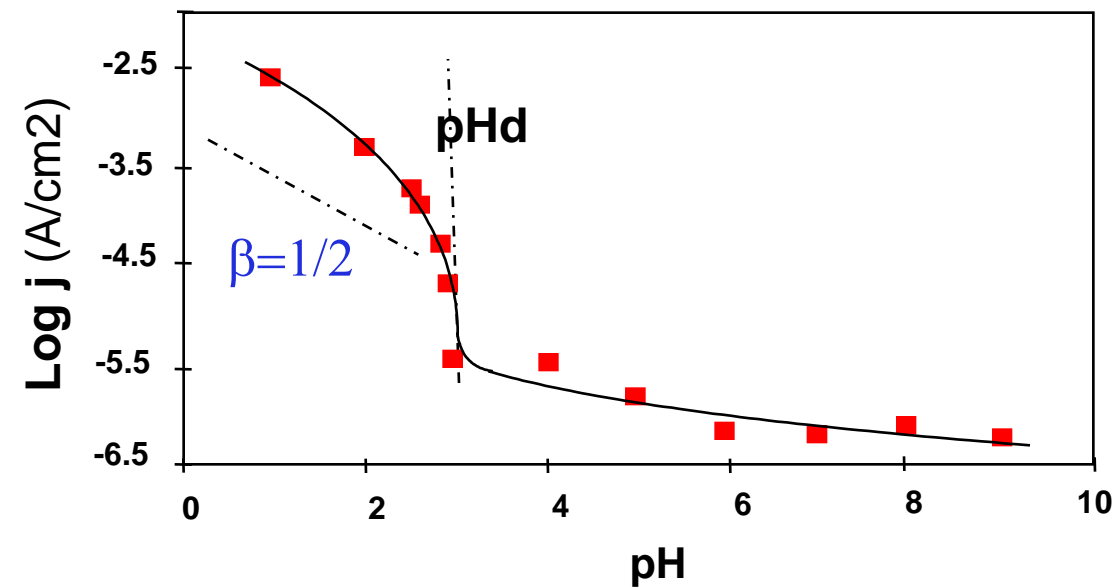


pH effect (Stainless steels)

$$V_{\text{crit}} = \text{cst.} + 2.3kT/q \text{ pH} \text{ (Nernst)}$$

$$\text{And } \log j_{\text{crit}} = \text{cst.} - \beta \cdot \text{pH}$$

(430 Ti in deaerated Na₂SO₄ 1M)



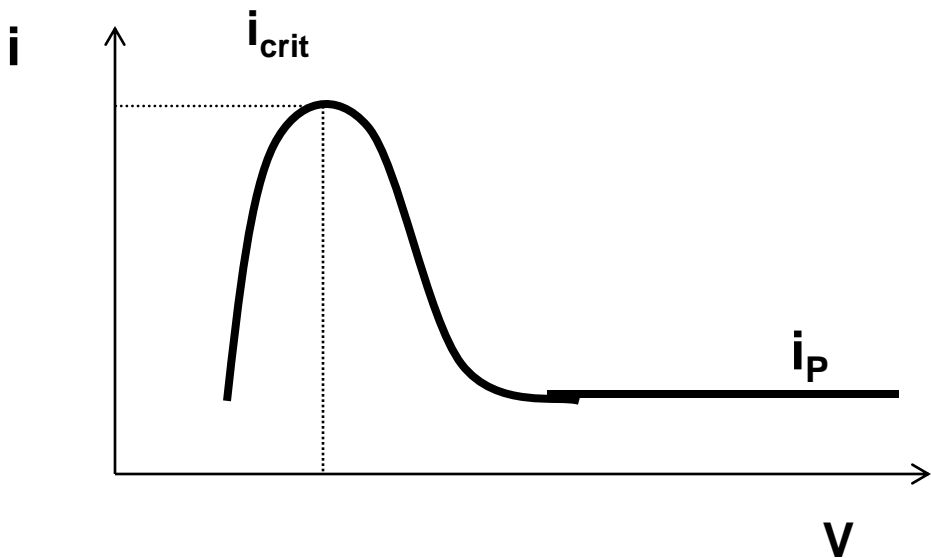
Theory

Experience

Polarisation Curve (general)

Le courant global i est la somme de 3 courants partiels:

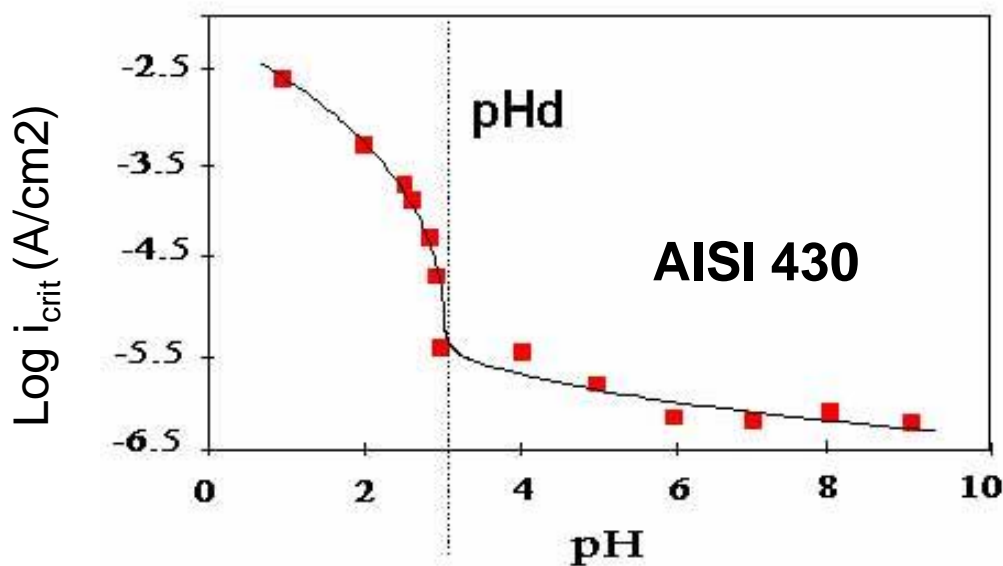
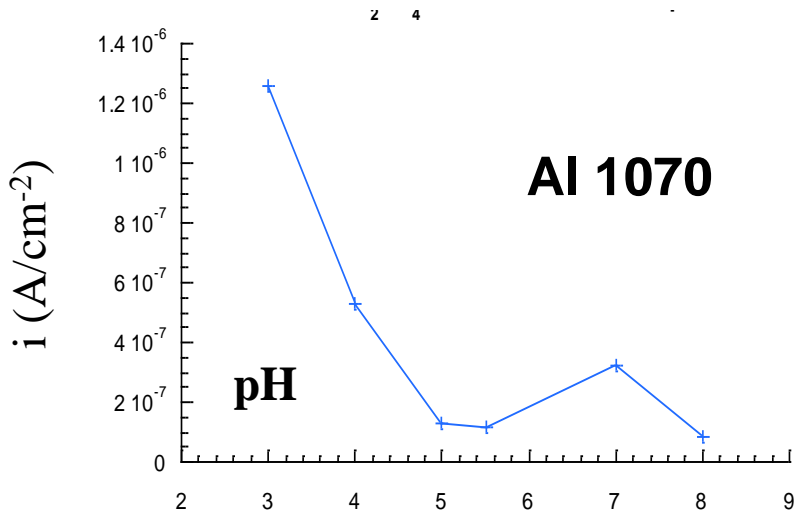
- 1) Le courant de dissolution anodique i_A
- 2) Le courant sur les sites oxydes, proportionnel à θ et tendant vers une constante i_P lorsque θ tend vers 1
- 3) Le courant cathodique i_K



Passivité de type
Fer, Cr, S.S. $i_P \ll i_{crit}$

Al : $i_P > i_{crit}$

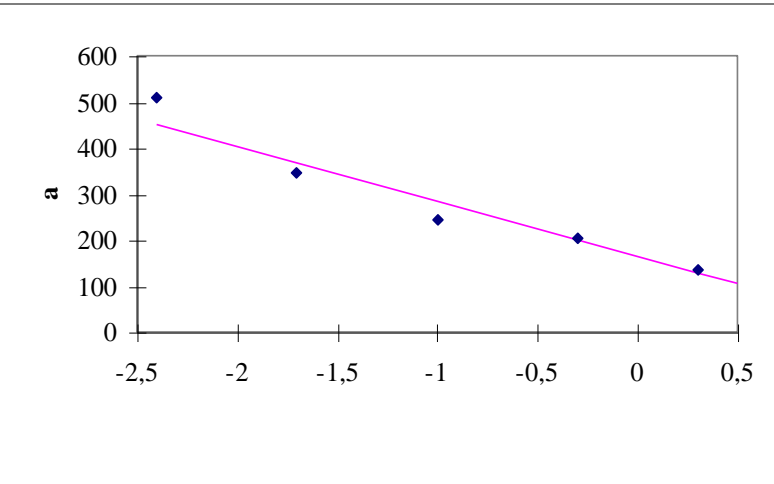
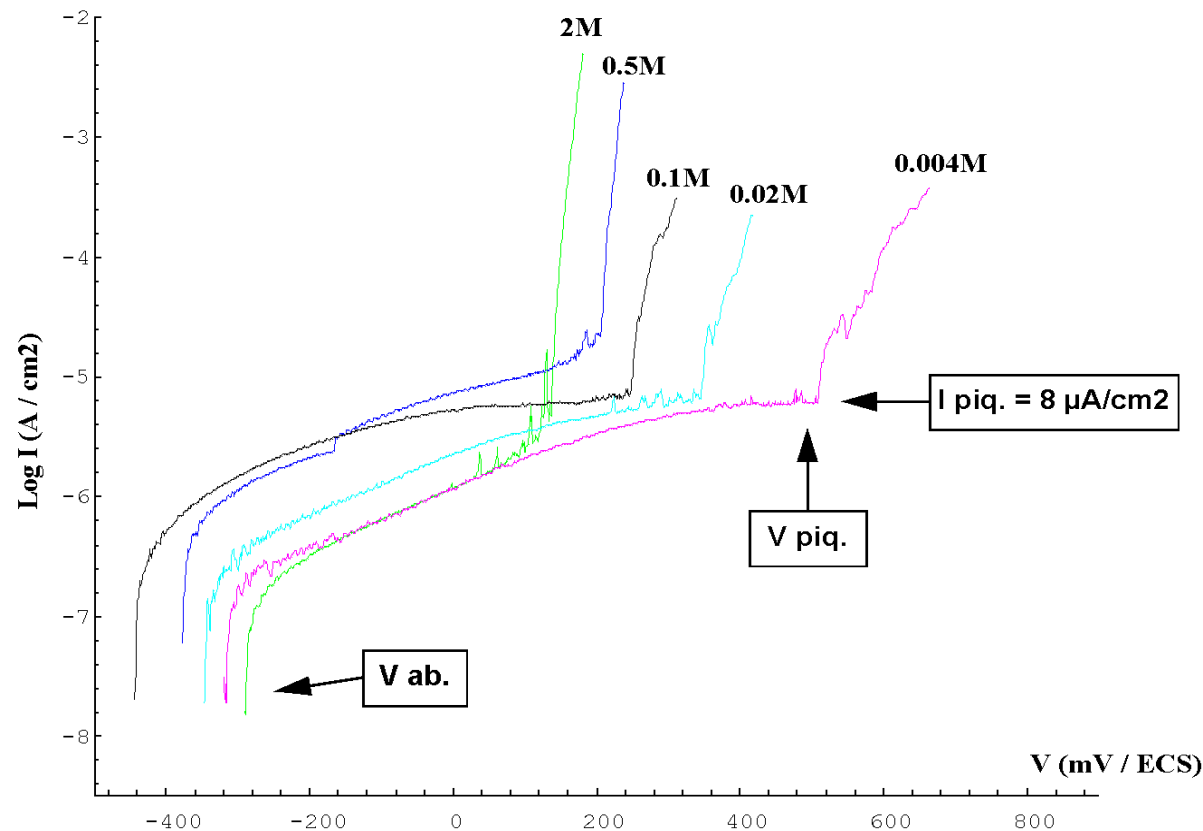
Corrosion current in acidified Na₂SO₄



critical passivation current in acidified Na₂SO₄

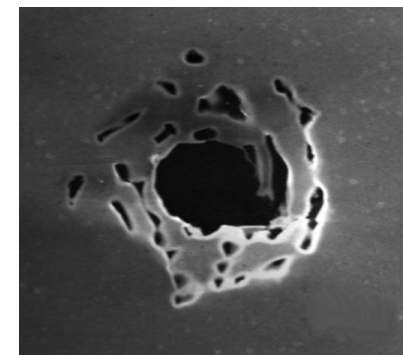
Behaviour of S.S. in neutral chloride containing media: the pitting Corrosion

(430 Ti in deaerated NaCl pH6.6)



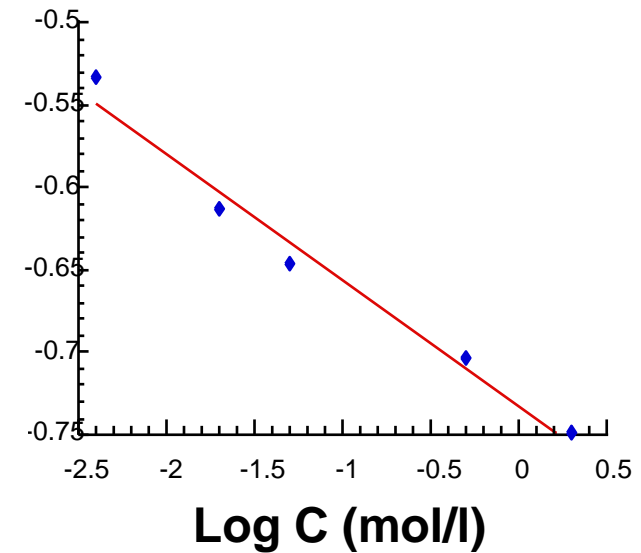
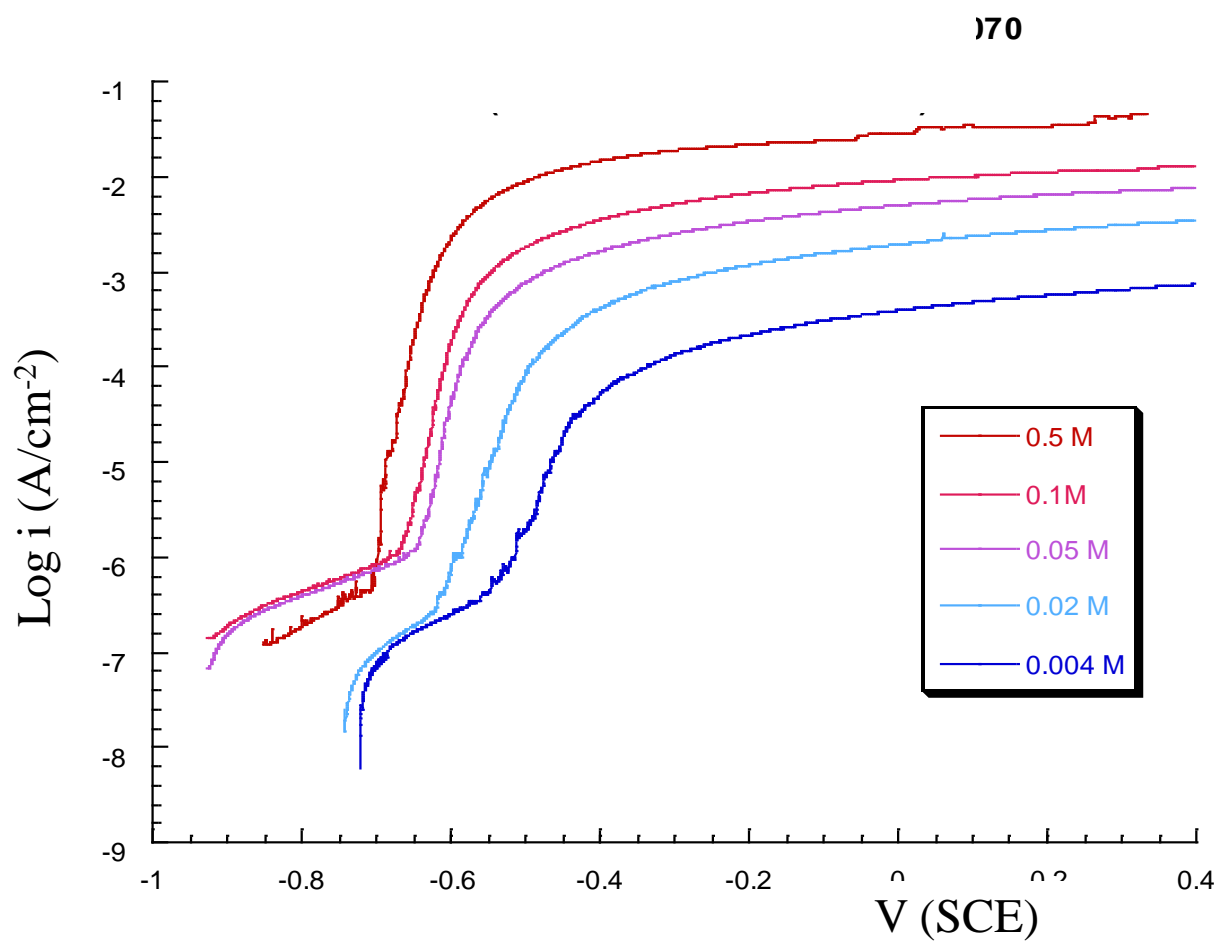
Log C (mol/l)

The pitting potential
decreases when
increasing the
Chloride content



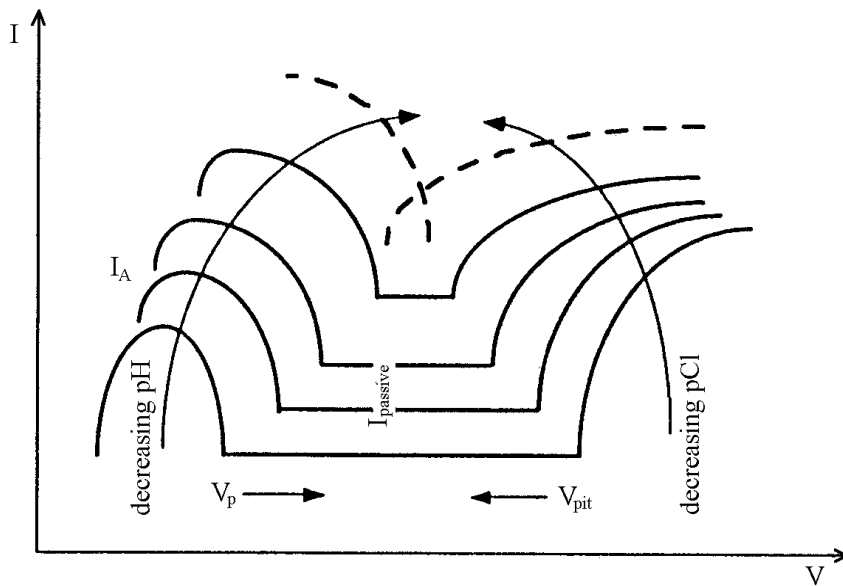
Behaviour of Al in neutral chloride containing media

(Al1070 in deaerated NaCl pH6.6)



As for Stainless steels, The pitting potential diminishes linearly with the logarithm of the chloride content.

The Corrosion risk in chloride containing acidic media

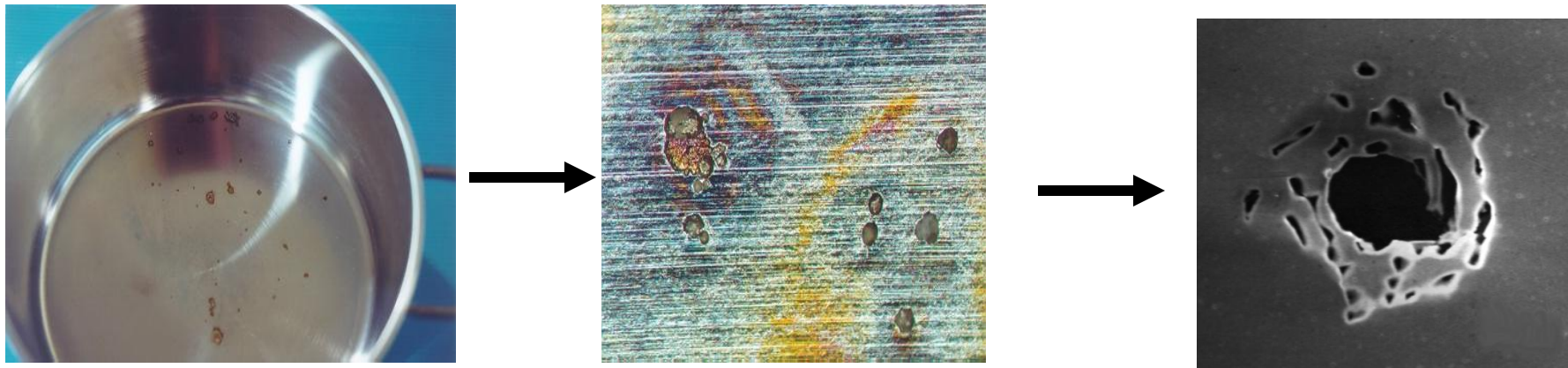


- The fall in pH and the increase in the Cl^- content reduces the passive range

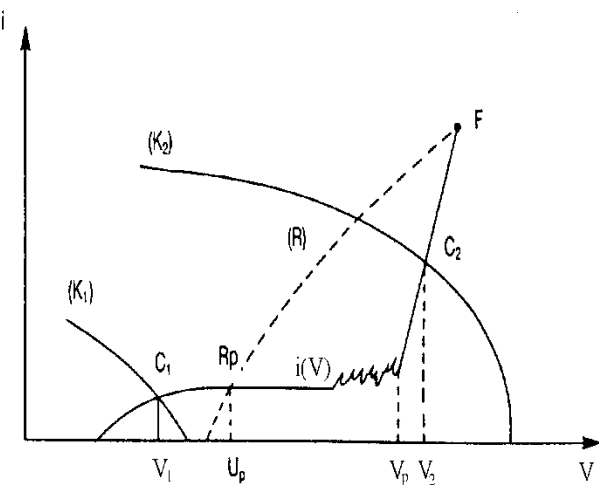
The successive stages of localised corrosion

- **Initiation**
 - The generic modes (Pitting, Crevice, SCC...)
 - Environment effects (*Marine, atmospheric, MIC...*)
 - Effect of the material (specific)
- **Propagation** (common mode)
 - Chloride enrichment
 - Hydrolysis of dissolved cations
 - High propagation rate

Pitting Corrosion in neutral chloride containing media



(AISI 304)

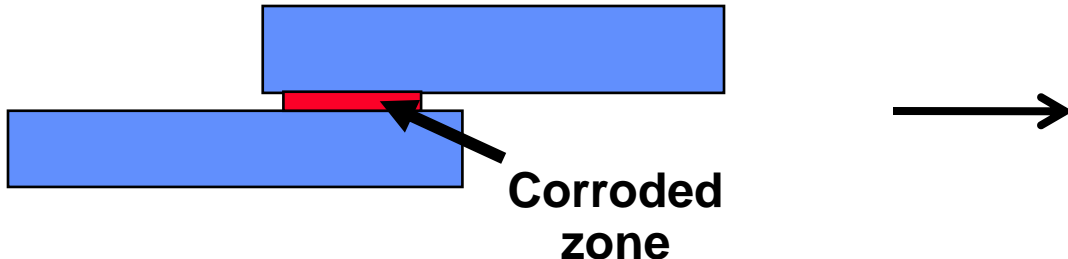


The pitting potential is an appropriate criterion for pitting corrosion resistance

The successive steps of pitting corrosion

- **Pit nucleation** (nanometric scale)
Local passive film breakdown.
- **Metastable pitting** (micrometric scale)
Possible repassivation, current transients.
- **Irreversible damage** (milimetric scale)
Pit propagation

Crevice corrosion?



What happens in a crevice?

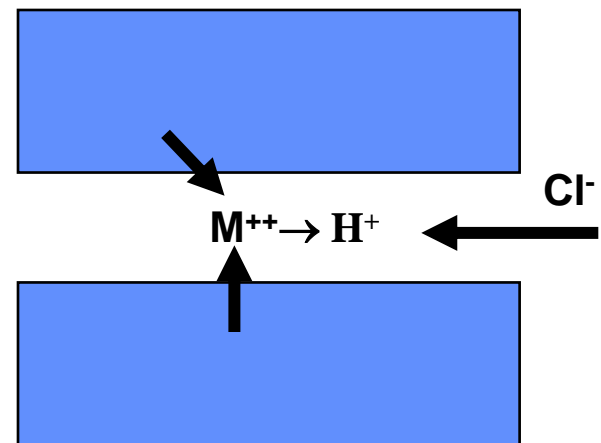
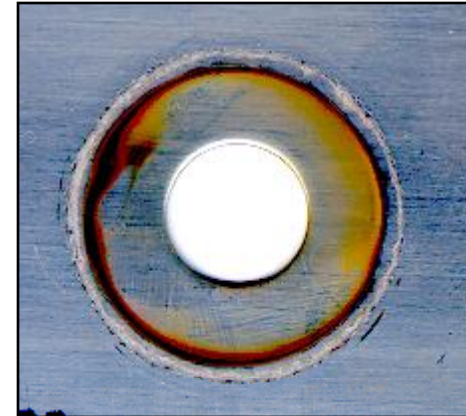
1) **Cathodic reaction** quickly exhaust oxygen in the crevice. Further cathodic reaction occurs then outside

2) **Anodic dissolution** across the passive surface, leads to an enrichment in dissolved cations

3) **Chloride enrichment** : Influx of the majority anion to compensate for the positive charges (electromigration)

4) **Hydrolysis of cations (\Rightarrow Hydrochloric acidity)**

limited by the migration and the diffusion of reaction products outside the zone.



The remedies:

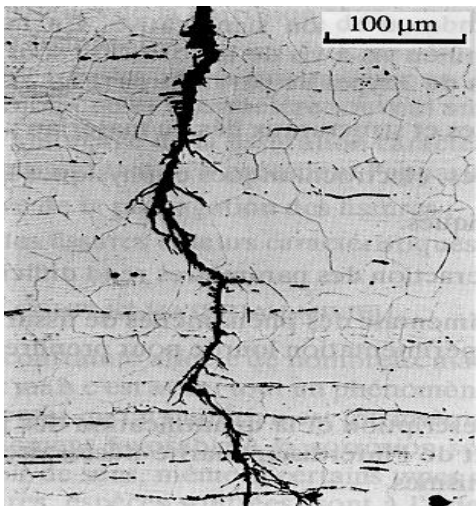
- 1) **Material selection** (for a “sufficient” resistance to acidic corrosion)
- 2) **To avoid crevices!**

Mechanical Effects

The Detrimental effect of Stress ...

- Stress corrosion cracking
- Corrosion-Fatigue
- Fretting Corrosion ...etc...

JE CROIS QUE
JE BOSSE TROP
EN C'MOMENT...



Stress corrosion cracking

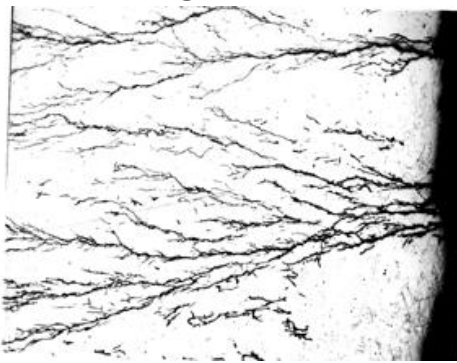
Conditions of occurrence:
hot chloride containing environment.

Remedy: selection of appropriate grades. For instance, the use of austeno-ferritic or ferritic steels is preferable to FeCrNi austenitic steels.

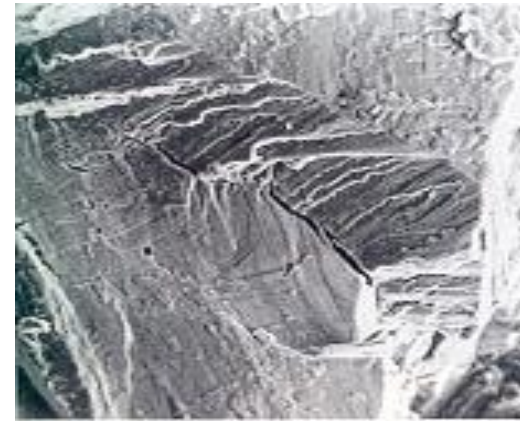
The association of mechanical stress and corrosive conditions:
may lead to damage which neither the mechanical stress nor the corrosion would have caused separately.

Optical microscopy

crack propagation rate



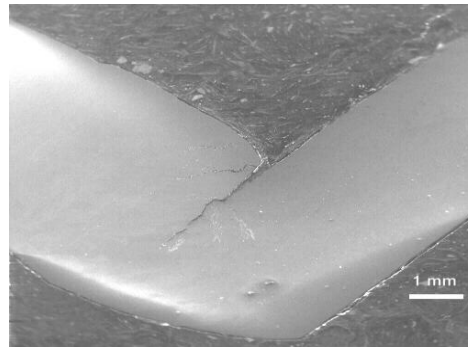
SCC facies



— 30 μm

Cracks in stainless steels can either be intergranular or transgranular or sometimes mixed.

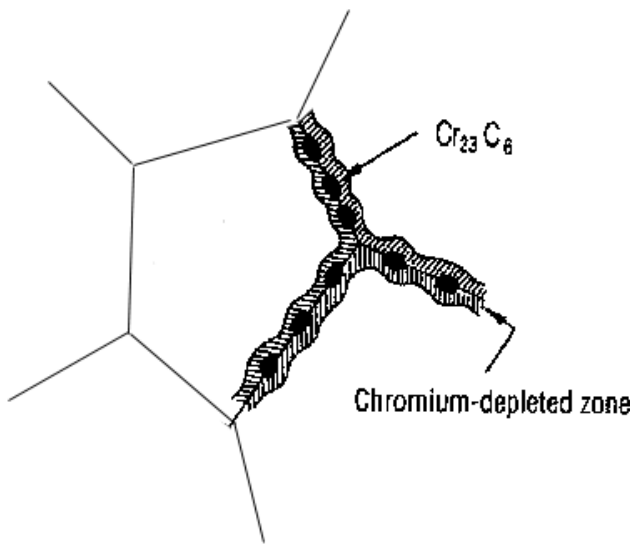
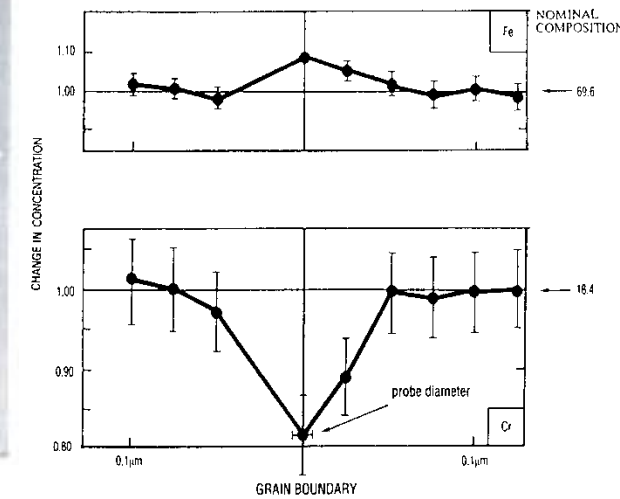
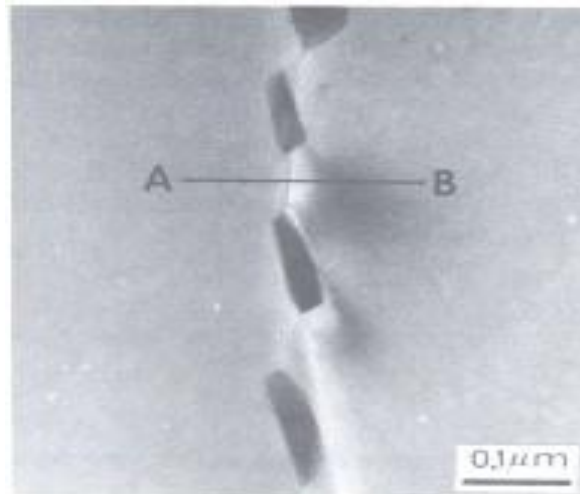
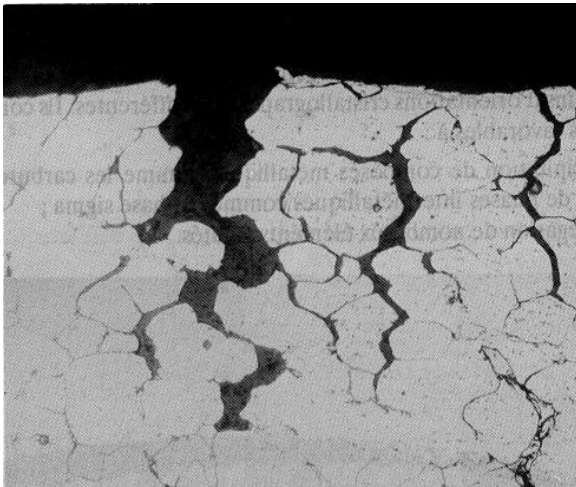
Transgranular cracks often show continuous striations, perpendicular to the crack growth direction, which are generally considered to mark successive stages of propagation (discontinuous propagation rate).



Effect of residual stresses

IV) Metalurgical effects

Intergranular Corrosion of stainless steels: Carbide Precipitation and Chromium depletion



Chromium depletion in the vicinity of a grain boundary in an austenitic steel:

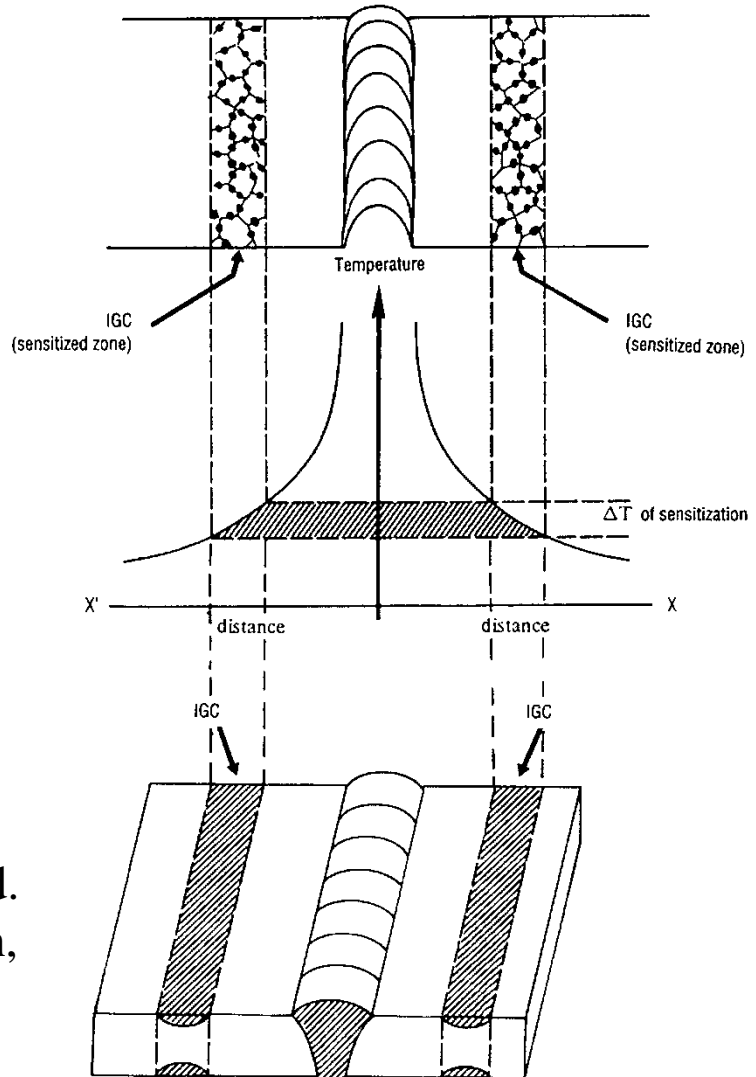
- transmission electron microscope image
- corresponding iron and chromium concentration profiles..

Heat Affected Zone close to the weldments



Example: Several secondary tubes are welded on a main tube. No post welding treatment was performed. Welds were then sensitised to intergranular corrosion, due to intergranular precipitation of chromium carbides in the heat affected zones.

The corrosion looks locally « uniform » all around the tube weldments



Austenitic Steels

IGC: The remedies

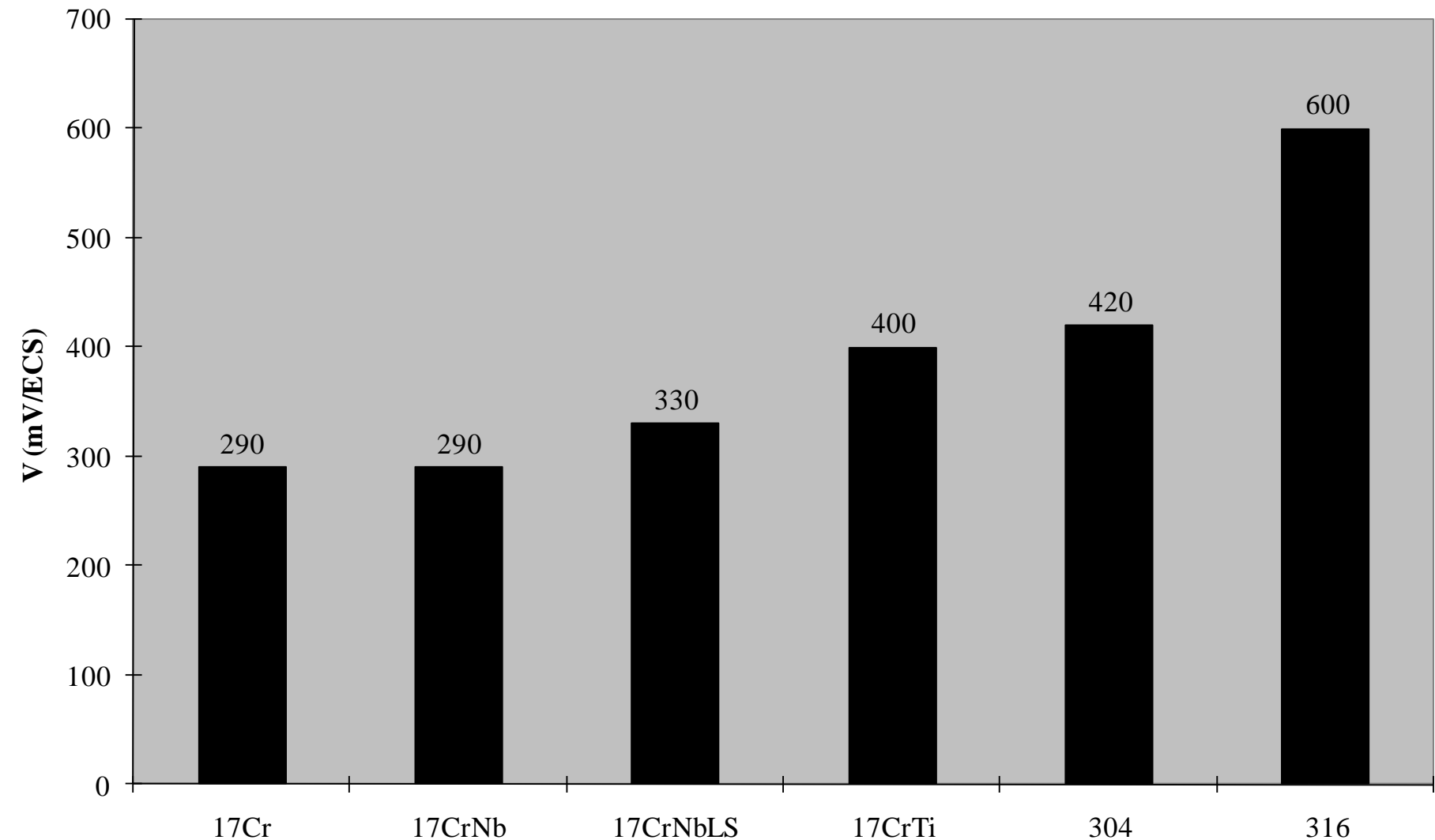
Ferritic Steels

- Heat Treatments
 - solution treatment
 - annealing after welding (rarely used)
- Low Carbon Steels: C<0.03%
 - (304L, 316L , etc ..)
- Stabilised Steels
 - Stabilising elements : Ti, Nb, Zr.
 - Ex: Ti stabilised steel (grade 321) : $Ti/C > 5$?
Maturation heat treatment

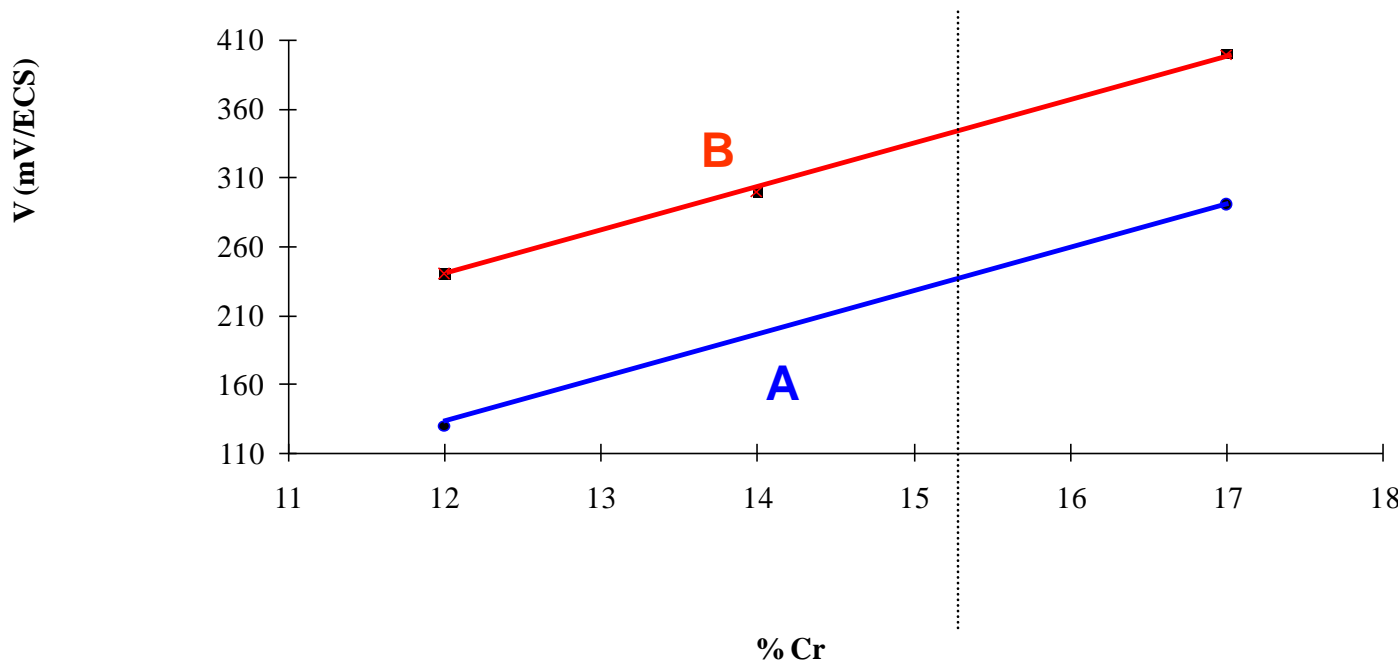
- Impossible solutions
 - Solution treatment
 - low carbon
- Possible solutions
 - annealing after welding
 - Stabilisation (Ti, Nb, Zr)
- Ex: Titanium stabilised steel
 - $Ti>0.15\% +4(C+N)$
 - Other effect: sulfur trapping
 \Rightarrow improvement of the pitting resistance

Pitting potentials of stainless steels

(In NaCl 0.02M)



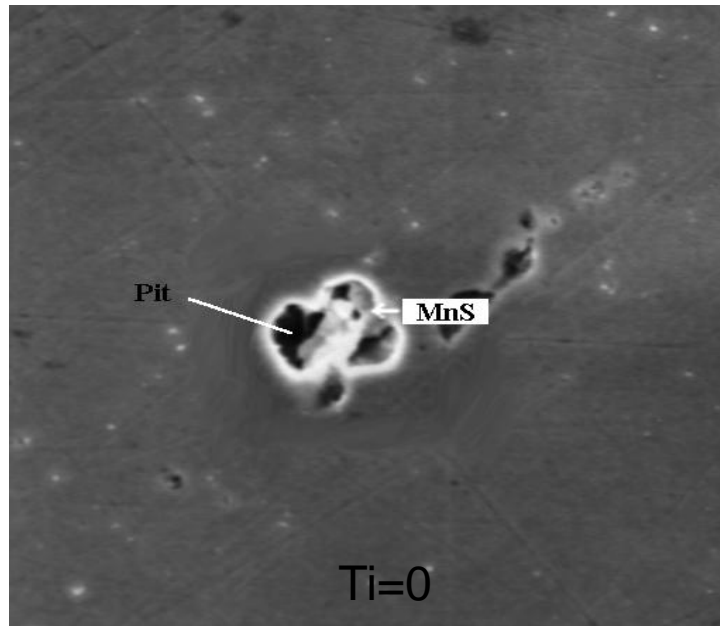
Effect of the chromium content in an Fe - Cr alloy



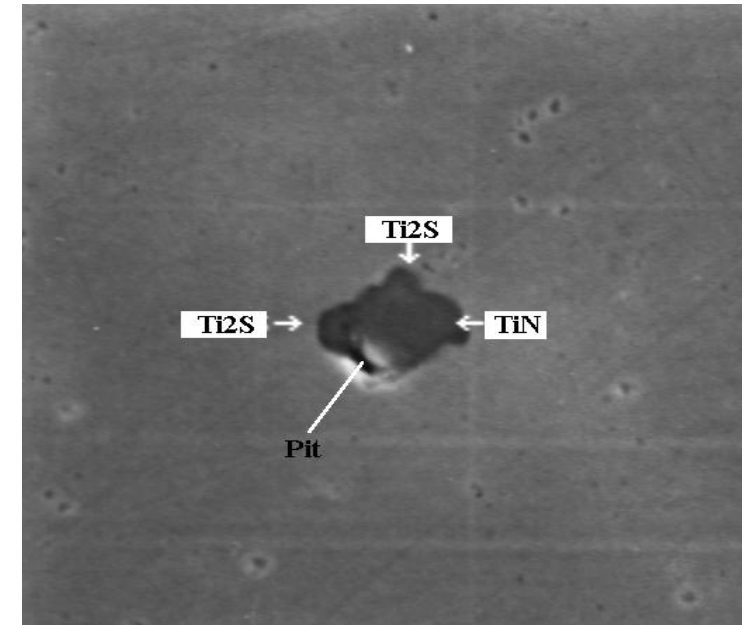
- **A: Steels with MnS (40 ppm S)**
- **B: Steels without MnS (+0,4%Ti)**

Pitting on sulphide inclusions

Scanning electron microscopy (x 3000)



Pitting on a manganese sulphide



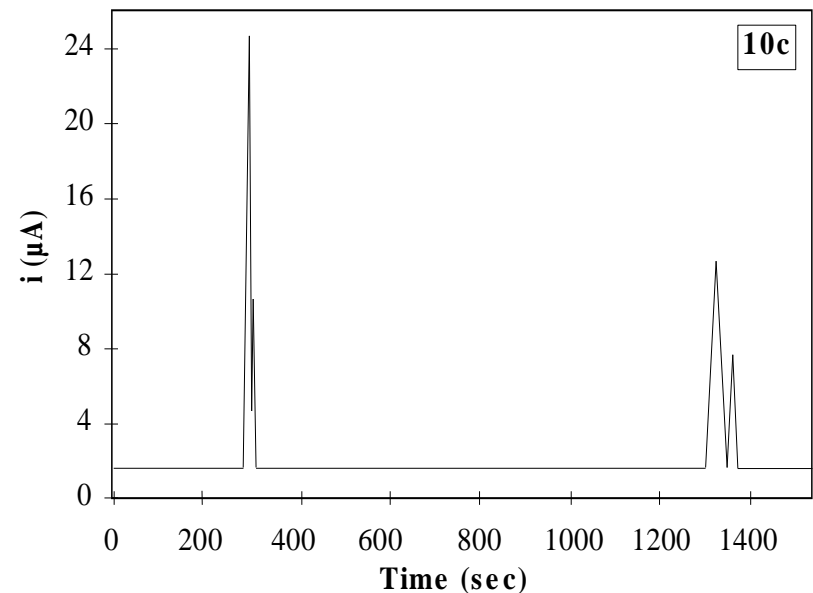
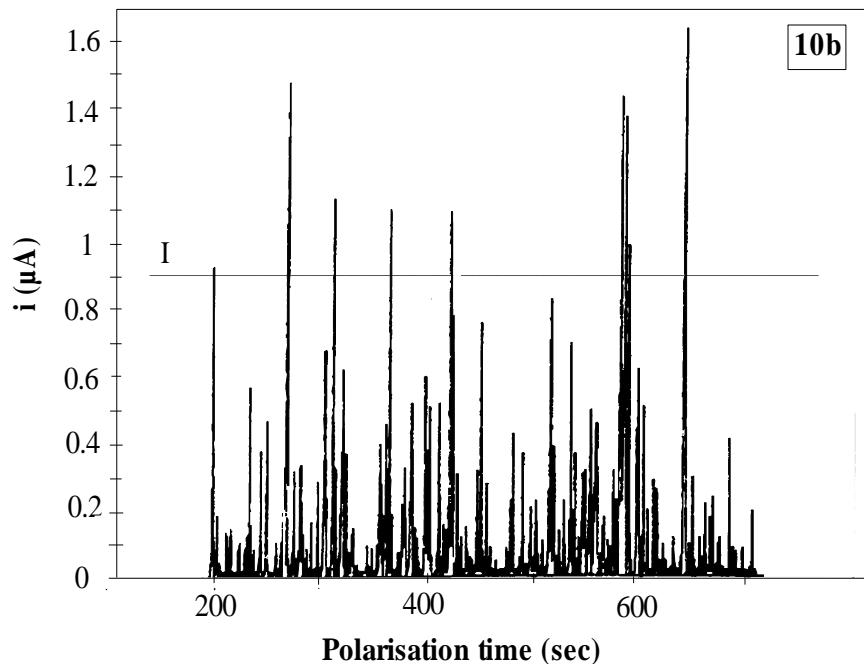
Pitting at the boundary of a Ti nitride

Fe16Cr

Mn=0.45% S= 40ppm

Prepitting events

during a polarisation at 200mV/SCE in NaCl 0.02M pH6.6

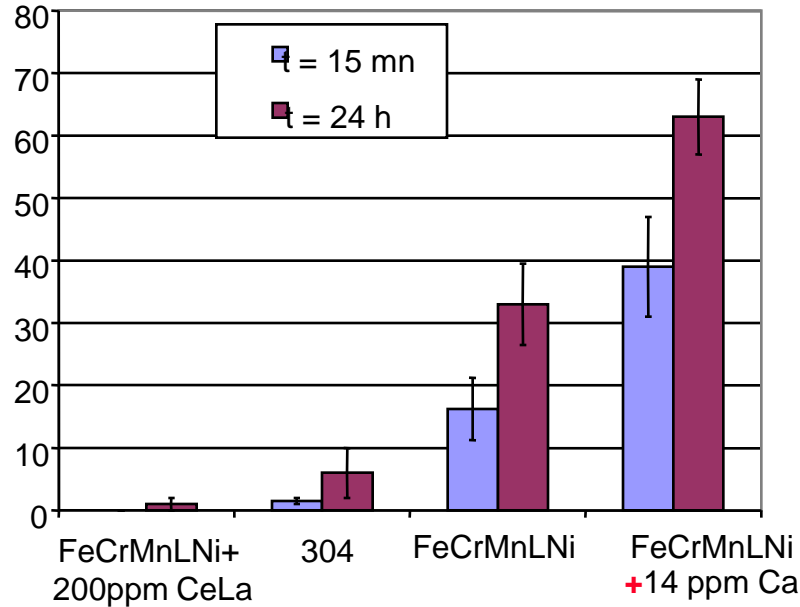


- *Left:* Typical anodic current variations for MnS containing steels.
- *Right:* Typical anodic micro-events for Ti bearing steels

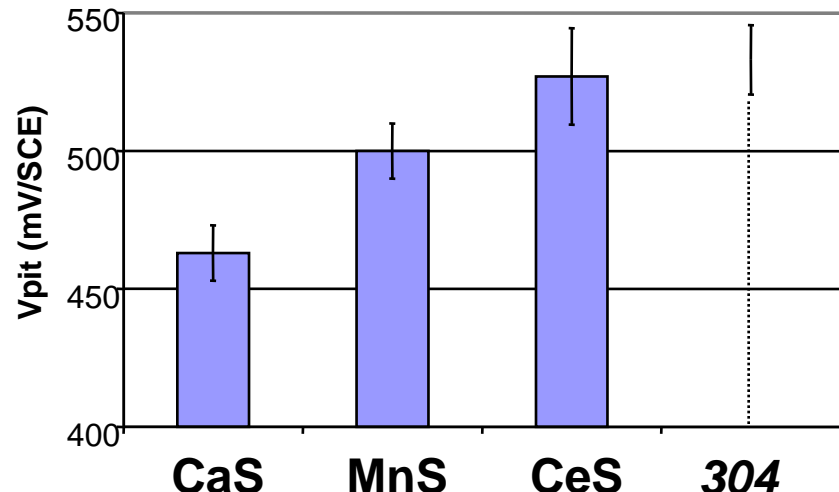
Effect of the sulfides solubility on the pitting potential

In "Critical Factors in localized corrosion IV": Salt lake city 2002. The importance of being a metallurgist

% of dissolved inclusions after immersion in neutral 0.02M NaCl (observed by SEM)



Pitting potential



CeS (Mn,Cr)S MnS CaS

C %	Cr %	Ni %	Mn	S (ppm)
0.07	16.4	1.6	7.3	9

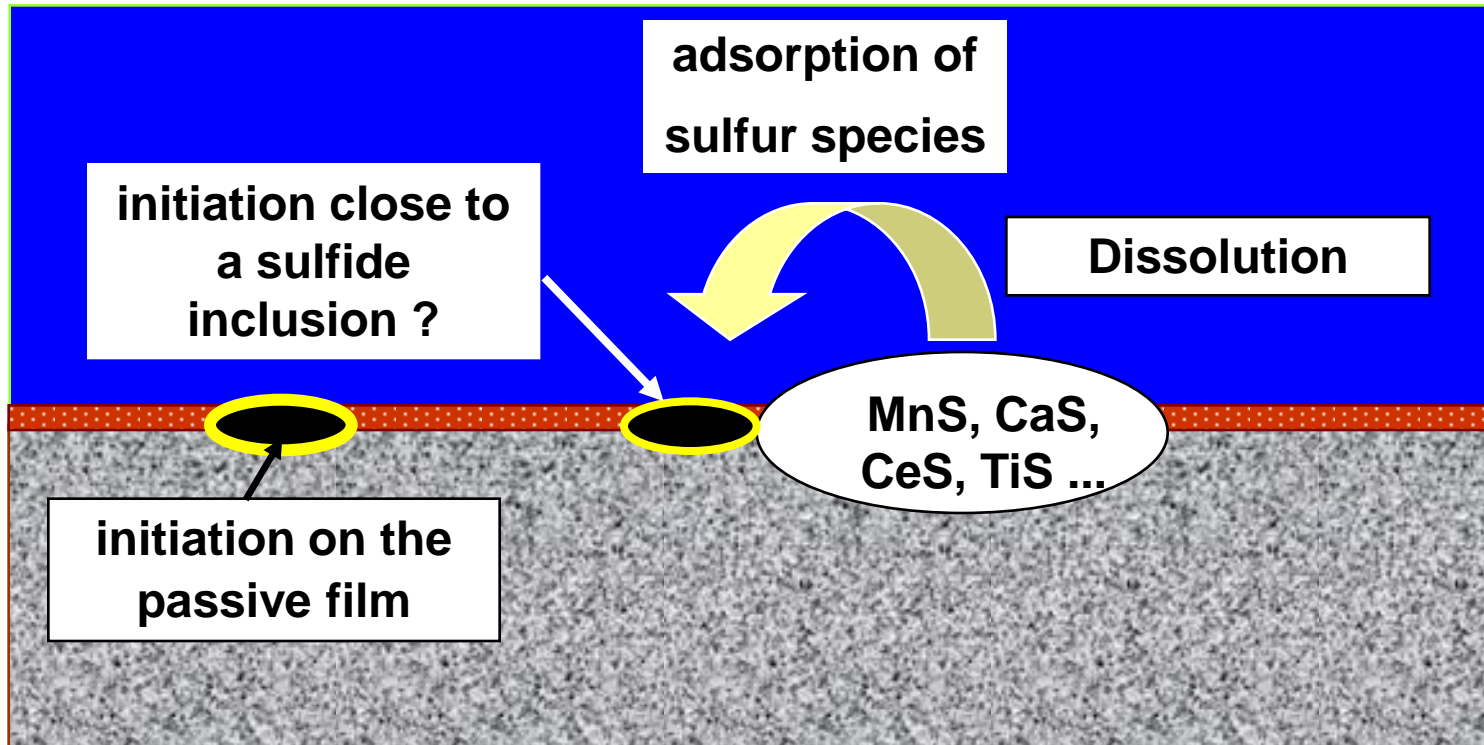
Low Ni austenitic stainless steel

The variations in pitting potential reveal

- 1) A significant effect of the sulfide solubility
- +
- 2) An effect of the matrix composition (Ni in 304)

Modeling the effect of sulfides

81



• The sulfides dissolve more or less rapidly, depending on their stability and on the solution corrosivity. In pitting initiation the sulfides act simply as sulfur species provider

• Sulfur containing species adsorb on the passive film close to the sulfide inclusion,

Promoting pit nucleation
(local film breakdown) or

Preventing repassivation
of nanopits

The pitting potential characterizes either
- the pit nucleation or
- the stabilization of pit nuclei

Modeling the effect of sulfides (2)

- **The earlier theories**
 - Sulfide dissolution, producing an unfilmed bare metal surface
 - Does not take into account the effect of passive film on pit initiation. Passive film could act only through the cathodic reaction (in OCP conditions)
- **Effect of thiosulfates**
 - Sulfide dissolution produce thiosulfates which prevent repassivation in the occluded zone formed by a metastable pit.
- **The effect of sulfide solubility**
 - Sulfide inclusions may act simply as sulfur species sources.
 - Sulfur containing species (elemental sulfur, thiosulfates...???) redeposit around the inclusion and make the passive film sensitive to pitting corrosion
 - Steel resistance to pitting decreases as sulfide inclusion solubility increases:
 - $\text{CaS} < \text{MnS} < (\text{Mn,Cr})\text{S} < \text{CrS} < \text{TiS} < \text{CeS}$
- **The Cr depletion theory** (Nature, Vol 415, 14 Feb. 2002) **does not meet basic metallurgical evidences**. More the effect of steel making process is ignored
 - In SS, Mn sulfides content a small amount of Cr (~5% in 304). The larger the Cr content or the smaller the Mn content, the larger the pitting resistance.
 - Ti containing steel, free from MnS but containing Ti_xS , resist better to pitting than MnS containing steels. They can pit however, but at higher potential , temperature or chloride content. Inclusions other than sulfides can also initiate pits
 - Metastable pitting was also observed even on « pure » (inclusion free) Fe17Cr alloys

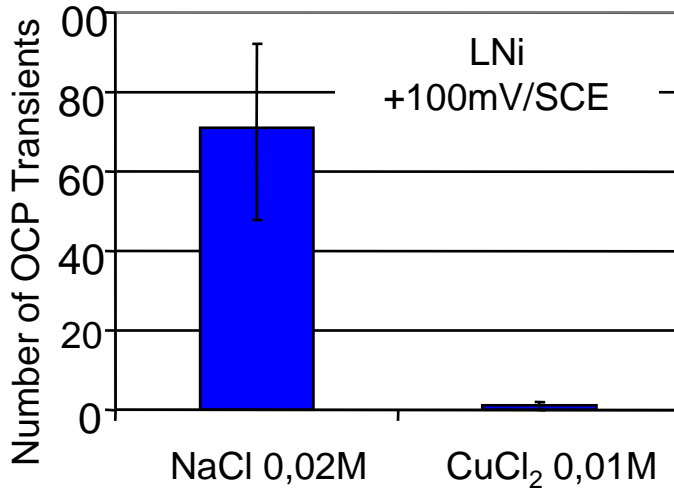
Conteracting the sulfur effects on pitting initiation

by T.Sourisseau and alias, Cors.Sci. 2005, 47, p1097

When added in aqueous solution,

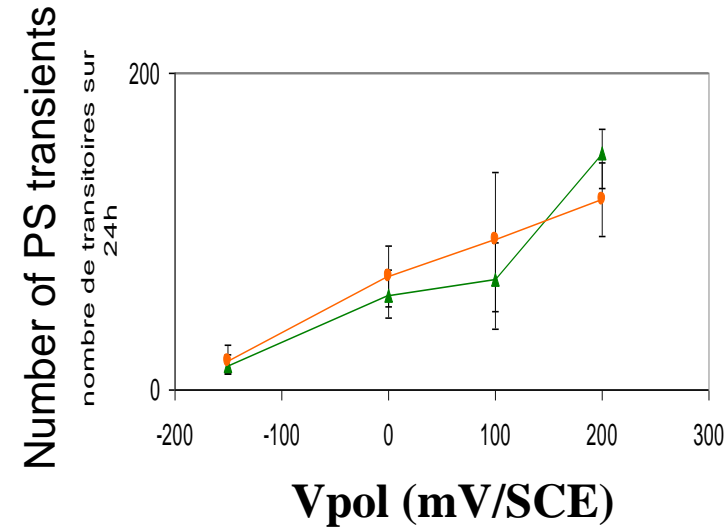
Cu Inhibits pits initiation

(formation of insoluble CuS-Cu₂S)



When added as alloying element

No effect is found on the number of transients



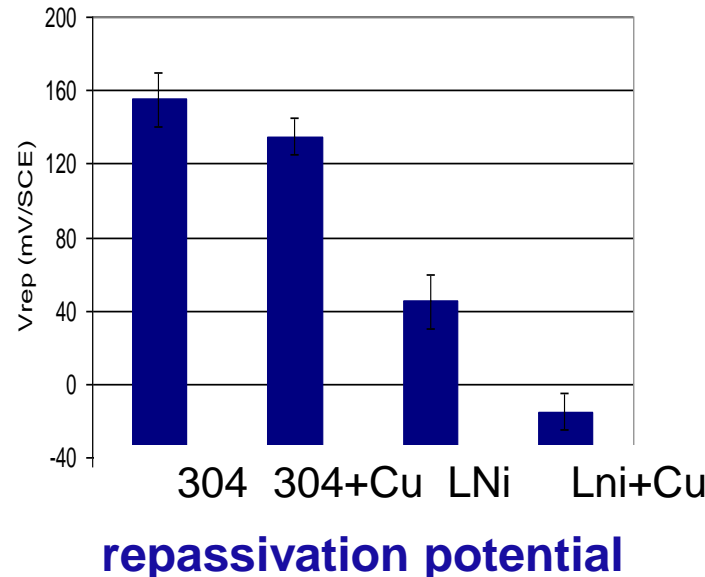
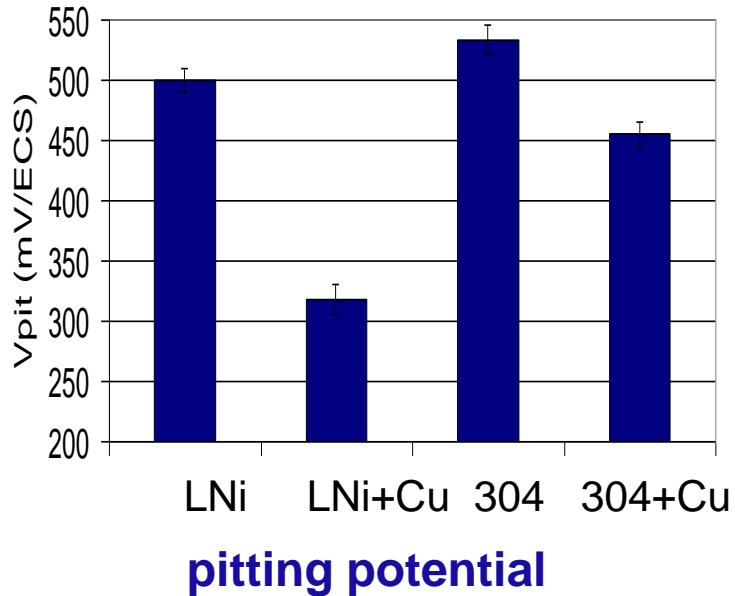
The favourable effect of dissolved copper in preventing pit initiation **is revealed by the number of pitting transients**

The possible effect of alloyed copper in preventing pit initiation **is not revealed** by the number of transients

Effect of metallic copper on the pitting potential

by T.Sourisseau and alias, Cors.Sci 2005.

Such an alloying addition of Cu is even found to decrease the pitting potential , and overmore the repassivation potential



1) Metallic Copper hinders repassivation

It was suggested that metallic Copper redeposits at pit bottom , inhibiting further Chromium oxidation, then preventing pit repassivation. The lower the pitting potential, the smaller the amount of dissolved Cu ions and then the larger the detrimental influence of Cu on the final result.

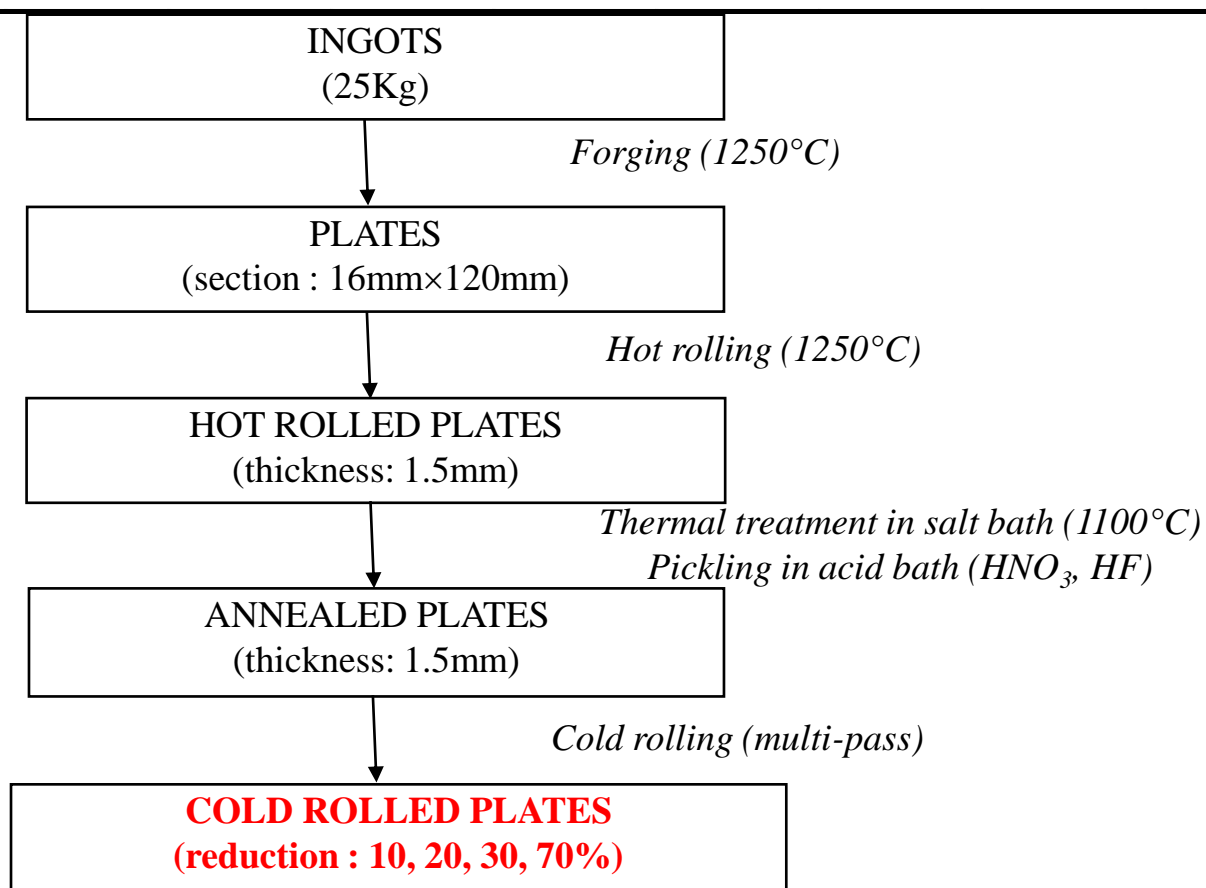
2) From the material performance viewpoint, it is worthy to note that this detrimental effect of Cu is revealed by both **repassivation and pitting potential**

The effect of cold rolling

by L..Peguet and alias, Cor.sci. In press)

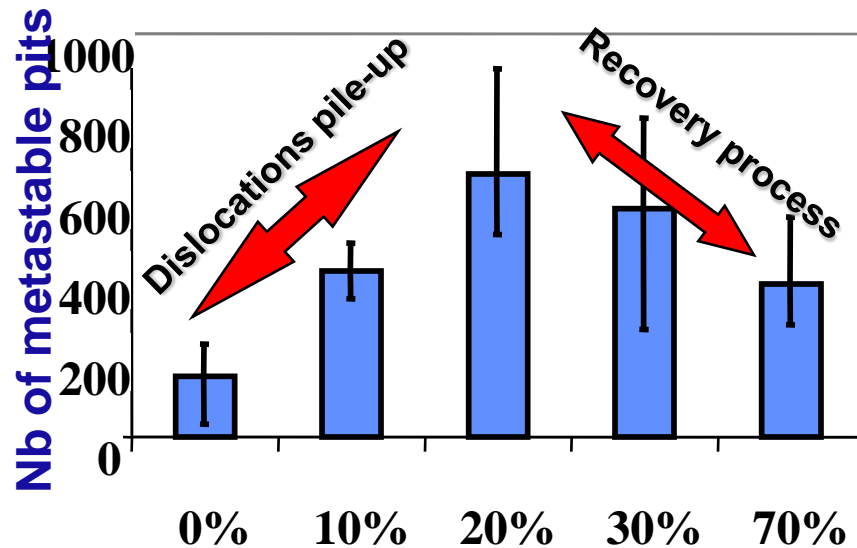
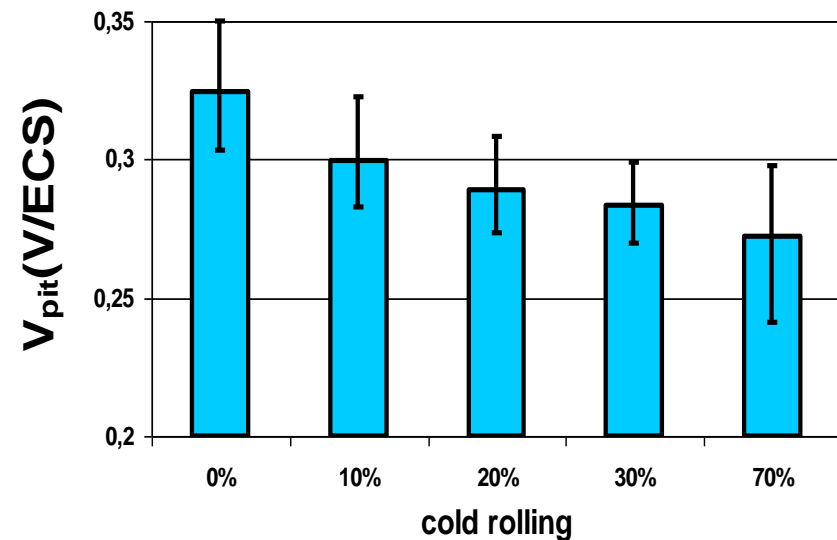
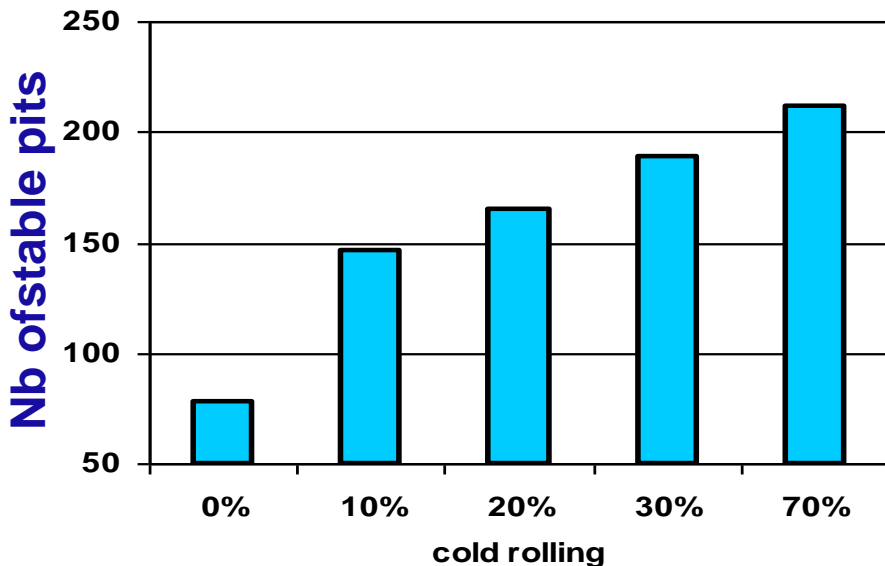
Chemical composition of the investigated material in weight %.

Grade	Elaboration	% C	% Mn	% Ni	% Cr	% Mo	% Cu	S (ppm)	% N
AISI 304	Laboratory	0.026	1.45	8.57	17.86	0.20	0.20	51	0.036



The effect of cold rolling: results

A fair correlation is evidenced between the pitting potential and Stable pitting but not with the number of metastable pitting transients



*In this case, the pitting potential is then correlated to stable pitting
but not to the pit initiation sensitivity*

Tensile deformation of a ferritic grade (no deformation martensite)

Chemical composition of the investigated materials in weight %.

Grade	Elaboration	% C	% Mn	% Ni	% Cr	% Mo	% Cu	S (ppm)	% N
AISI 304	<i>Industrial</i>	0.037	1.42	8.66	18.18	0.25	0.22	12	0.038
AISI 430	<i>Industrial</i>	0.042	0.38	0.16	16.26	0.03	0.04	21	0.027

Annealed



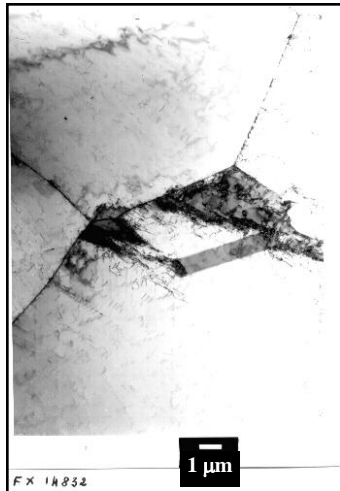
⇒ Disks stamped from strained samples to be used in electrochemical characterization.

Number of metastable pits initiated during 24h at free potential in NaCl 1M + FeCl₃ 10⁻³ M.

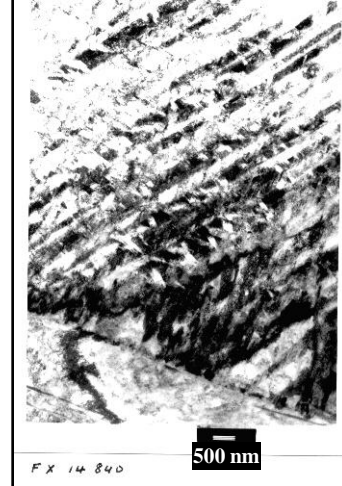
	annealed	10%	20%	35%	60%
AISI 304	116	297	-	64	40
AISI 430	371	515	309	-	-

⇒ Even a ferritic grade exhibits a maximum in pit initiation.

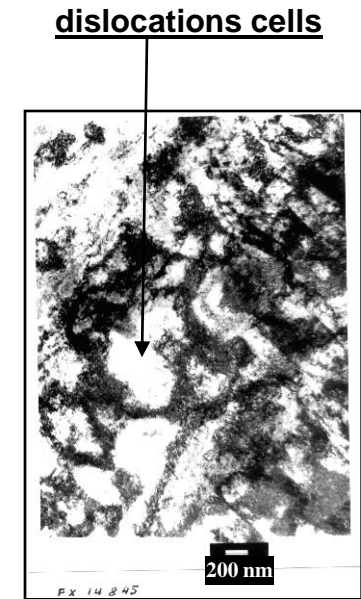
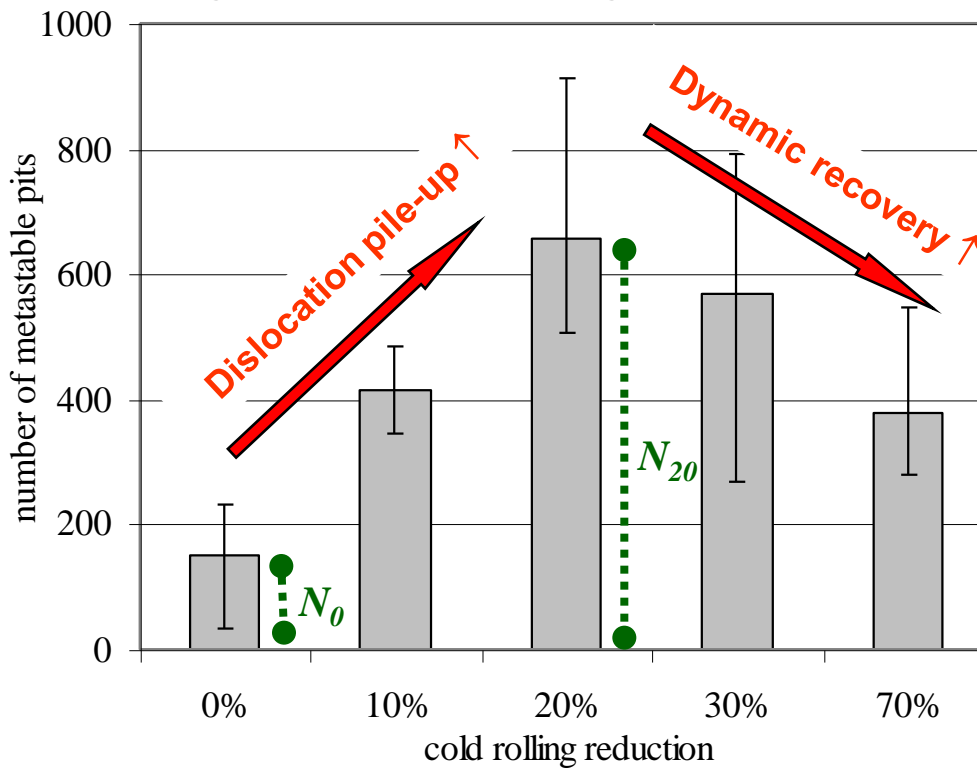
Dislocations substructure



Annealed



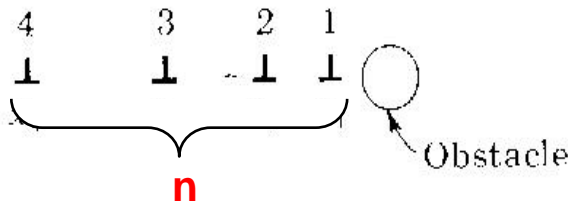
20% cold-rolled
Moderate strain : Fine lamellar structure by twinning, shear bands favoring dislocation pile-ups



70% cold rolled
Large strain : Recovery process illustrated by dislocations cells and pile-ups destruction.

Mechano-electrochemical modeling

Dislocation Pile-ups

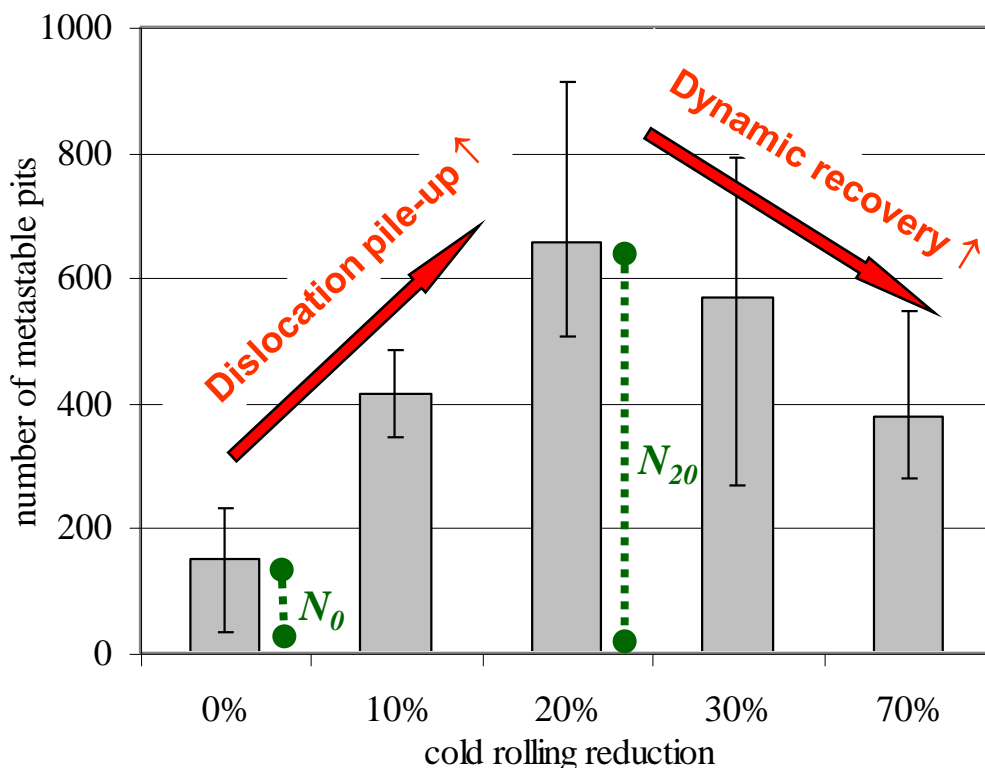


⇒ inducing large stress concentration:

$$\sigma \propto n$$

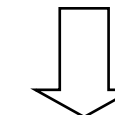
⇒ causing local electrochemical heterogeneities:

$$\Delta\phi = -n\Delta\tau \frac{R}{\alpha R' zF}$$



S.F.E. ↓ ⇒ Dislocation Pile-ups ↑

- dissociation ↑
- cross slip ↓



To work on selected SS grades with various S.F.E.

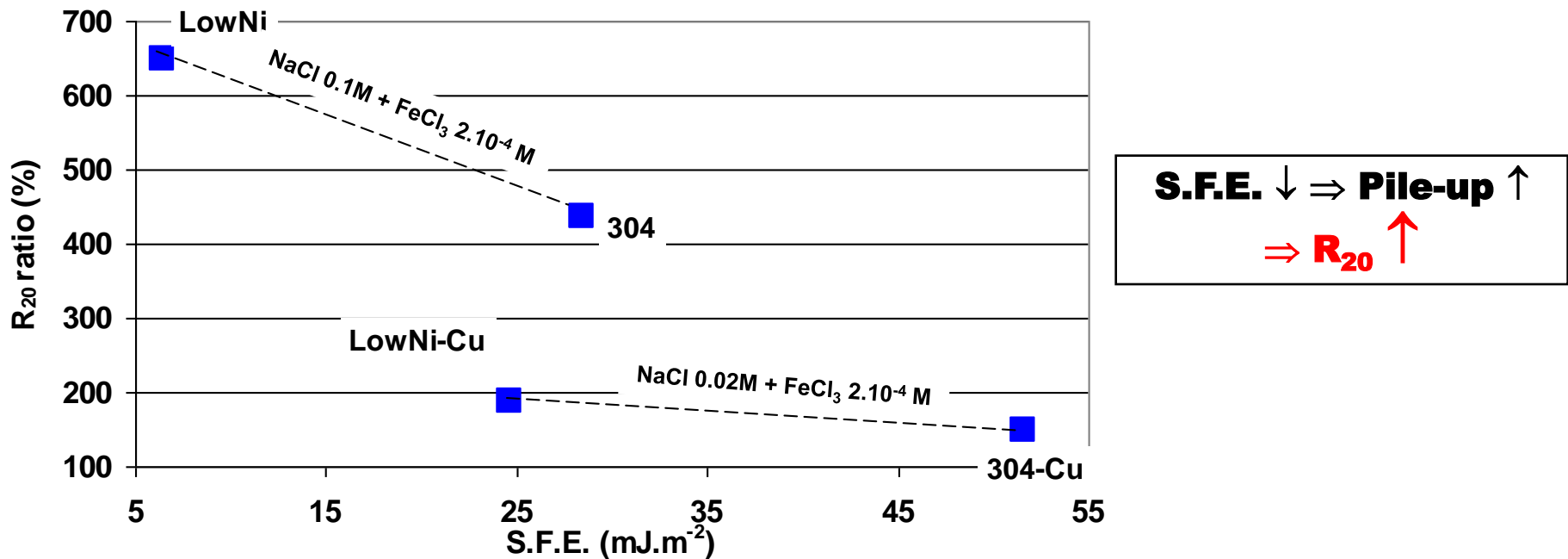
$$R_{20} = \frac{N_{20}}{N_0} = \frac{\text{Number of metastable pits at 20\%}}{\text{Number of metastable pits in the annealed state}}$$

Alloying elements affect the extent of pit initiation frequency maximum via their influence on dislocation pile-ups stability.

	C	N	S (ppm)	Cr	Mn	Ni	Cu
304	0.03	0.04	51	17.9	1.5	8.5	0.2
LowNi	0.07	0.24	9	16.4	7.3	1.6	0.2
304-Cu	0.04	0.04	45	18.2	1.4	8.7	3.0
LowNi-Cu	0.06	0.19	20	16.5	7.7	1.8	2.9

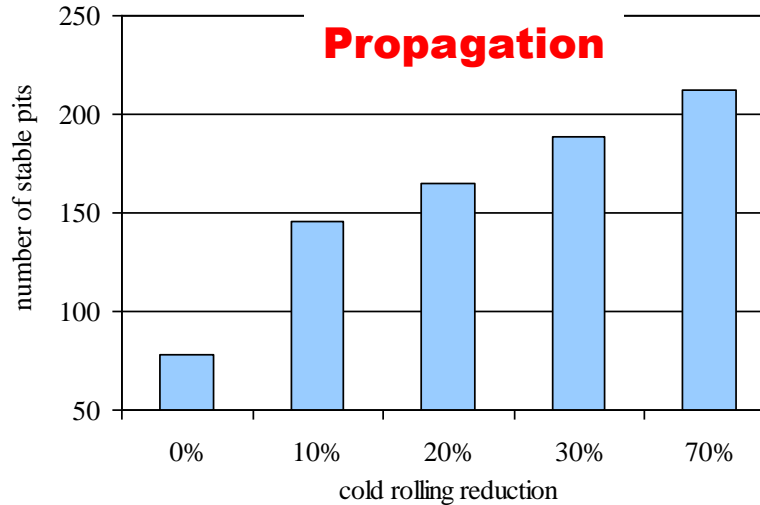
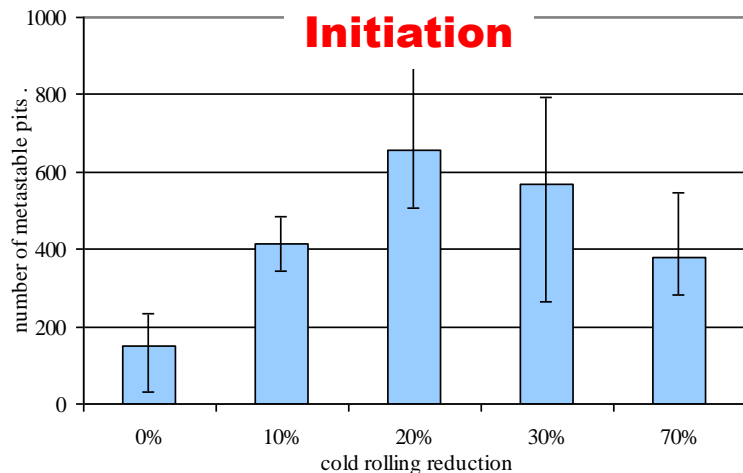
$$\text{SFE (mJ.m}^{-2}\text{)} = 25.7 + 2(\% \text{Ni}) + 410(\% \text{C}) - 0.9(\% \text{Cr}) - 77(\% \text{N}) - 13(\% \text{Si}) - 1.2(\% \text{Mn}) + 4(\% \text{Cu})$$

Pickering (1984) - Dulieu, Nutting (1964)



The effect of cold rolling: Conclusions

⇒ Plastic deformation acts differently depending on the pitting stage under consideration.



⇒ The unexpected maximum in pit initiation frequency does not depend on the deformation process nor on the presence of induced-martensite.

⇒ A major influence of dislocation pile-ups via the mecano-electrochemical effect is suspected. This explanation is supported by the role of alloying elements in the extent of pit initiation frequency maximum.

Effect of the surface finish condition on metastable pitting

by G.Berthomé and alias, Cors Sci.

The last stage of steel making process after cold rolling is the final annealing.

Two main conditions are of industrial interest for S.S. sheets:

2B condition:

Cold rolled sheet + annealing in oxidizing atmosphere

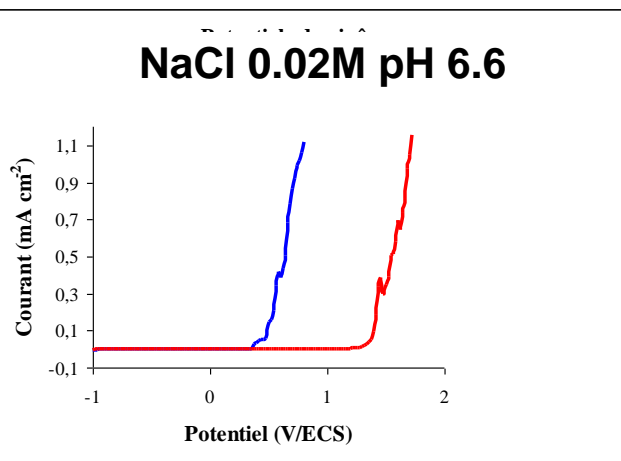
+ pickling in acidic bath then rinsing
+ skin pass

BA condition:

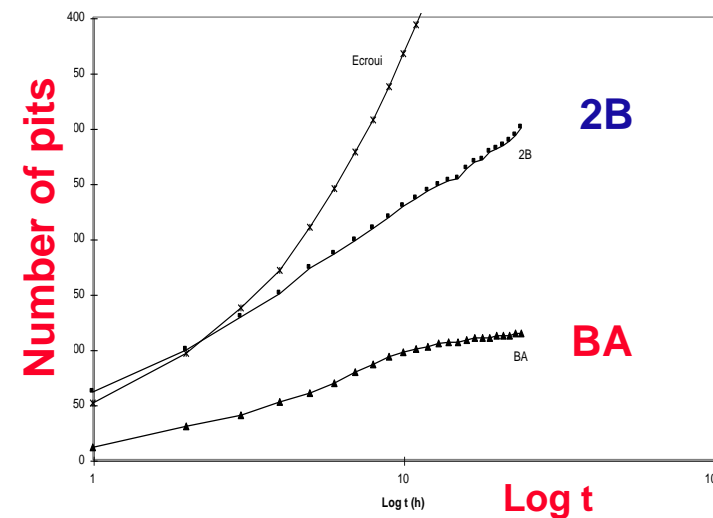
Cold rolled sheet + annealing in H₂ containing atmosphere + skin pass

This produces some passive films of different Cr content and of different pitting corrosion resistances

The pitting potential is larger for BA than for 2B and the number of OCP pitting transients is smaller



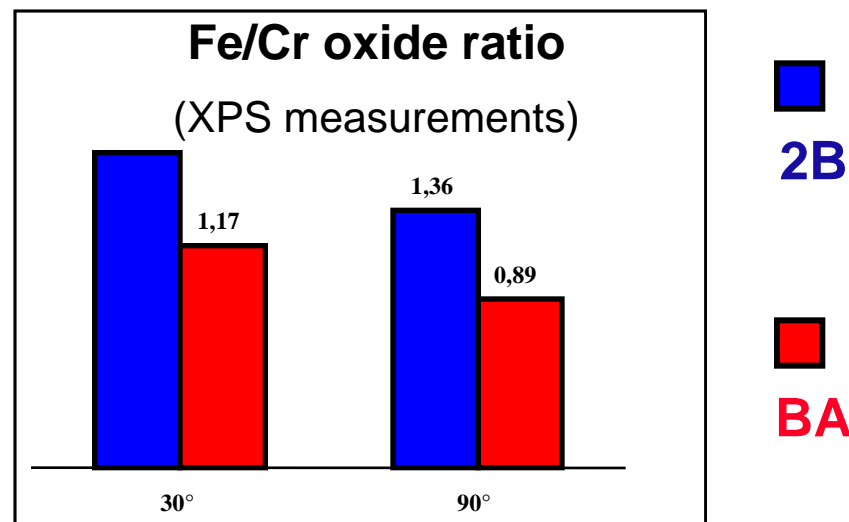
Pitting potential: BA > 2B



Number of pitting transients:
As rolled > 2B > BA

XPS analysis

The passive films formed on 2B and BA differ by their chromium content and their semi conductive properties

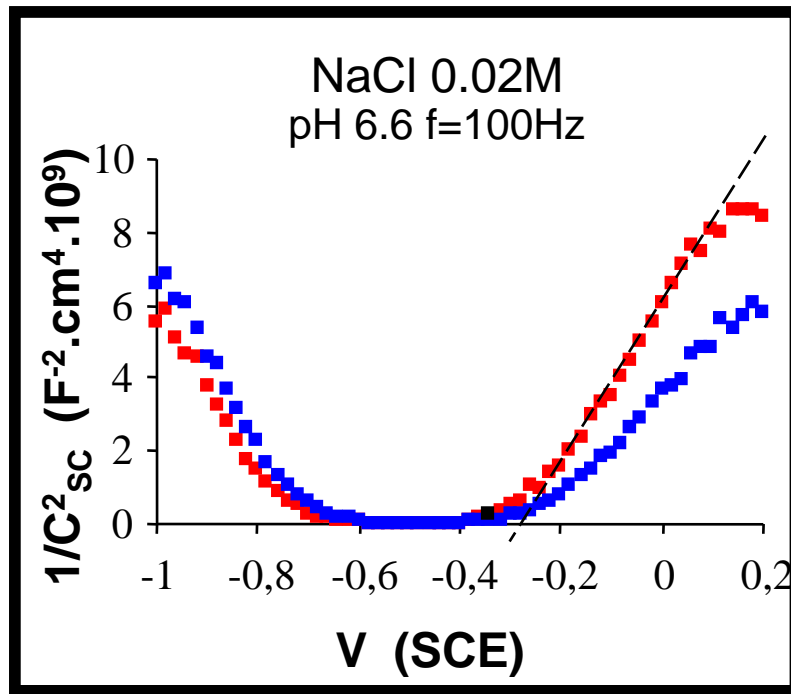


In the two cases the Cr content is higher in the inner passive film than in the outer, and larger for BA than for 2B condition

Semiconductive behaviour

by J.Amri and alias: in preparation

The passive film exhibits a p-type inner part and a n-type outer part. The electron states densities (acceptors in the inner part, donors in the outer part) are given by the Mott Schottky plots



$$\frac{1}{C_{sc}^2} = \left| \frac{2}{\epsilon_r \cdot \epsilon_0 \cdot q \cdot N_d} (V - V_{fb}) \right|$$

Mott-Schottky plots

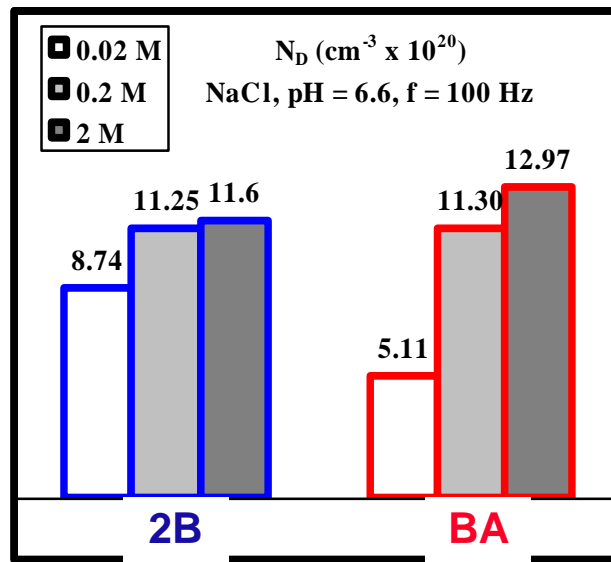
2B : $N_d = 8.74 \cdot 10^{20} \text{ cm}^3$

BA : $N_d = 5.11 \cdot 10^{20} \text{ cm}^3$

The electron donor concentration in the outer passive film (which is likely related to the concentration in point defects) is smaller for BA than for 2B,

Going further (2)

by J.Amri and alias: *in preparation*



The density of donor states increases with the electrolyte chloride content,
 Suggesting that the corresponding point defects are due to Chloride ions adsorption or incorporation in the outer passive film

Following this idea, the 2B film is less corrosion resistant due to its larger affinity for chloride ions

In this case the rate determining step is likely the nucleation step, and
 the pitting potential and the number of transients are fairly correlated to the Pit nucleation sensitivity

Material: Fe17Cr

Effect of the Surface Condition on the resistance to CC

Surface finishing :

BA (Bright annealed)

2B (Pickled surface)

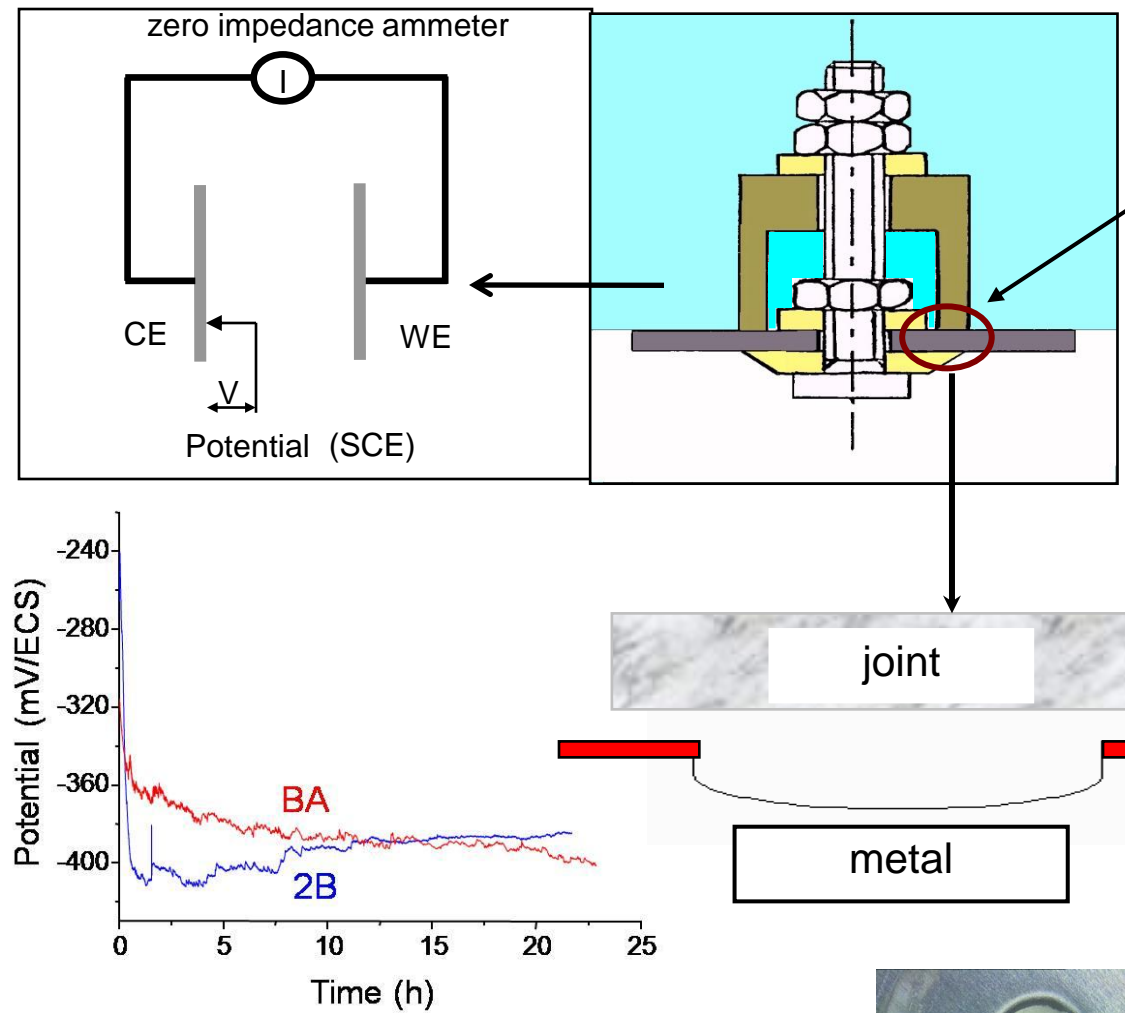
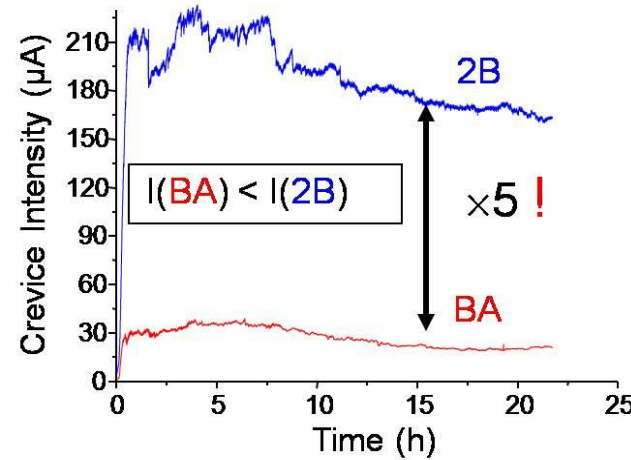
Test conditions:

NaCl 0.5M pH 6.6 / 50°C

Screw/wing system

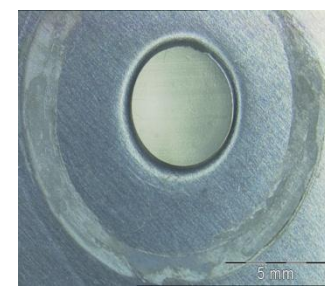
tightening = 0,2 N.m

$S_{crev} = 0.85 \text{ cm}^2$

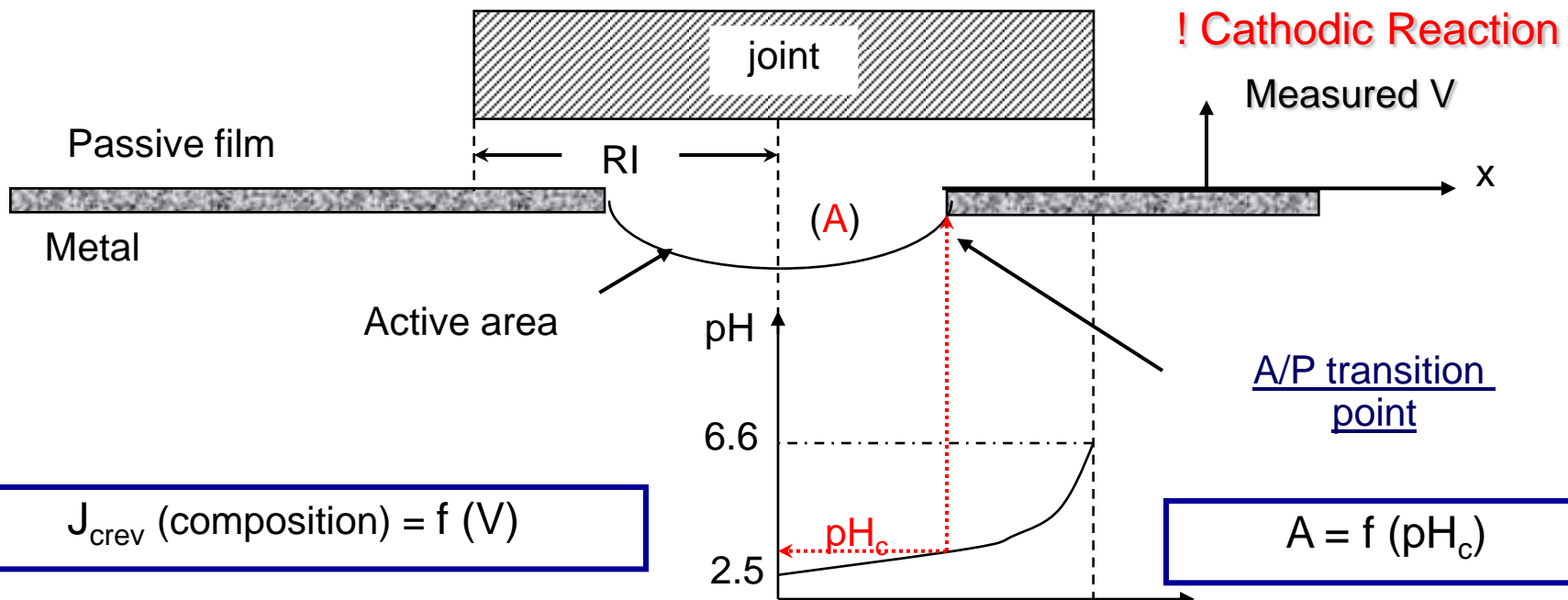


The active area 2B is ~ 5 times larger for 2B than for BA

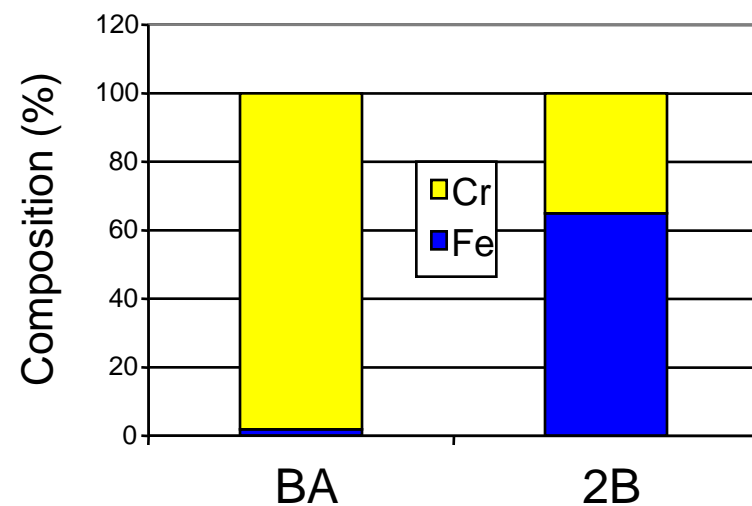
Then $j_{crev}(2B) = j_{crev}(2B)$



Effect of the Surface Condition (2)



- ✓ BA finish exhibits better crevice corrosion resistance than 2B.
- ✓ The corrosion current is controlled by the active area, depending on the critical depassivation pH



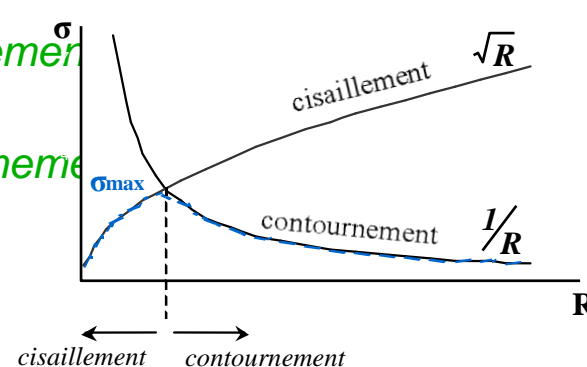
Corrosion feuilletante des alliages d'aluminium

Alliages 7000 (aéronautique) à durcissement structural : précipitation durcissante type MgZn₂
Franchissement des obstacles (précipités) par les dislocations:

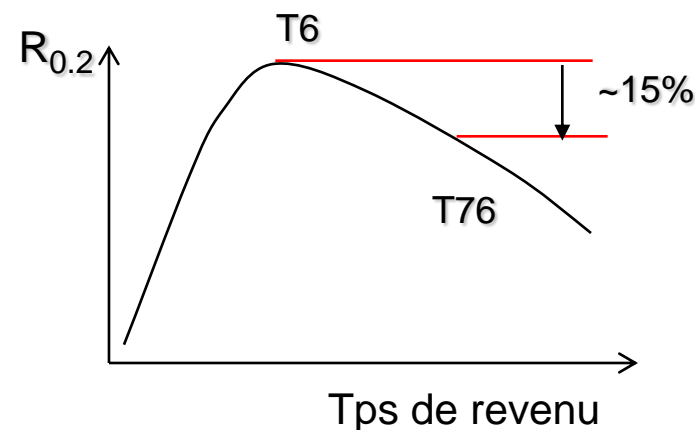
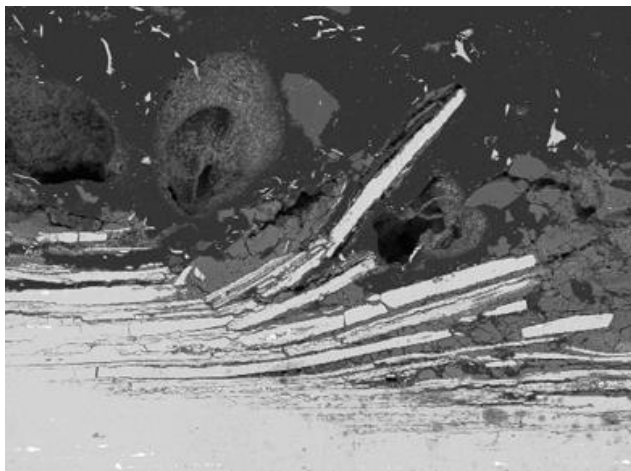
$$\Delta\tau = K \cdot f_v^{1/2} \cdot r^{-1/2} \text{ Cisaillement}$$

$$\Delta\tau = K \cdot f_v^{1/2} \cdot \frac{1}{r} \text{ Contournement}$$

⇒ Taille optimale de précipités



- . Excellentes propriétés mécaniques (R_{0.2} : 430-700 Mpa) MAIS sensibilité à la corrosion feuilletante



• T6 : Revenu au pic = maximum de caractéristiques mécaniques

• T76 : Sur-revenu = compromis entre CM et sensibilité à la corrosion feuilletante

Essai galvanostatique

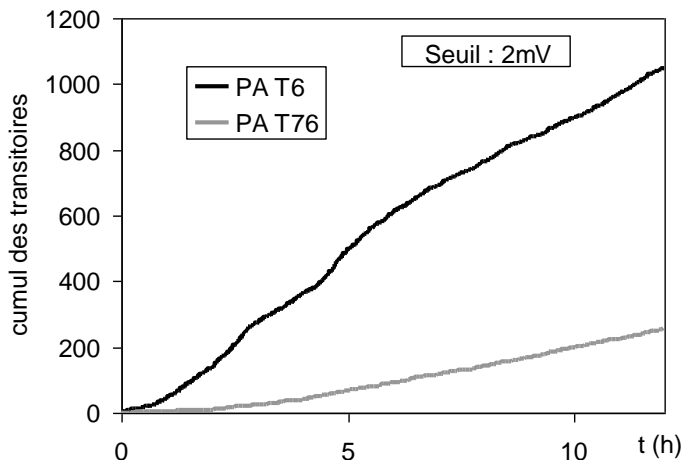
Solution :

NaCl 1M, NaNO₃ 0.25M, AlCl₃ 0.033M

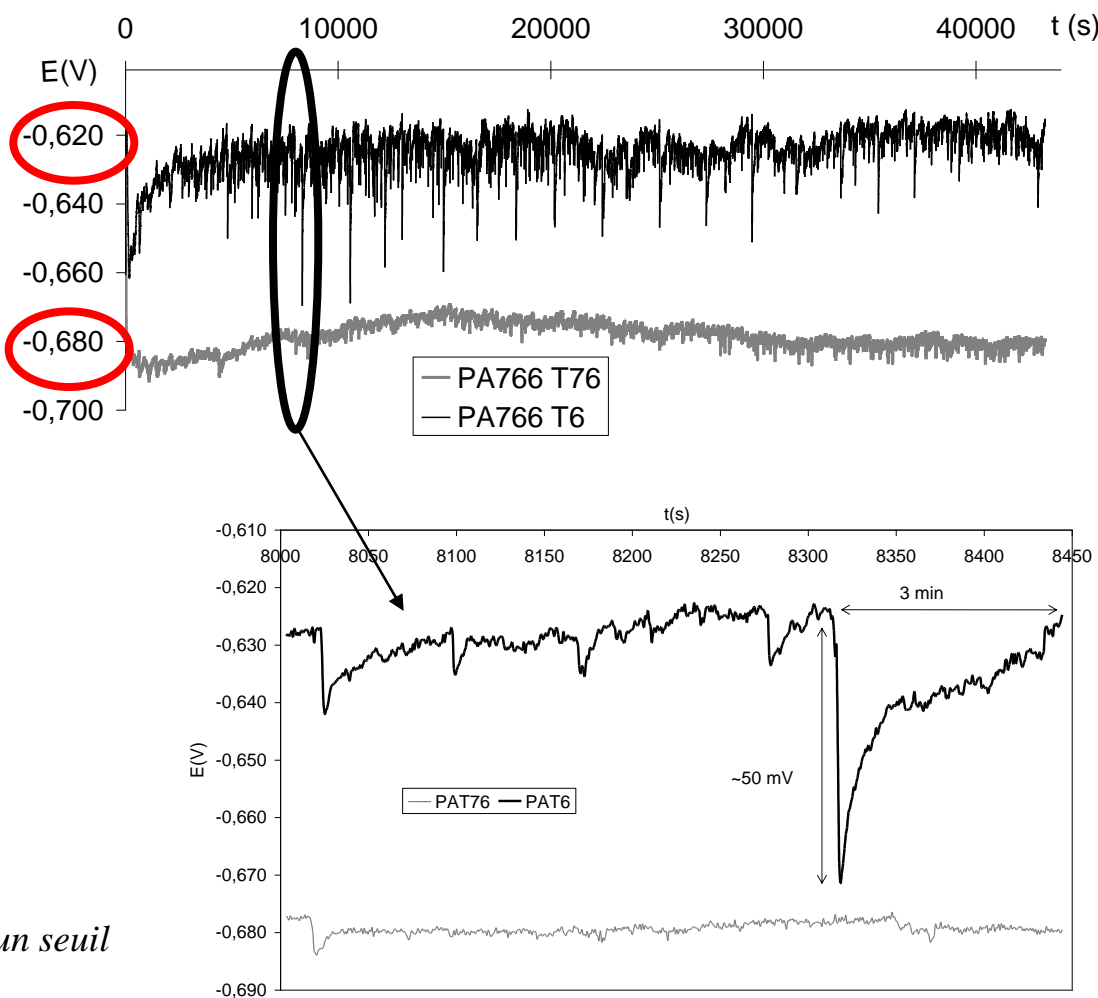
Intensité : 2.5mA/cm²

Aspect: T6 = feuillets, T76 = poudre

Les transitoires en potentiel =
Corrosion feuilletante

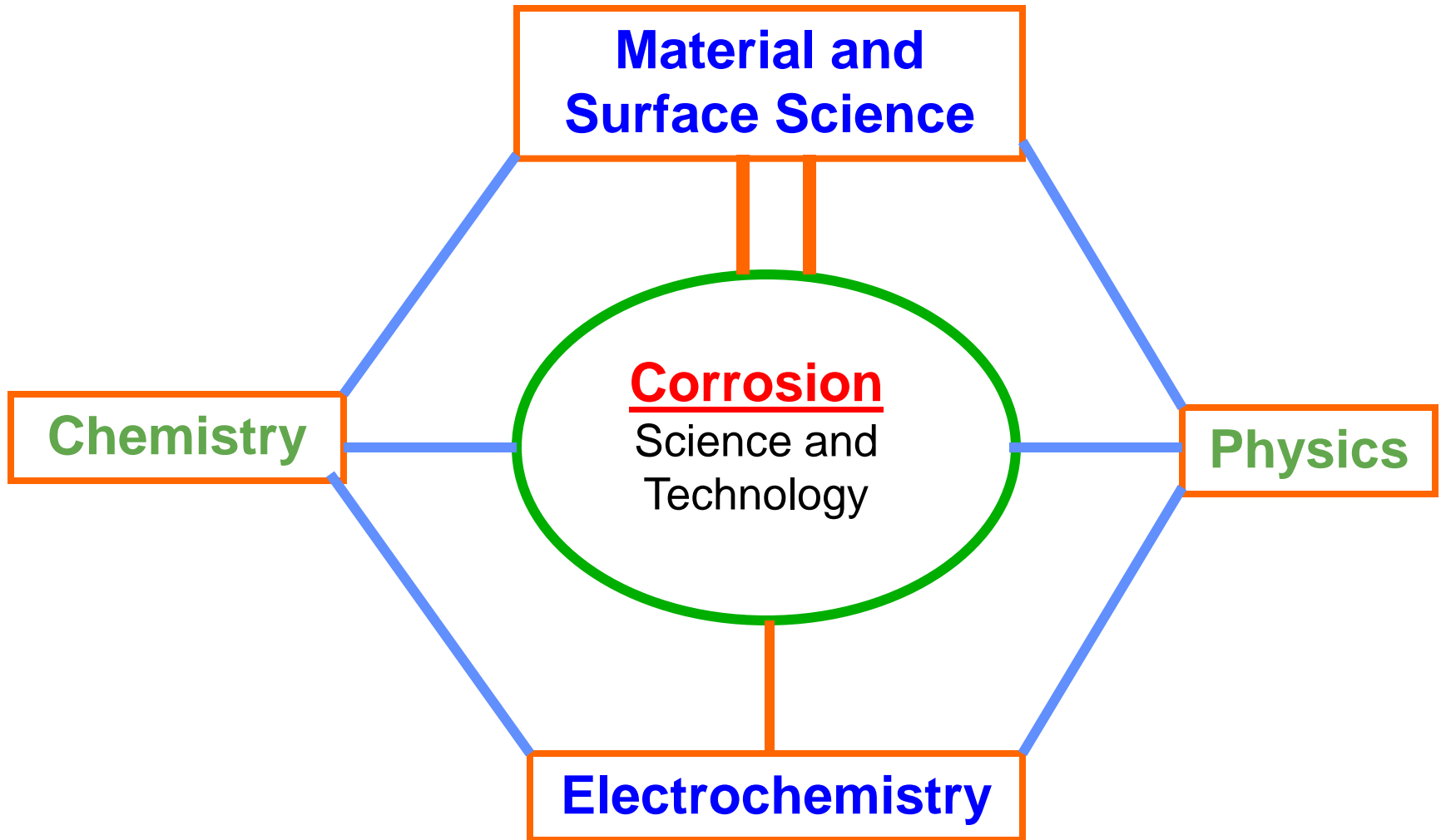


Cumul du nombre de transitoires supérieurs à un seuil de 2mV à droite



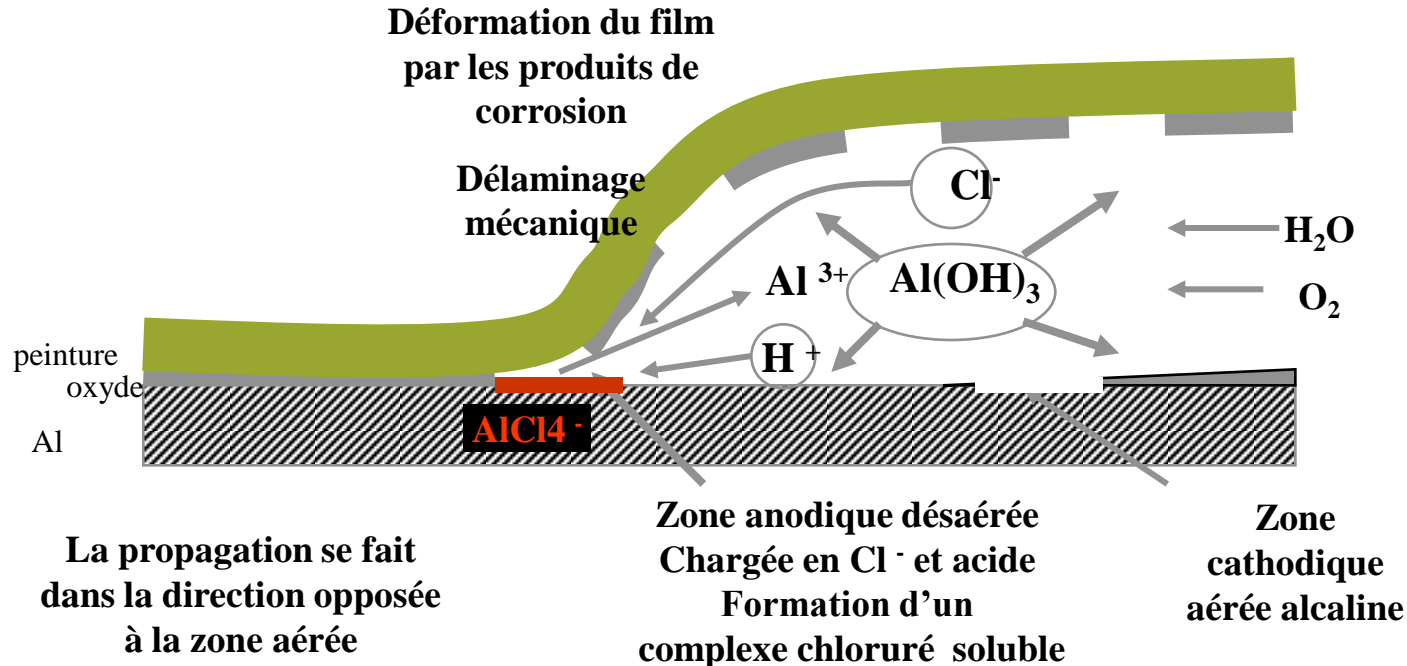
Conclusion:

The importance of being a metallurgist



Délamination des peintures

Délamination anodique



Délamination cathodique (*Propagation à l'interface peinture/oxyde*)

